University of Kent

Kent Academic Repository

Contreras Peña, C., Lucas, P. W., Minniti, D., Kurtev, R., Stimson, W., Molina, C. Navarro, Borissova, J., Kumar, M. S. N., Thompson, M.A., Gledhill, T. and others (2016) *A population of eruptive variable protostars in VVV.* Monthly Notices of the Royal Astronomical Society, 465 (3). pp. 3011-3038. ISSN 0035-8711.

Downloaded from

https://kar.kent.ac.uk/58436/ The University of Kent's Academic Repository KAR

The version of record is available from

https://doi.org/10.1093/mnras/stw2801

This document version

Author's Accepted Manuscript

DOI for this version

Licence for this version

UNSPECIFIED

Additional information

Versions of research works

Versions of Record

If this version is the version of record, it is the same as the published version available on the publisher's web site. Cite as the published version.

Author Accepted Manuscripts

If this document is identified as the Author Accepted Manuscript it is the version after peer review but before type setting, copy editing or publisher branding. Cite as Surname, Initial. (Year) 'Title of article'. To be published in *Title of Journal* , Volume and issue numbers [peer-reviewed accepted version]. Available at: DOI or URL (Accessed: date).

Enquiries

If you have questions about this document contact ResearchSupport@kent.ac.uk. Please include the URL of the record in KAR. If you believe that your, or a third party's rights have been compromised through this document please see our Take Down policy (available from https://www.kent.ac.uk/guides/kar-the-kent-academic-repository#policies).

Mon. Not. R. Astron. Soc. **000**, 1–?? (2002) Printed 1 November 2016 (MN LATEX style file v2.2)

A population of eruptive variable protostars in VVV

C. Contreras Peña[1,4,2,⋆] P. W. Lucas[2], D. Minniti[1,7], R. Kurtev[3,4], W. Stimson[2], C. Navarro Molina[4,3], J. Borissova[3,4], M. S. N. Kumar[2], M.A. Thompson[2], T. Gledhill[2], R. Terzi[2], D. Froebrich[5], and A. Caratti o Garatti[6]

[1] *Departamento de Ciencias Fisicas, Universidad Andres Bello, Republica 220, Santiago, Chile*
[2] *Centre for Astrophysics Research, University of Hertfordshire, Hatfield, AL10 9AB, UK*
[3] *Instituto de Física y Astronomía, Universidad de Valparaíso, ave. Gran Bretaña, 1111, Casilla 5030, Valparaíso, Chile*
[4] *Millennium Institute of Astrophysics, Av. Vicuna Mackenna 4860, 782-0436, Macul, Santiago, Chile*
[5] *Centre for Astrophysics and Planetary Science, University of Kent, Canterbury CT2 7NH, UK*
[6] *Dublin Institute for Advanced Studies, School of Cosmic Physics, Astronomy & Astrophysics Section, 31 Fitzwilliam Place, Dublin 2, Ireland*
[7] *Vatican Observatory, V00120 Vatican City State, Italy*

arXiv:1602.06267v2 [astro-ph.SR] 30 Oct 2016

1 November 2016

ABSTRACT

We present the discovery of 816 high amplitude infrared variable stars ($\Delta K_s > 1$ mag) in 119 deg^2 of the Galactic midplane covered by the Vista Variables in the Via Lactea (VVV) survey. Almost all are new discoveries and about 50% are YSOs. This provides further evidence that YSOs are the commonest high amplitude infrared variable stars in the Galactic plane. In the 2010-2014 time series of likely YSOs we find that the amplitude of variability increases towards younger evolutionary classes (class I and flat-spectrum sources) except on short timescales (<25 days) where this trend is reversed. Dividing the likely YSOs by light curve morphology, we find 106 with eruptive light curves, 45 dippers, 39 faders, 24 eclipsing binaries, 65 long-term periodic variables (P>100 days) and 162 short-term variables. Eruptive YSOs and faders tend to have the highest amplitudes and eruptive systems have the reddest SEDs. Follow up spectroscopy in a companion paper verifies high accretion rates in the eruptive systems. Variable extinction is disfavoured by the 2 epochs of colour data. These discoveries increase the number of eruptive variable YSOs by a factor of at least 5, most being at earlier stages of evolution than the known FUor and EXor types. We find that eruptive variability is at least an order of magnitude more common in class I YSOs than class II YSOs. Typical outburst durations are 1 to 4 years, between those of EXors and FUors. They occur in 3 to 6% of class I YSOs over a 4 year time span.

Key words: infrared: stars – stars: low-mass – stars: pre-main-sequence – stars: AGB and post-AGB – stars: protostars – stars: variables: T Tauri, Herbig Ae/Be.

1 INTRODUCTION

The VISTA Variables in the Via Lactea (VVV, Minniti et al. 2010) survey has mapped a 560 deg^2 area containing $\sim 3 \times 10^8$ point sources with multi-epoch near-infrared photometry. The surveyed area includes the Milky Way bulge and an adjacent section of the mid plane. The survey has already produced a deep near-infrared Atlas in 5 bandpasses (Z, Y, J, H, K_s), and the final product will include a 2nd epoch of the multi-filter data and a catalogue of more than 10^6 variable sources.

One of the main scientific goals expected to arise from the final product of VVV is the finding of rare variable sources such as Cataclysmic Variables and RS CVn stars, among others (see Catelan et al. 2013, for a discussion on classes of near-infrared variable stars that are being studied with VVV). One of the most important outcomes is the possibility of finding eruptive variable Young Stellar Objects (YSOs) undergoing unstable accretion. Such objects are usually assigned to one of two sub-classes: FUors, named after FU Orionis, have long duration outbursts (from tens to hundreds of years); EXors, named for EX Lupi, have outbursts of much shorter duration (from few weeks to several months). Both categories were optically defined in the first instance and fewer than 20 are known in total (see e.g., Reipurth & Aspin 2010; Scholz et al. 2013; Audard et al. 2014), very likely because YSOs with high accretion rates tend to suffer high optical extinction by circumstellar mat-

⋆ E-mail:cecontrep@gmail.com (CCP)

© 2002 RAS

ter. For thorough reviews of the theory and observations in this subject see Hartmann & Kenyon (1996); Reipurth & Aspin (2010); Audard et al. (2014). Given that VVV is the first near infrared time domain survey of a large portion of the Galaxy, it is reasonable to hope for a substantial yield of new eruptive variable YSOs in the dataset. In particular, we would expect the survey to probe for high amplitude variability that occurs on typical timescales of up to a few years, which corresponds more to EXors (or their younger, more obscured counterparts) than to FUors. Eruptive variable YSOs are important because it is thought that highly variable accretion may be common amongst protostars, though rarely observed owing to a duty cycle consisting of long periods of slow accretion and much shorter periods of unstable accretion at a much higher rate. If this is true, it might explain both the observed under-luminosity of low-mass, class I YSOs (the "Luminosity problem" (see e.g Kenyon et al. 1990; Evans et al. 2009; Caratti o Garatti et al. 2012)) and the wide scatter seen in the Hertzsprung-Russell (HR) diagrams of pre-main-sequence (PMS) clusters (Baraffe, Chabrier, & Gallardo 2009; Baraffe, Vorobyov, & Chabrier 2012).

In the search for this rare class of eruptive variable stars, Contreras Peña et al. (2014) studied near-infrared high-amplitude variability in the Galactic plane using the two epochs of UKIDSS Galactic Plane Survey (UGPS) K band data (Lawrence et al. 2007; Lucas et al. 2008). Contreras Peña et al. found that $\sim 66\%$ of high-amplitude variable stars selected from UGPS data releases DR5 and DR7 are located in star forming regions (SFRs) and have characteristics of YSOs. They concluded that YSOs likely dominate the Galactic disc population of high-amplitude variable stars in the near-infrared. Spectroscopic follow-up confirmed four new additions to the eruptive variable class. These objects showed a mixture of the characteristics of the optically-defined EXor and FUor subclasses. Two of them were deeply embedded sources with very steep 1 to 5 μm spectral energy distributions (SEDs), though showing "flat spectrum" SEDs at longer wavelengths. Such deeply embedded eruptive variables are regarded as a potentially distinct additional subclass, though only a few had been detected previously: OO Ser, V2775 Ori, HOPS 383 and GM Cha (see Hodapp et al. 1996; Kóspál et al. 2007; Persi et al. 2007; Caratti o Garatti et al. 2011; Safron et al. 2015). With the aims of determining the incidence of eruptive variability among YSOs and characterising the phenomenon, we have undertaken a search of the multi-epoch VVV dataset. In contrast to UGPS, the ongoing VVV survey offers several dozen epochs of K_s data over a time baseline of a few years. We expect that the VVV survey will also be used to identify YSOs by the common low amplitude variability seen in nearly all such objects (e.g. Rice et al. 2012). This will complement studies in nearby star formation regions and in external galaxies, such as the *Spitzer* YSOVAR programme (e.g. Wolk et al. 2015) and a 2 epoch study of the LMC with *Spitzer* SAGE survey data (Vijh et al. 2009).

We have divided the results of this work in two publications. In this first study we present the method of the search and a general discussion on the photometric characteristics of the whole sample of high amplitude variables in the near-infrared. We present the follow-up and spectroscopic characteristics of a large sub-sample of candidate eruptive variable stars in a companion publication (hereinafter referred to as paper II).

In Sect. 2 of this work we describe the VVV survey, the data and the method used to select high amplitude infrared variables. Section 3 describes the make up and general properties of the sample, the evidence for clustering and the apparent association with SFRs. In this section we also classify the light curves of variables found outside SFRs and use this information to estimate the contamination of our high amplitude YSO sample by other types of variable star. We then estimate the high amplitude YSO source density from our sample and compare the average space density with those of other high amplitude infrared variables. In Sect. 4 we discuss the physical mechanisms that drive variability in YSOs and classify our YSOs via light curve morphology. This yields some ideas concerning which of the known mechanisms might be responsible for the observed variability. We test these mechanisms using two epoch JHK_s data. Then we discuss the trends in the likely YSOs as a function of evolutionary status based on their spectral energy distribution. Finally we discuss the large sample of likely eruptive variables. Section 6 presents a summary of our results.

2 VVV

The regions covered by the VVV survey comprise the Bulge region within $-10^\circ < l < +10^\circ$ and $-10^\circ < b < +5^\circ$ and the disc region in $295^\circ < l < 350^\circ$ and $-2^\circ < b < +2^\circ$ (see e.g., Minniti et al. 2010).

The data is collected by the Visible and Infrared Survey Telescope for Astronomy (VISTA). The 4m telescope is located at Cerro Paranal Observatory in Chile and is equipped with a near-infrared camera (VIRCAM) consisting of an array of sixteen 2048×2048 pix detectors, with a typical pixel scale of $0.''339$, with each detector covering 694×694 arcsec^2. The detectors are set in a 4×4 array and have large spacing along the X and Y axis. Therefore a single pointing, called a "pawprint", covers 0.59° giving partial coverage of a particular field of view. A continuous coverage of a particular field is achieved by combining six single pointing with appropriate offsets. This combined image is called a tile. The VVV survey uses the five broad-band filters available in VIRCAM, $Z(\lambda_{eff} = 0.87\mu\text{m})$, $Y(\lambda_{eff} = 1.02\mu\text{m})$, $J(\lambda_{eff} = 1.25\mu\text{m})$, $H(\lambda_{eff} = 1.64\mu\text{m})$ and $K_s(\lambda_{eff} = 2.14\mu\text{m})$.

The VVV survey area is comprised of 348 tiles, 196 in the bulge and 152 in the disc area. Each tile was observed in a single near-contemporaneous multi-filter ($ZYJHK_s$) epoch at the beginning of the campaign, with an exposure time of 80 s per filter. A second epoch of contemporaneous JHK_s was observed in 2015. The variability monitoring was performed only in K_s with an exposure time of 16 s.

The images are combined and processed at the Cambridge Astronomical Survey Unit (CASU). The tile catalogues are produced from the image resulting from combining six pawprints. The catalogues provide parameters such as positions and fluxes from different aperture sizes. A flag indicating the most probable morphological classification is also provided, with "-1" indicating stellar sources, "-2" borderline stellar, "1" non-stellar , "0" noise, "-7" indicating sources containing bad pixels and finally class=-9 related to

saturation (for more details on all of the above, see Saito et al. 2012).

Quality control (QC) grades are also given by the European Southern Observatory (ESO) according to requirements provided by the observer. The constraints for VVV K_s variability data are: seeing <2 arcsec, sky transparency defined as "thin cirrus" or better. The "master epoch" of multi-filter data taken for each tile in a contemporaneous JHK_s observing block and a separate ZY observing block have more stringent constraints: seeing <1.0, 1.0, 0.9, 0.9, 0.8 in Z, Y, J, H, K_s respectively and sky transparency of "clear" or better. According to whether observations fulfil the constraints established by the observer, these are classified as fully satisfied (QC A), almost satisfied, where for example some of the parameters are outside the specified constraints by < 10% (QC B) and finally not satisfied (QC C).

2.1 Selection method

In order to search for variable stars we used the multi-epoch database of VVV comprising the observations of disc tiles with $|b| \leqslant 1^\circ$ taken between 2010 and 2012. We added the 2013, 2014 and 2015[1] data later to assist our analysis but they were not used in the selection. The catalogues were requested and downloaded from the CASU. We used catalogues of observations with QC grades A, B or C. Catalogues with QC grades C are still considered in order to increase the number of epochs. Some of them were still useful for our purposes. However, a small number of catalogues still presented some issues (e.g. zero point errors, bad seeing) making them useless, and as such were eliminated from the analysis. The number of catalogues in each tile varied from 14 to 23 epochs, with a median of 17 epochs per tile. When the 2013-15 data were added, the number of epochs available for the light curves rose to between 44 and 59. K_s photometry is derived from *apermag3* aperture fluxes ($2''$ diameter aperture).

For each tile, the individual catalogues are merged into a single master catalogue. The first catalogue to be used as a reference was selected as the catalogue with the highest number of sources on it. In every case this corresponded to the catalogue from the deep K_s observation (80 s on source), which was taken contemporaneously with the J and H band data (in 2010). For all other epochs the time on source was 16 s.

Figure 1 shows the typical scatter shown by stars at different magnitudes across the analysed range. In here we can see considerable scatter at bright magnitudes, due to effects of saturation, and the faint end of the distribution, which is dominated by photon noise. High amplitude variable star candidates are selected from the master catalogue from stars which fulfilled the following criteria in the 2010-12 data:

[1] We included a single K_s datapoint from 2015 observations, corresponding to the epoch with contemporaneous JHK_s photometry. Note that our analysis of the light curve morphologies and periods is based on the 2010-2014 data only (Sect. 4.1). The 2015 data became available only after that was complete but they were used in the colour variability analysis (see Sect. 4.2).

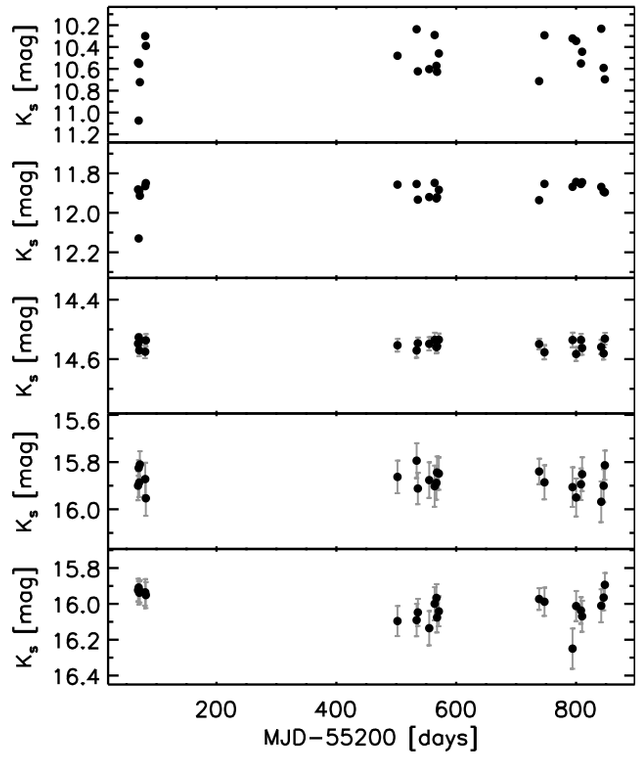

Figure 1. 2010-2012 light curves of "non-variable" VVV objects (i.e. not classified as high-amplitude variables in our analysis). These are presented to show the typical scatter in magnitude across the analysed magnitude range. We note that photometry for the brightest star is the standard CASU pipeline photometry.

(i) Detection with a stellar morphological classification (class= −1) in every available epoch.

(ii) Ellipticity with ell< 0.3 in every epoch.

(iii) The absolute difference (ΔK_s) between the brightest ($K_{s,max}$) and faintest point ($K_{s,min}$) in the light curve of the source to be larger than 1 magnitude (similar to the analysis in Contreras Peña et al. 2014).

The requirement for a detection at every available epoch in the 2010-12 interval was designed to exclude most transient objects such as novae, as well as reducing the number of false positives. This was the initial classification scheme. However, we observed that for each tile we were selecting a large number of sources as variable star candidates. Figure 2 shows the average K_s magnitude vs ΔK_s for variable stars in one of the VVV tiles. The figure shows that the majority of stars selected in the original classification scheme are located at the bright and faint ends of the distribution. The latter arise due to unreliable photometry at this faintest part. The VISTA detectors also become increasingly non-linear when reaching the saturation level. This non-linearity is corrected for in the creation of the catalogues, but differences between the magnitudes of the same object can still be observed, even for objects classified as stellar sources (Saito et al. 2012). Figure 10 in Saito et al. (2012) shows that when comparing the K_s magnitudes of stellar sources found in overlapping regions of adjacent disc tiles, stars found at the brighter end show an increasing difference in magnitude (an effect also observed in Cioni et al. 2011; Gonzalez et al. 2011). This effect would explain the large differences observed at

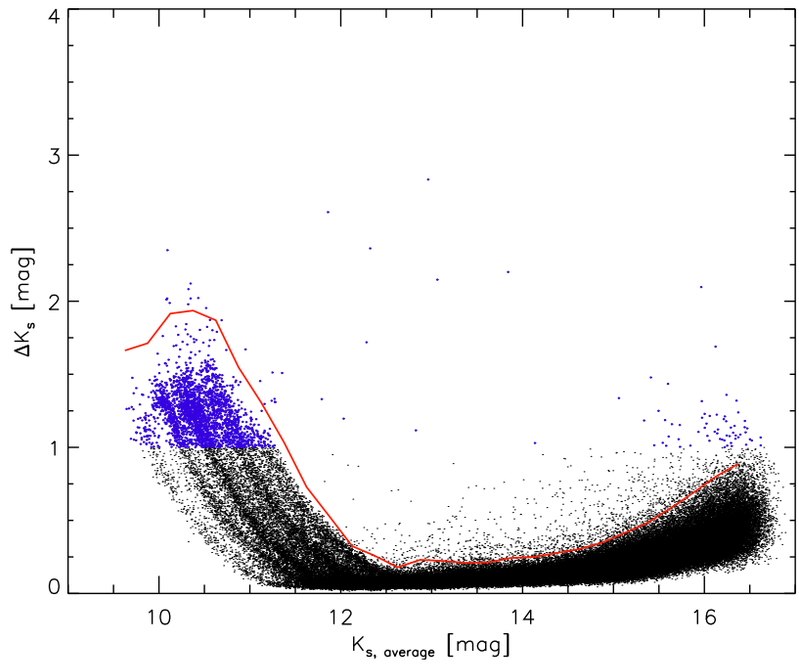

Figure 2. K_s vs ΔK_s for one of the VVV tiles studied in this work, showing stars with class= -1 and ellipticity < 0.3 in every epoch (black circles). Variable star candidates which fulfil the condition $\Delta K_s > 1$ magnitude are shown as blue circles. The red solid line marks the additional 3σ cut applied to the objects as explained in the text. Stars above this line are selected for subsequent visual inspection.

the brighter end of Fig. 2. This part of the distribution also shows marked "finger-like" sequences. Each of the sequences can be explained by the fact that the VISTA detectors have different saturation levels. In order to minimize these effects we applied an additional cut.

(iv) We separated the average K_s distribution of Fig. 2 into bins of 0.5 magnitudes and derived the mean and standard deviation, σ, on ΔK_s for each bin. In order to select an object as a candidate variable star we required its ΔK_s to be 3σ above the mean ΔK_s at the corresponding magnitude level. This 3σ line is shown in red in Fig. 2 where we can see that it is able to account for the non-linearity effects at the bright end of the distribution.

This additional constraint reduced the number of variable star candidates by a large factor. The initial requirements yield 158478 stars; the additional cut reduced this to 5085 stars. After the catalogue-based selection, we constructed $1' \times 1'$ cut-out images around each candidate for every available epoch. Variable stars were confirmed as real through visual inspection of the individual images (an example is shown in Fig. 3). In some cases we performed manual photometry with IRAF in order to confirm the variability of the star. The most common causes for the appearance of false positives were, bad pixels in the images, saturation of bright sources, diffraction spikes and stars that were found on the edge of tiles. In the case of saturation, if this effect was present it was quite evident in individual images. In most cases saturation was observed in every single epoch, thus the variability observed in the light curve plots was not real, and the source was marked as such.

This selection method yielded a total of 840 real variable stars. However, 25 of them are found twice as they are covered by adjacent tiles in VVV. The final list of VVV high-amplitude infrared variables consists of 816 stars. This includes one variable star, VVVv815, that showed large variability in 2010 but did not meet all the selection criteria (see below). The average magnitude for objects in the selected sample was found in the range $10.3 < K_s < 16.9$ mag.

Our requirement for a high quality detection at every epoch between 2010 and 2012 (see items (i) and (ii)) is bound to cause us to miss some real variables, very likely including some of the faintest or highest amplitude variables if they dropped below $K_s \sim 16$ during that time, or if they became saturated and were therefore no longer classified as point sources. A significant fraction of all VVV sources are blended with adjacent stars and they can fail to pass our cuts on the morphological class and ellipticity at one or more epochs in consequence. The same can be true for YSOs with extended reflection nebulae or strong H_2 jets, as they might have slightly extended morphologies and fail to be classified as point sources (see e.g. Chen et al. 2009; Ward et al. 2016). However, sources that pass these quality cuts are likely to be unblended and therefore to have reliable photometry (photometry from the VISTA pipeline is not always reliable for faint stars in crowded fields, see e.g. Saito et al. 2012). In order to check the reliability of the pipeline photometry, especially for faint sources with $K_s = 15 - 16$ magnitudes, we obtained point spread function (PSF) fitting photometry of all stars in tile d069 with DoPHOT (Schechter et al. 1993). The results confirmed that the variables found by our selection have reliable pipeline photometry. This is illustrated in Fig. 4 for variable star VVVv316, where the comparison of DoPHOT and VISTA pipeline photometry shows close agreement.

We investigated the incompleteness of our selection by examining two widely separated VVV disc tiles (d064 and d083), in which we removed our class and ellipticity cuts

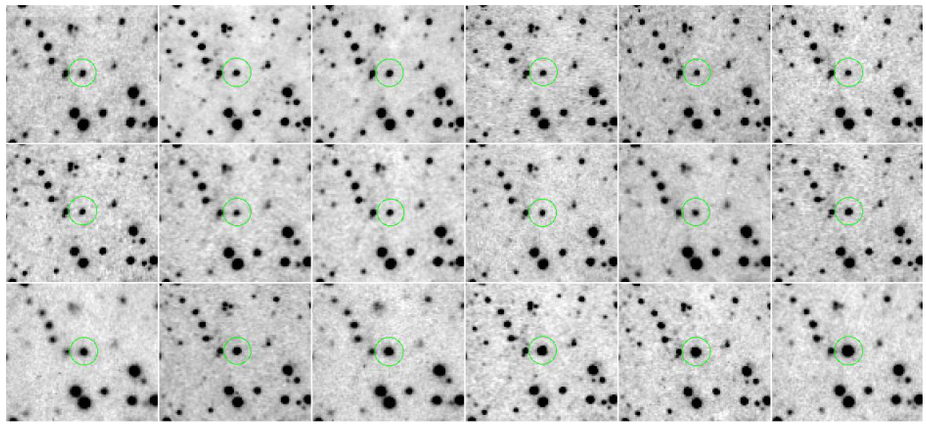

Figure 3. Example of the images used to visually inspect variable star candidates. In this case we show the images, taken between 2010 and 2012, of variable star VVVv322. Each image has a size of $1' \times 1'$. The star gets brighter towards the end of the sequence.

and required a minimum of only one detection in each year from 2010 to 2012 (with a stellar profile classification). This continues to select against transients and perhaps the most extreme variable YSOs but it allows us to assess incompleteness due to blending, which can cause sources to be absent or to have different profile classifications at different epochs. We found that this more relaxed selection added over 400 additional candidates in the two tiles down to (mean) $K_{\rm s}$=15.5, an increase of more than a factor of 10. Following visual inspection (see below), we found that the number of real high amplitude variables was increased by a factor of ∼2, up to a limit of $K_{\rm s}$= 15.5. At fainter mean magnitudes the completeness of our selection with criteria (i) to (iv) falls more steeply because most high amplitude variables will not satisfy the quality cuts at every epoch as the sensitivity limit is approached.

A case of this selection effect is found in a variable star VVVv815 mentioned above. It showed a large variation ($\Delta K_{\rm s} > 1$ magnitude) in the analysis of an early release of 2010 data. However, the star does not show up as a variable star candidate in the analysis described above. Inspection of the master catalogue for the respective tile shows that the star has a classification different from stellar in 3 out of 18 epochs available for tile d090 in the 2010-2012 period. This star is included in our final list of VVV high-amplitude variables because it is also part of the sample that has follow up spectroscopic observations.

The number of stars in the analysed VVV area that fulfil criteria (i) and (ii) above is 12 789 000 stars. Considering the number of real variable stars we see that high-amplitude infrared variability was observed in approximately 1 out of 15000 stars in the Galactic mid-plane at $295 < l < 350°$.

2.2 Issues with saturation

The aforementioned problems of saturation still affect a small number of stars in our sample. This effect can become important when individual epochs of stars in our sample are brighter than $K_{\rm s} = 12$ magnitudes. Saturation will reduce the flux at the inner core of the star, thus the magnitude of the star derived by using smaller diameter aperture than the default $2''$ aperture, will be fainter than the magnitude obtained from the default aperture.

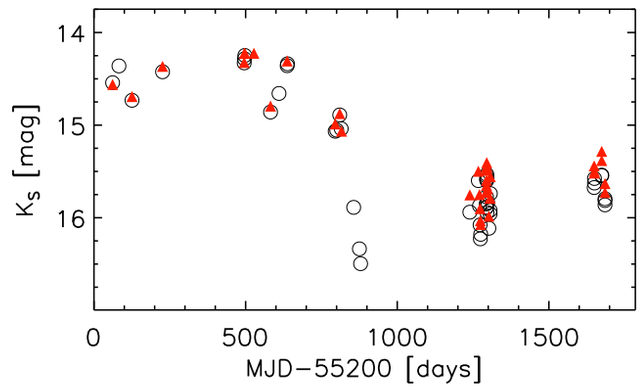

Figure 4. PSF (red triangles) vs aperture photometry (open circles) of star VVVv316. PSF photometry is shown only for data points classified as "good" or "good but faint" by DoPHOT.

In order to check whether the star is saturated we first obtain the magnitudes from aperture photometry using the measure fluxed from five different diameters for the apertures. These diameters are $1''$ (Apermag1), $1.41''$ (Apermag2), $2''$ (Apermag3), $2.82''$ (Apermag4) and $4''$ (Apermag5). We find that saturated stars show relatively large differences between the magnitudes from the first three apertures, and we set a threshold for saturation as stars having both Apermag1-Apermag3>0.05 mag and Apermag2-Apermag3>0.02 mag. Thus any individual epoch of a star with Apermag3< 12 mag (in the $K_{\rm s}$ passband) and having these differences is flagged as saturated.

In order to correct for saturation, we follow Irwin (2009) and defined a ring outside the saturated core, to obtain a new flux estimate. We then determine an aperture correction for the ring from a set of bright, unsaturated stars found within $5'$ of our object of interest. In our analysis we derived new fluxes using the ring defined by Apermag2 and Apermag4. Comparison with 2MASS K_s photometry indicates that this choice of apertures extends the dynamic range by 2.5 magnitudes, relative to the pipeline photometry. We caution that comparison with 2MASS K_s photometry indicates that while this approach provides correct magnitudes, the uncertainties are large, typically 0.2 magnitudes.

ID	MJD-55200 (days)	K_s (mag)	$K_{s,err}$ (mag)
VVVv1	69.1171875	14.400	0.016
VVVv1	70.1484375	14.436	0.010
VVVv1	71.1445312	14.381	0.016
VVVv1	72.1406250	14.225	0.014
VVVv1	81.0781250	14.606	0.022
VVVv1	82.1015625	14.680	0.024
VVVv1	501.9882812	14.297	0.017
VVVv1	533.9648438	15.271	0.044
VVVv1	535.9726562	15.133	0.033
VVVv1	554.9726562	14.853	0.029
VVVv1	564.0117188	14.223	0.019

Table 1. K_s photometry of the 816 high-amplitude variable stars from VVV. The full version of the table is available online.

In Table 1 we present the 2010-2015 photometry for the 816 high-amplitude variable stars from VVV.

3 HIGH AMPLITUDE INFRARED VARIABLES FROM VVV

3.1 General characteristics

Object ID	VVV Designation	α (J2000)	δ (J2000)	l (degrees)	b (degrees)	Z (mag)	Z_{err} (mag)	Y (mag)	Y_{err} (mag)	J (mag)	J_{err} (mag)	H (mag)	H_{err} (mag)	$K_{\rm s}$ (mag)	$K_{\rm s,err}$ (mag)	$\Delta K_{\rm s}$ (mag)	α_{class}	SFR	Class[a]	Period [b] (days)
VVVv1	VVV J114135.16-622055.51	11:41:35.16	-62:20:55.51	294.92603	-0.56770	–	–	–	–	17.99	0.06	15.95	0.02	14.44	0.01	1.34	-0.29	y	STV	72
VVVv2	VVV J114412.94-623449.09	11:44:12.94	-62:34:49.09	295.28005	-0.71146	–	–	–	–	–	–	18.78	0.23	15.71	0.03	2.52	1.22	y	STV	–
VVVv3	VVV J115113.03-623729.29	11:51:13.03	-62:37:29.29	296.07199	-0.55784	13.17	0.01	12.93	0.01	12.90	0.01	12.70	0.01	12.24	0.01	2.21	–	n	Known	–
VVVv4	VVV J115808.69-630708.60	11:58:08.69	-63:07:08.60	296.95057	-0.86785	–	–	–	–	18.23	0.08	16.62	0.04	15.32	0.02	1.10	-0.24	y	STV	–
VVVv5	VVV J115959.68-622613.20	11:59:59.68	-62:26:13.20	297.02026	-0.15716	17.69	0.02	16.62	0.01	15.87	0.01	15.25	0.01	13.53	0.01	1.30	–	n	LPV	–
VVVv6	VVV J115937.81-631109.77	11:59:37.81	-63:11:09.77	297.12836	-0.89953	19.02	0.05	18.08	0.04	16.80	0.02	15.95	0.02	15.50	0.02	1.02	–	n	EB	1.64
VVVv7	VVV J120202.67-623615.60	12:02:02.67	-62:36:15.60	297.28472	-0.27538	–	–	–	–	–	–	–	–	17.22	0.12	1.60	2.39	y	Eruptive	–
VVVv8	VVV J120059.11-631636.18	12:00:59.11	-63:16:36.18	297.29582	-0.95838	–	–	–	–	–	–	–	–	16.86	0.09	1.38	0.64	y	Eruptive	–
VVVv9	VVV J120217.23-623647.83	12:02:17.23	-62:36:47.83	297.31381	-0.27888	–	–	–	–	18.29	0.08	16.33	0.03	14.64	0.01	2.78	-0.39	y	Dipper	–
VVVv10	VVV J120250.85-622437.62	12:02:50.85	-62:24:37.62	297.33912	-0.06749	18.57	0.04	18.23	0.05	16.97	0.03	16.35	0.03	16.07	0.04	1.19	–	n	STV	–
VVVv11	VVV J120436.62-625704.60	12:04:36.62	-62:57:04.60	297.63741	-0.56188	20.20	0.19	19.01	0.13	17.87	0.07	16.79	0.05	16.08	0.08	1.10	–	n	STV	–
VVVv12	VVV J121033.19-630755.71	12:10:33.19	-63:07:55.71	298.33185	-0.62611	–	–	–	–	–	–	16.30	0.03	15.04	0.03	1.74	0.28	y	Fader	–
VVVv13	VVV J121216.83-624838.32	12:12:16.83	-62:48:38.32	298.47603	-0.27814	–	–	–	–	–	–	–	–	16.72	0.14	1.40	1.39	y	STV	–
VVVv14	VVV J121218.13-624904.48	12:12:18.13	-62:49:04.48	298.47958	-0.28495	19.48	0.10	18.88	0.12	17.84	0.06	16.74	0.05	15.56	0.05	1.29	0.88	y	LPV-YSO	124
VVVv15	VVV J121226.09-624416.97	12:12:26.09	-62:44:16.97	298.48252	-0.20371	19.00	0.07	17.72	0.04	16.57	0.02	15.60	0.02	15.04	0.03	1.09	–	y	EB	2.27
VVVv16	VVV J121329.76-624107.74	12:13:29.76	-62:41:07.74	298.59498	-0.13364	18.01	0.03	17.13	0.02	16.06	0.01	14.72	0.01	13.66	0.01	1.29	0.92	y	Eruptive	–
VVVv17	VVV J121352.08-625549.90	12:13:52.08	-62:55:49.90	298.67278	-0.36986	–	–	–	–	–	–	17.79	0.12	16.41	0.10	1.22	0.44	y	STV	–
VVVv18	VVV J121950.31-632142.24	12:19:50.31	-63:21:42.24	299.39868	-0.70695	17.82	0.02	17.29	0.02	16.20	0.01	15.52	0.01	15.32	0.02	1.04	–	n	STV	–
VVVv19	VVV J122255.30-632352.56	12:22:55.30	-63:23:52.56	299.74594	-0.70270	19.56	0.08	18.67	0.06	17.55	0.04	16.40	0.03	15.61	0.03	1.82	–	n	EB	16.88
VVVv20	VVV J122827.97-625713.97	12:28:27.97	-62:57:13.97	300.32402	-0.19849	–	–	–	–	17.38	0.04	14.10	0.01	11.70	0.01	1.71	0.60	y	Eruptive	–
VVVv21	VVV J122902.24-625234.10	12:29:02.24	-62:52:34.10	300.38193	-0.11533	–	–	–	–	–	–	17.12	0.05	15.80	0.03	1.79	0.86	y	LPV-YSO	603
VVVv22	VVV J123105.60-624457.34	12:31:05.60	-62:44:57.34	300.60547	0.03057	–	–	–	–	18.81	0.14	16.94	0.05	15.55	0.03	1.73	-0.34	y	STV	–
VVVv23	VVV J123128.53-624433.10	12:31:28.53	-62:44:33.10	300.64855	0.04070	19.44	0.07	18.37	0.05	17.14	0.03	15.57	0.02	14.40	0.01	1.51	-0.20	y	Fader	–
VVVv24	VVV J123235.68-634319.61	12:32:35.68	-63:43:19.61	300.84794	-0.92662	17.17	0.01	16.13	0.01	14.05	0.01	12.95	0.01	12.23	0.01	1.20	–	n	LPV	430
VVVv25	VVV J123514.37-624715.63	12:35:14.37	-62:47:15.63	301.08129	0.02587	–	–	–	–	–	–	16.01	0.02	12.34	0.01	1.68	0.22	y	Eruptive	–
VVVv26	VVV J123845.66-631136.03	12:38:45.66	-63:11:36.03	301.50320	-0.35674	–	–	–	–	19.67	0.29	16.70	0.04	14.71	0.01	2.45	1.07	y	Eruptive	–
VVVv27	VVV J123848.33-633939.15	12:38:48.33	-63:39:39.15	301.53114	-0.82347	–	–	–	–	–	–	–	–	12.04	0.01	2.73	–	n	LPV	1329
VVVv28	VVV J123911.54-630524.76	12:39:11.54	-63:05:24.76	301.54688	-0.25138	–	–	–	–	–	–	18.91	0.32	16.78	0.09	1.39	0.54	y	STV	3.68
VVVv29	VVV J123931.48-630720.38	12:39:31.48	-63:07:20.38	301.58593	-0.28170	–	–	–	–	–	–	–	–	16.94	0.10	2.13	1.32	y	Eruptive	–
VVVv30	VVV J124140.56-635033.57	12:41:40.56	-63:50:33.57	301.85616	-0.99128	17.92	0.02	17.22	0.02	16.40	0.02	15.66	0.02	15.23	0.02	1.22	–	n	EB	1.91
VVVv31	VVV J124140.15-635918.05	12:41:40.15	-63:59:18.05	301.86093	-1.13689	13.91	0.01	13.27	0.01	12.46	0.01	12.08	0.01	11.69	0.01	1.15	–	n	LPV	760
VVVv32	VVV J124357.15-625445.09	12:43:57.15	-62:54:45.09	302.07991	-0.05314	19.58	0.07	18.08	0.04	16.07	0.01	14.07	0.01	12.45	0.01	2.49	0.33	y	LPV-YSO	–
VVVv33	VVV J124425.05-631355.76	12:44:25.05	-63:13:55.76	302.14153	-0.37116	–	–	–	–	–	–	18.10	0.16	16.43	0.07	1.37	–	n	STV	–
VVVv34	VVV J125029.87-625124.93	12:50:29.87	-62:51:24.93	302.82470	0.01465	19.22	0.05	18.32	0.05	17.86	0.06	16.70	0.04	15.71	0.03	1.30	-0.34	y	STV	–
VVVv35	VVV J125206.52-635711.52	12:52:06.52	-63:57:11.52	303.00557	-1.08152	17.62	0.01	16.85	0.01	17.13	0.03	16.21	0.03	15.97	0.04	1.24	–	n	EB	1.12
VVVv36	VVV J125917.72-633008.44	12:59:17.72	-63:30:08.44	303.80825	-0.64394	14.38	0.01	13.84	0.01	13.27	0.01	12.56	0.01	11.81	0.01	1.03	-0.11	y	Eruptive	–
VVVv37	VVV J130243.05-631130.00	13:02:43.05	-63:11:30.00	304.20331	-0.34774	18.80	0.03	17.75	0.03	16.74	0.02	15.89	0.02	15.38	0.03	1.34	–	n	STV	–
VVVv38	VVV J130311.38-631439.09	13:03:11.38	-63:14:39.09	304.25411	-0.40259	–	–	–	–	–	–	17.79	0.13	16.32	0.07	1.41	1.20	y	STV	48.96
VVVv39	VVV J130440.98-635313.45	13:04:40.98	-63:53:13.45	304.38893	-1.05277	18.67	0.03	17.89	0.03	17.57	0.05	16.38	0.04	15.49	0.03	1.51	–	n	STV	–
VVVv40	VVV J130600.43-630144.40	13:06:00.43	-63:01:44.40	304.58298	-0.20394	20.71	0.20	19.49	0.14	16.52	0.02	15.42	0.02	14.69	0.01	1.24	–	n	EB	10.29

a. LPV:long-period variable; LPV-Mira:long-period variable found in SFR but with Mira-like characteristics; LPV-YSO:long-period variable found in SFR with YSO-like characteristics. STV:short-term variable; EB:eclipsing binary

b. We note that in some objects classified as long-period variables (LPV, LPV-MIRA and LPV-YSO), the light curve shows a clear periodic behaviour over long timescales ($>$ 100 days). However, we are unable to measure an exact period. In those cases this column is left blank.

Table 2. Parameters of the high-amplitude variables from VVV. For the description of the columns see Sect. 3.1. Here we show the first 40 sources in the list. The complete list is available online.

The selection method of Sect.2.1 yields 816 high amplitude (ΔK_s >1 mag) infrared variables. In order to study the properties of these stars, we searched for additional information in available public databases. This search can be summarized as follows:

• **SIMBAD** We query the SIMBAD database (Wenger et al. 2000) for astronomical objects within a radius of $5'$ centred on the VVV object.
• **Vizier** Additional information was provided with the use of the Vizier database (Ochsenbein et al. 2000). In here we queried whether the VVV object was found within $2''$ of objects found in astronomical catalogues that were not available in SIMBAD.
• **The NASA/IPAC Infrared Science Archive (IRSA)** In here we queried for additional information in several near- and mid-infrared public surveys, which include 2MASS (Skrutskie et al. 2006), DENIS (Epchtein et al. 1994), *Spitzer*/GLIMPSE surveys (see e.g., Benjamin et al. 2003), WISE (Wright et al. 2010), Akari (Murakami et al. 2007) and MSX6C (Price et al. 2001). The search was done automatically using the IDL scripts provided at the IRSA website. The catalogues were queried for objects found within a $10''$ radius of the VVV object. In most cases, several objects are found at these distances, then we only selected the nearest object to our star. In order to confirm whether these detections correspond to our variable star, $1'\times1'$ VVV images around the star were visually inspected.

In addition, we used the WISE image service within IRSA to inspect multi-colour images of the areas around our variable stars, in order to establish a possible association of the the VVV object with a SFR.

The general properties of the sample can be found in Table 2. Column 1 presents the original designation given to the sources. Column 2 corresponds to the full VVV designation for the source. Coordinates for the objects are given in Columns 3 and 4, with columns 5 and 6 presenting the Galactic coordinates of the sources. In columns 7, 8, 9, 10 and 11 we present the nearly contemporaneous Z, Y, J, H, K_s photometry from VVV. Column 12 gives ΔK_s, the absolute value of the peak-to-trough difference from the 2010-2014 light curves from VVV. Column 13 presents α_{class}, the 2 to 23 μm spectral index parameter that relates to the evolutionary class of sources that appear to be associated with SFRs (the method and data used to estimate this parameter is explained in Sect. 4.3). In column 14 we present whether the object is likely associated with SFRs or not, whilst column 15 presents the classification of the object from its light curve. The latter is discussed throughout the text. Finally, in column 16 we present the approximate period for variable stars where we are able to measure this parameter.

Most of the variable stars are unknown from searches in SIMBAD and Vizier (∼ 98 per cent). Among the known variables there are 2 novae, Nova Cen 2005 and Nova Cen 2008 (Hughes et al. 2010; Saito et al. 2013), 2 eclipsing binaries (EBs), EROS2-GSA J132758-631449 and PT Cen (Derue et al. 2002; Budding et al. 2004), 1 high-mass X-ray binary, BR Cir (see e.g. Tudose et al. 2008) and 9 OH/IR stars. Among the objects not previously classified as variable stars, 159 are found in the Spitzer/GLIMPSE catalogue of intrinsically red sources from Robitaille et al. (2008), with the majority being classified as likely YSOs from their mid-IR colours and brightness.

3.2 YSO population

At this point, the reader should note that most of the variables are listed as spatially associated with SFRs (∼65%, falling to ∼54% after allowing for chance projection by non-YSOs, see Sect. 3.3, 3.4 and 4) and these stars have spectral indices that indicate a class I or flat spectrum evolutionary status, therefore they are likely in an early evolutionary stage. They are usually sufficiently red to be undetected ($i > 21$ mag) in sensitive panoramic optical surveys such as VPHAS+ (Drew et al. 2014) unlike most of the known FUor and EXors. The spectral indices of the YSOs are discussed later in Sect.4.3 following classification of the light curves and an attempt to decontaminate chance projections of other variables in SFRs.

3.3 Association with SFRs

Figure 5 shows the distribution for the 816 VVV variables across the Galactic midplane. It can be seen that our objects appear to be highly clustered, with their distribution following that of the SFRs from the Avedisova et al.(2002) catalogue (red diamonds in the bottom plot of Fig. 5). To study the apparent clustering, we derive the two-point angular correlation function, $w(\theta)$ and the nearest neighbour distribution of the sample of high amplitude variables. To derive $w(\theta)$, we follow Bate et al. (1998) and first estimate the mean surface density of companions (MSDC). For each star, we compute the angular separation, θ, to all other stars, and bin the separation into annuli of separation θ to $\theta + \delta\theta$. The MSDC results from dividing the number of pairs found, N_p, at a given separation by the area of the annulus, and dividing by the total number of stars, N_*, or

$$MSDC = \frac{N_P}{2\pi\theta\delta\theta N_*}$$

The latter relates to $w(\theta)$ as

$$w(\theta) = MSDC \times \frac{A}{N_*} - 1$$

where A is the area covered by the survey (Bate et al. 1998, and references therein). This correlation function is valid as long as the separations θ are smaller than the angular length of the sample. We show the two-point correlation function in Fig. 6. We can see that we do not find any pairs for separations $\theta < 20''$, hence $w(\theta) = -1$. For separations between $20''$ and $100''$ $w(\theta)$ is larger than the values expected for random pairings ($w(\theta) = 0$) and it remains somewhat above zero for separations up to a few hundred arcseconds. This nearest neighbour distribution of Fig. 6, also shows an excess of close neighbours at distances $R < 200''$, compared to the expected number from a random (Poisson) distribution. Thus we are confident that we are tracing clustering in the VVV sample, on a spatial scale similar to that of distant Galactic clusters and star formation regions.

As an illustration of how variable stars in VVV are preferentially located in areas of star formation, Fig. 7 shows the

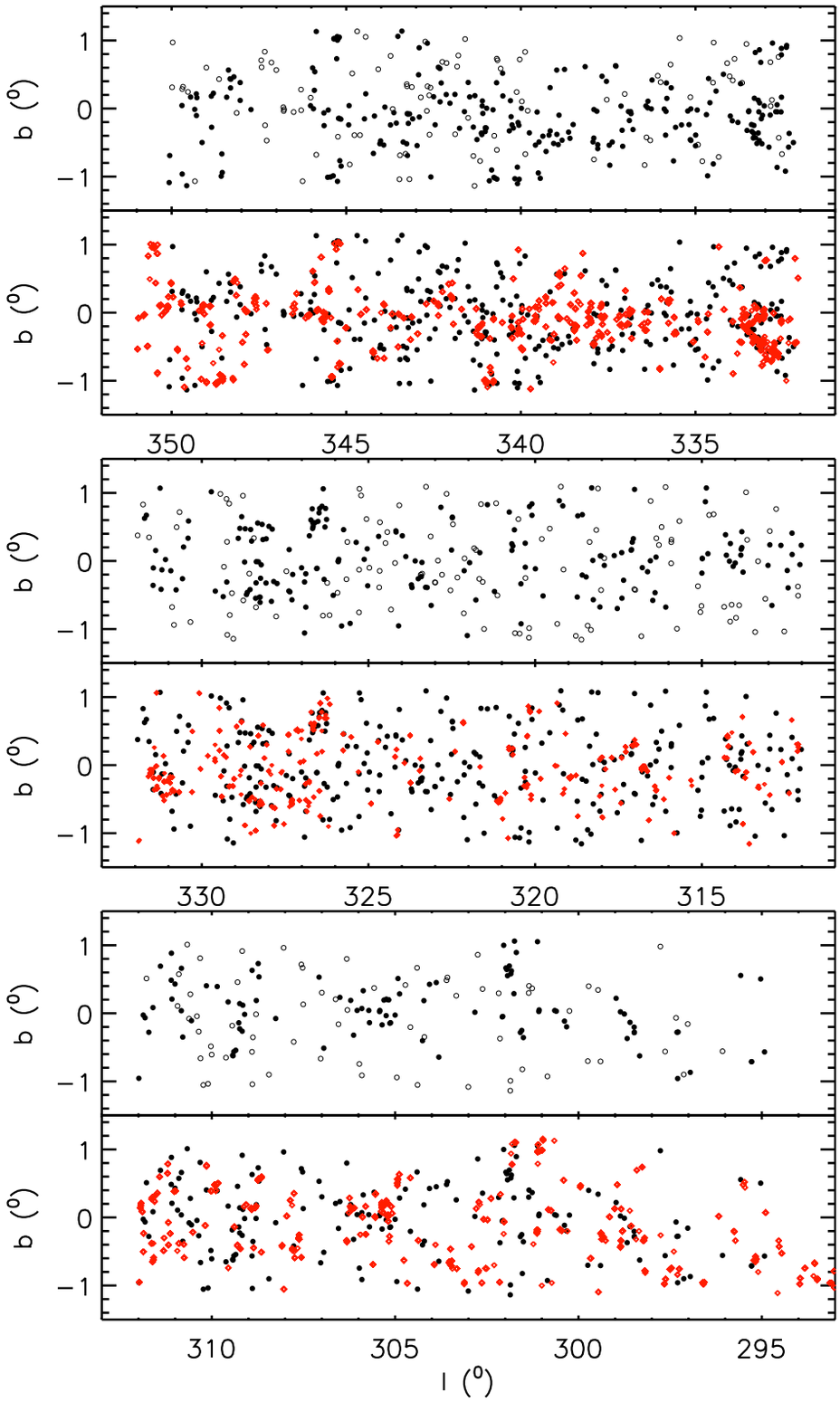

Figure 5. (top) Galactic distribution of high amplitude variable stars selected from VVV. These are divided into objects likely associated with SFRs (black filled circles) and those that are found outside these regions (black open circles) . The bottom graph shows the same distribution for the 816 high amplitude variables (black circles), but this time including the areas of star formation from the Avedisova (2002) catalogue (red diamonds).

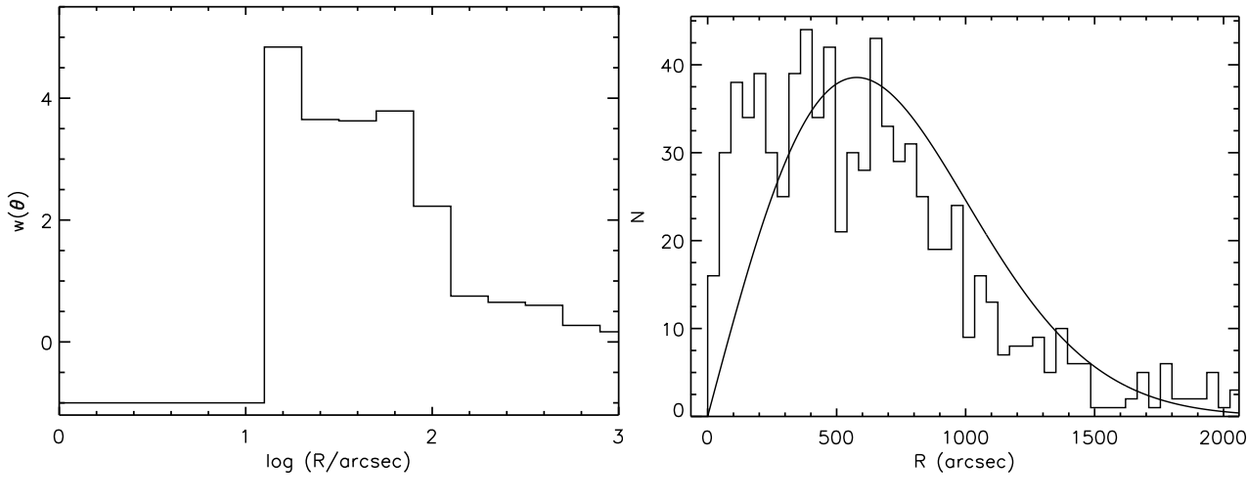

Figure 6. (left) Two-point angular correlation function of the sample of VVV high-amplitude variables. (right) Nearest neighbour distribution for the same sample. The smooth curve represents the expected distribution of a random (Poisson) distribution.

K_s image of the area covered in tile d065. Twenty five highly variable stars are found in this tile, and it is clear that these are not evenly distributed along the area covered in d065, and instead are found clustered around an area of star formation, which is better appreciated in the cut-out image from WISE (Wright et al. 2010).

To establish a likely association with a SFR we used the criteria established in the UGPS search (see Contreras Peña et al. 2014), which were based on entries in the SIMBAD database and the Avedisova catalogue within a 5′ radius of each high amplitude variable. In addition we also check WISE images for evidence of star formation in the area of the object, e.g. evidence of bright extended 12 μm emission near the location of the objects or the finding of several stars with red W1-W2 colours (sources appearing green, yellow or red in WISE colour images) around the VVV object. We find that 530 of our variable stars are spatially associated with SFRs, which represents 65% of the sample, remarkably similar to the observed association in UGPS objects (Contreras Peña et al. 2014).

3.4 Contamination by non-YSOs

In Contreras Peña et al. (2014), we estimated that about 10% of objects are probable chance associations with SFRs. This number is likely to be larger in our current analysis given that: (i) we are sampling mid-plane sightlines across the Galactic disc; (ii) the higher extinction in the Galactic midplane and the brighter saturation limit of VVV than UGPS, allows for a larger number of bright evolved variable stars to show up in our results. To determine the percentage of objects that might be catalogued as likely associated with SFRs by chance, we used the following method:

a) Create a master catalogue of objects in the 76 tiles that were classified as stars in each of the epochs from the 2010-2012 analysis.

b) Select 816 stars randomly from this catalogue and query SIMBAD for objects found in a 5′ radius.

c) Count the number of objects within this radius that were classified in any of the categories that could relate to star formation. This categories included T Tauri and Herbig Ae/Be stars, HII regions, Dark clouds, dense cores, mm and submm sources, FU Orionis stars, among others.

d) Repeat items b through c 40 times.

Figure 8 shows the number of stars found within 5′ of the VVV object and that were classified in the categories shown above, N_{simbad} vs the percentage of VVV objects with this number. It is already apparent that the percentage of chance selection will be higher than that estimated from GPS. However, we note that in order for an object to be flagged as associated with an SFR in Table 2, we needed at least 4 SIMBAD objects to appear within the 5′ radius, thus giving us an estimate that ∼30% of the non-YSO population is spatially associated with an SFR by chance. Inspection of WISE images of 100 randomly selected sources yields a similar fraction of chance associations but most of these were also identified as SFR-associated from the SIMBAD results, so the WISE data only slightly increased the chance association fraction. The Avedisova catalogue added an even smaller fraction of chance associations not indicated by the SIMBAD and WISE data, so the final chance association probability for non-YSOs with star formation regions is 35%.

The number of non-YSOs in the SFR-associated sample is less than 35% because non-YSOs do not dominate the full high amplitude sample but constitute about half of it. We found 286/816 (35%) of variables outside SFRs, i.e. in 65% of the area, suggesting that 54% (35/0.65) of the sample is composed of objects other than YSOs but this neglects the fact that some YSOs will be members of SFRs that are not known in the literature nor visible in WISE images (see Sect. 3.5). Consequently, random addition of 35% of half of the total sample of 816 variables to the SFR-associated sample would be expected to cause only 27% contamination of the SFR-associated subsample by non-YSOs. This conclusion that the SFR-associated population of variables is dominated by bona-fide YSOs is supported by the two colour diagrams (figures 10 and 22) and light curves of the population (see Sect. 3.5 and Sect. 4.1), which differ from those outside SFRs. We note that the results of spectro-

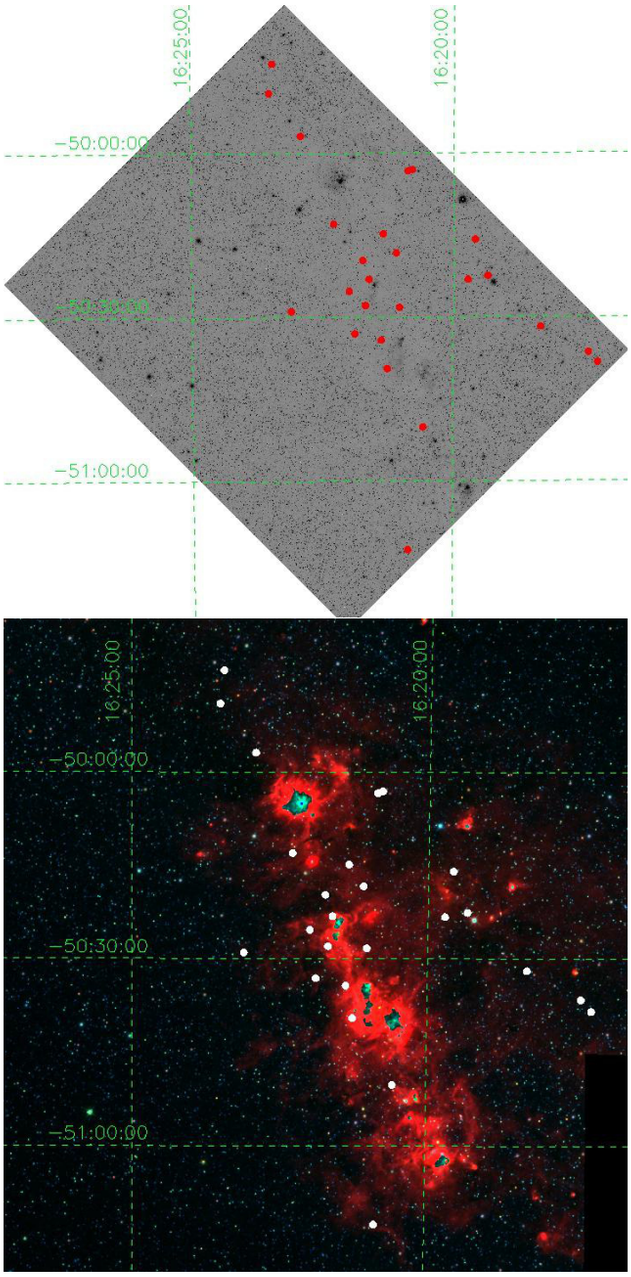

Figure 7. The top graph shows the K_s image of tile d065 along with the high amplitude variable stars found in this region. The clustering of the variable stars is already apparent in this image. The bottom graph shows the WISE false colour image of the same region (blue=3.5 μm, green=4.6 μm, red=12 μm). In here, the fact that variable stars preferentially locate around areas of star formation can be better appreciated.

scopic follow-up of a subsample of VVV objects associated with SFRs (Paper II) show a figure of 25%, a consistent figure despite some additional selection effects in that subsample.

3.5 Properties of variables outside SFRs

To establish the nature of the objects that could be contaminating our sample of likely YSOs, and may also be interesting variable stars, we study the properties of objects found outside areas of star formation. Many of these are listed in SIMBAD as IR sources (from the IRAS and MSX6C catalogues) and associated with OH masers, as well as being catalogued as evolved stars in previous surveys. Visual inspection of their light curves also shows that a large percentage of objects have periodic variability, with $P > 100$ days, whilst the remainder of the sample shows variability over shorter timescales in the order of $P < 20$ days. We use the phase dispersion minimization (PDM, Stellingwerf 1978) algorithm found in the NOAO package in IRAF to search for a period in the light curve of these objects. This allows us to derive the periods or at least the approximate timescale of the variability of objects found outside areas of star formation. To provide a comparison with the PDM results we also used the GATSPY LombScargleFast implementation of the Lomb Scargle algorithm, which benefits from automatic optimisation of the frequency grid so that significant periods are not missed. We found that PDM was generally better for the purpose of this initial investigation. The Lomb Scargle algorithm is designed to detect sinusoidal variations whereas PDM makes no assumptions about the form of the light curve and is therefore much more sensitive to the periods of eclipsing binaries, for example. The Lomb Scargle method did help with the classification of a small number of long period variables (LPVs).

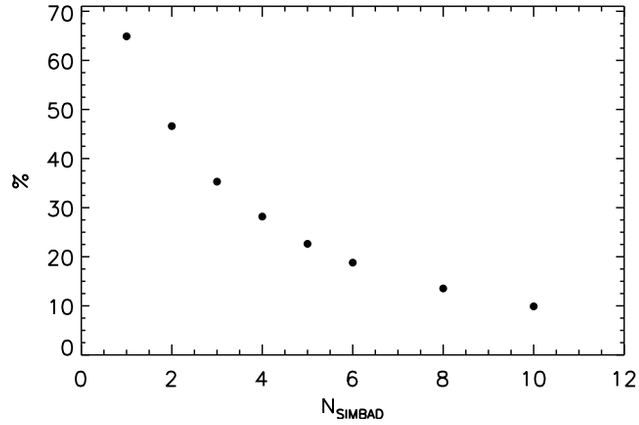

Figure 8. Percentage of objects flagged as likely associated with SFRs as a function of the number of objects classified in the categories that could relate to star formation found within a 5′ radius query in SIMBAD.

Out of the 286 stars in this subsample, 5 objects correspond to known objects from the literature (novae, EBs and a high mass X-ray binary), 45% of them are LPVs and 17% are EBs where we are able to measure a period. In addition, 30% of the sample is comprised of objects in which variability seems to occur on short timescales. The light curves of many objects in the latter group resemble those of EBs with measured periods, but with only 1 or 2 dips sampled in the dataset. We suspect that most of these could also be EBs but we are not able to establish the periods. Finally, we also find 18 objects (6%) that do not appear to belong to any of the former classes. In Fig. 9 we show two examples of objects belonging to these different subclasses where a period could be derived. The LPV VVVv215 is typical of many of the dusty Mira variables in the dataset that show long term

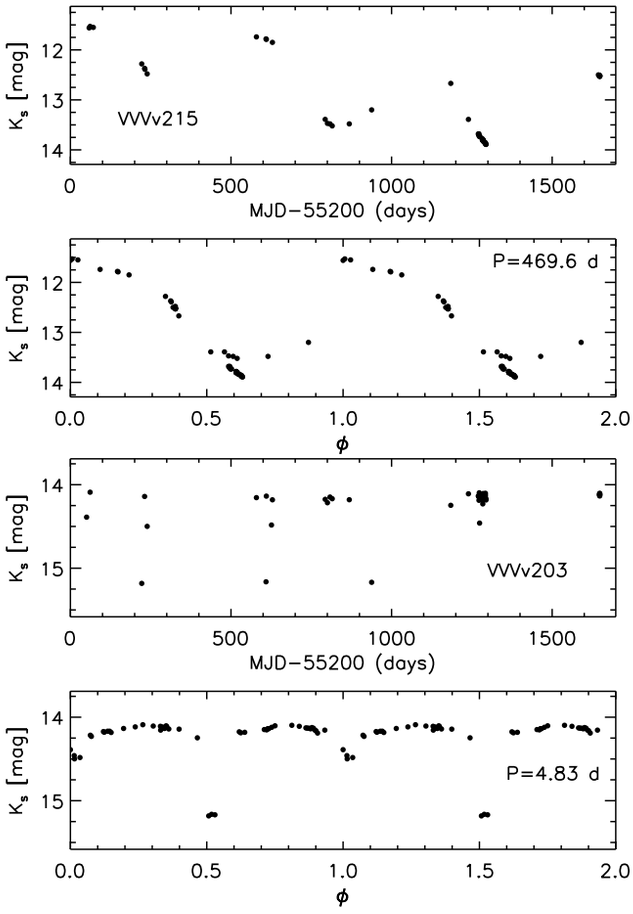

Figure 9. Examples of K_s light curves for objects not associated with SFRs. (top) the long period variable VVVv215. (bottom) the eclipsing binary VVVv203.

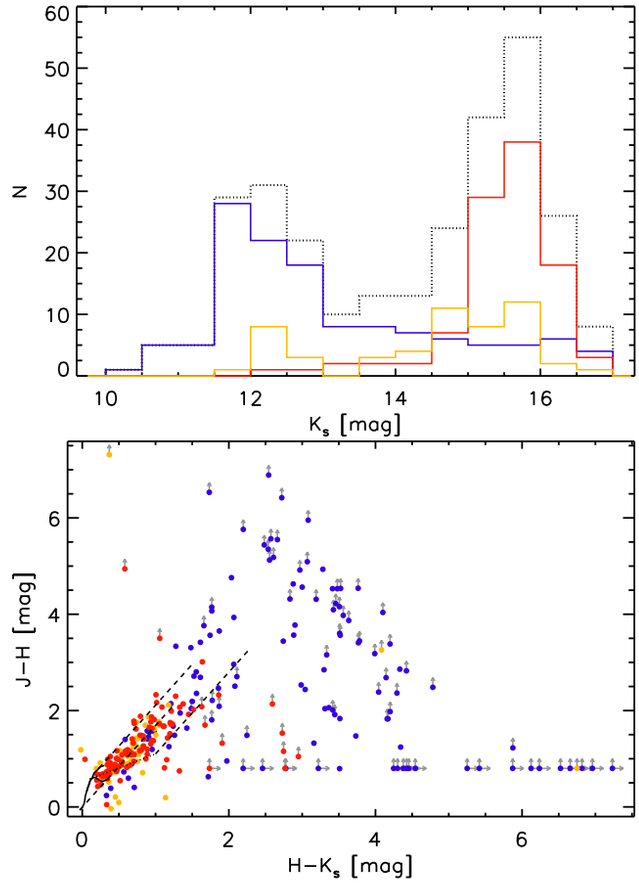

Figure 10. (top) Overall K_s distribution (from 2010 data) of objects not associated with SFRs (dotted line), and the same distribution separated for LPVs (solid blue line), EBs and known objects (solid orange line), and other classes of variable stars (solid red line). (bottom) $(J-H)$, $(H-K_s)$ colour-colour diagram for LPVs (blue circles), EBs and known objects (orange circles), and other classes of variable stars (red circles). In the diagram, arrows mark lower limits. The solid curve at the lower left indicates the colours of main sequence stars. The short-dashed line is the CTTS locus of Meyer et al. (1997) and the long-dashed lines are reddening vectors.

trends caused by changes in the extinction of the circumstellar dust shell. These trends are superimposed on the pulsational, approximately sinusoidal variations, with the result that the K_s magnitude as a given point in the phase curve can differ between cycles.

The objects belonging to different classes show very different properties. Figure 10 shows the K_s distribution for these objects, where it can be seen that the LPVs dominate the bright end of the distribution with a peak at $K_s \sim 11.8$ magnitudes, and showing a sharp drop at brighter magnitudes, probably due to the effects of saturation. EBs and other classes are usually found at fainter magnitudes. The near-infrared colours of the two samples (bottom plot of Fig. 10) show that LPVs tend to be highly reddened objects or have larger $(H-K_s)$ colours than EBs and other classes, which usually have the colours of lightly reddened main sequence and giant stars. We will see in Sect. 4 that this low reddening and lack of K band excess (in most cases) distinguishes the EBs and other shorter period variables from the sample spatially associated with SFRs, so contamination of the SFR sample by these shorter-period variables should not be very significant.

The colour-colour diagram of Fig. 10 also supports the idea that this sample might contain some bona fide YSOs that are not revealed by our searches of SIMBAD and the WISE images, as mentioned in our discussion of contamination. In the figure we observe objects (red circles) that show $(H-K_s)$ colour excesses and are neither known variables nor classified as LPVs or EBs. By simply selecting red circles located to the right of the reddening vector passing through the reddest main sequence stars we estimate that 44 objects have colours consistent with a YSO nature. This would represent 15% of objects outside SFRs and 5% of the full sample of 816 variables. A more detailed study would of course be needed to confirm their nature as YSOs. We also note that the lower left part of the classical T Tauri stars (CTTS) locus plotted in the figure extends into the region occupied by lightly reddened main sequence stars, so in principle some of these individual red circles can potentially be YSOs.

The bright LPVs are very likely pulsating Asymptotic Giant Branch (AGB) stars. These type of stars are usually divided into Mira variables, which are characterized by displaying variability of $\Delta K > 0.4$ magnitudes and with pe-

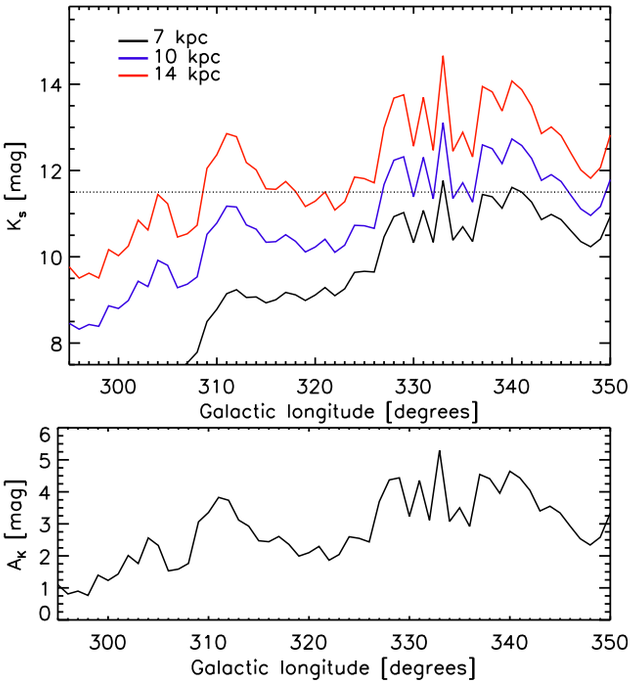

Figure 11. (top) Apparent $K_{\rm s}$ magnitude, derived as explained in the text, for a Mira variable located at the Galactic disc edge (solid red line). The same value is shown for a Mira located at lower Galactic radii $R_{GC} = 10$ kpc (blue line) and $R_{GC} = 7$ kpc (black line). The magnitude where the number of detections for LPVs drops ($K_{\rm s} = 11.5$ magnitudes) is marked by a dotted line. (bottom) K-band Galactic extinction column as a function of Galactic longitude.

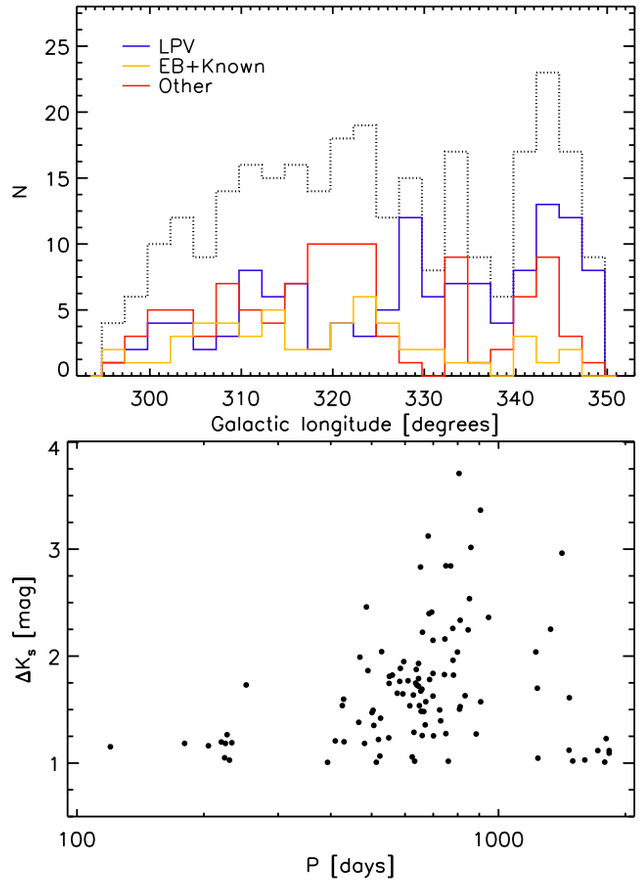

Figure 12. (top) Overall Galactic longitude distribution of objects outside SFRs (black line). We also show the same distribution divided into LPVs (blue line), EBs and known objects (orange line), and other classes of variable stars (red line). (bottom) Period vs $K_{\rm s}$ amplitude for LPVs with a measured period.

riods in the range 100 < P< 400 d, and dust-enshrouded AGB stars, which are heavily obscured in the optical due to the thick circumstellar envelopes (CSE) developed by heavy mass loss ($\sim 10^{-4}$ $M_\odot$ yr^{-1}). The latter group, comprised of carbon-rich and oxygen-rich stars (the latter often referred to as OH/IR stars if they display OH maser emission), show larger amplitudes in the K-band (up to 4 magnitudes) and have periods between 400 < P< 2000 d (for the above, see e.g, Jiménez-Esteban et al. 2006a; Whitelock et al. 2008).

AGB stars are bright objects and should be saturated at the magnitudes covered in VVV. However, due to the large extinctions towards the Galactic mid-plane we are more likely to observe these type of objects in VVV compared to our previous UKIDSS study. We can estimate the apparent magnitude of Mira variables at the different Galactic longitudes covered in VVV, and by assuming that these objects are located at the Galactic disc edge ($R_{GC} = 14$ kpc Minniti et al. 2011) and then considering other Galactocentric radii. At a given longitude, l, we derive A_V as the mean value of the interstellar extinction found at latitudes b between -1° and 1°. The interstellar extinction is taken from the Schlegel et al. (1998) reddening maps, and corrected following Schlafly & Finkbeiner (2011), i.e. $E(B-V) = 0.86E(B-V)_{Schlegel}$. We then assume that extinction increases linearly with distance, at a rate A_V/D_{edge} (mag kpc^{-1}), with D_{edge} the distance to the Galactic disc edge at the corresponding l. We finally take the absolute magnitude as $M_K = -7.25$ (Whitelock et al. 2008).

Figure 11 shows the estimated apparent magnitudes of Mira variables at different l and at varying R_{GC}. In the figure we also show the magnitude, $K_{\rm s} = 11.5$, that marks the drop in the number of the detection of these objects, as observed in the histograms of the $K_{\rm s}$ distribution (Fig. 10). We can see as we move away from the Galactic center, a Mira variable would most likely saturate in VVV, especially at $l < 310^\circ$. This occurs due to the effects of having relatively larger extinctions towards the Galactic center (see bottom plot of Fig.11) and that a star at $R_{GC} = 14$ kpc is located farther away from the observer as l approaches $l = 0^\circ$. We note that Ishihara et al. (2011) finds that most AGB stars are found at $R_{GC} < 10$ kpc so if we place a Mira variable at smaller Galactic radii (R_{GC} =7, 10 kpc), we see that it is less likely for such a star to show up in our sample. However, variable dust-enshrouded AGB stars which undergo heavy mass loss, suffer heavy extinction due to their thick circumstellar envelope, and thus are fainter than Mira variables (AGB stars with optically thick envelopes are found to be $\sim$5 $K_{\rm s}$ magnitudes fainter than objects with optically thin envelopes in the work of Jiménez-Esteban et al. 2006b) and thus less likely to saturate in VVV, even at large distances. Then most AGB stars in our sample are probably dust-enshrouded objects.

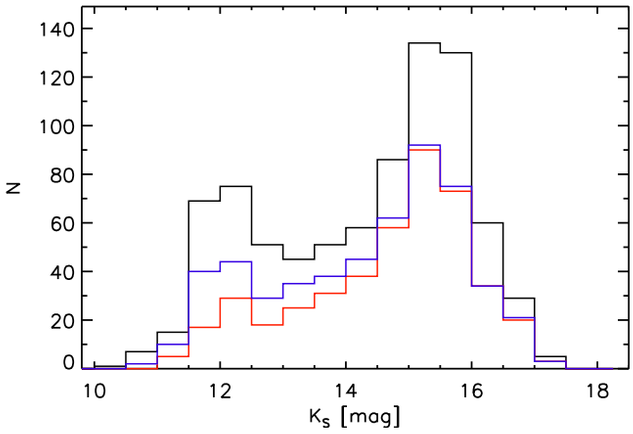

Figure 13. K_s distribution (from 2010 data) of the 816 VVV selected variable stars (solid black line). We show the same distribution for the overall sample of stars found to be likely associated with areas of star formation (blue line) and for the same sample but removing objects that show Mira-like light curves in Sect. 4.1 (red line).

The observations confirm the trend expected from the analysis above. Figure 12 shows that the number of LPVs increases as we come closer to the Galactic center. In addition, when taking into account AGB stars with measured periods, we confirm that the majority of AGB stars show periods longer than 400 days and large amplitudes (see lower panel in Fig. 12), as expected in heavily obscured AGB stars. It is interesting to see in the same figure, that variable objects with periods longer than 1500 days show lower amplitudes than expected for their long periods. This is similar to the observed trend in the variable OH/IR stars of Jiménez-Esteban et al. (2006a). According to the authors, these objects correspond to stars at the end of the AGB. We note that the apparent lack of high amplitude objects at longer periods could relate to the fact that more luminous (longer period) objects have smaller amplitudes expressed in magnitudes (red supergiants often display $\Delta K < 1$ mag, see e.g. van Loon et al. 2008).

This population of bright pulsating AGB stars can also explain the observed bimodality of the K_s distribution for the full sample of VVV high amplitude variable stars (see Fig. 13). The peaks of the distribution occur at $K_s \sim 11.8$ and $K_s \sim 15.8$. The peak at the bright end is at the same magnitude as the peak for LPVs.

When we only plot objects which are found to be likely associated with areas of star formation, the peak at the bright end becomes less evident (see blue histogram in Fig. 13). When we plot only SFR-associated sources that do not have LPV-like light curves (see Sect. 4.1) the bimodality almost disappears, as shown by the red histogram in Fig. 13. AGB stars are probably the main source of contamination in our search for eruptive YSOs in SFRs, especially dust-enshrouded AGB stars which can have infrared colours resembling those of YSOs. Hence it is fortunate that we can remove most of this contamination by selecting against LPV-like light curves.

3.6 YSO source density

Our finding in Sect. 3.3 that YSOs constitute about half of the detected population of high amplitude variables in VVV disc fields indicates that they represent the largest single population of high-amplitude infrared variables in the Galactic mid-plane, at least in the range $11 < K < 17$. We note that extragalactic studies of high-amplitude stellar variables are dominated by the more luminous AGB star population (see e.g. Javadi et al. 2015). Our analysis only considered the VVV disc tiles with $|b| < 1^\circ$, this amounts to 76 tiles, covering each 1.636 deg^2 of the sky. After allowing for the small overlaps between adjacent tiles, the total area covered in this part of the survey is 119.21 deg^2. Adopting a 50% YSO fraction for the full sample of 816 variables implies a source density of 3.4 deg^{-2}. As noted in Sect. 2.1, the stringent data quality cuts in our selection procedure excluded $\sim 50\%$ of high amplitude variables down to K_s=15.5, and a high fraction at fainter magnitudes where completeness falls (see Fig. 13). The corrected source density is therefore $\sim$7 deg^{-2}.

When considering the source density of high amplitude infrared variables in the UGPS, Contreras Peña et al. (2014) argued that the observed source density under-estimates the actual source density due to three main effects: (1) with only two epochs of K-band data most high amplitude variables will be missed; (2) the source density rises towards the magnitude cut of K< 16, indicating that many low luminosity PMS variables that are detected at distances of 1.4 to 2 kpc would be missed at larger distances; and (3) the dataset used in the UGPS search of Contreras Peña et al. excludes the mid-plane and is therefore strongly biased against SFRs. The UGPS YSO source density is estimated to reach 12.7 deg^{-2} when correcting for these 3 factors. In the case of VVV, given the higher number of epochs obtained from this survey, and that this analysis is not biased against areas of star formation, the source density is only likely to be affected by item (2) of the UGPS analysis. Figure 13 shows the magnitude distribution of the VVV variables associated with SFRs, where we can see a similar behaviour to the UGPS results, with the density of sources rising steeply towards faint magnitudes. Contrary to the UGPS search, we do not have a hard magnitude cut in the VVV sample, which includes sources as faint as $K_s \sim 17$. However, the number of sources decreases at $K_s > 16$, so we estimate an effective magnitude detection limit of $K_s = 16.25$ magnitudes. This implies that if typical sources from VVV have similar characteristics to UGPS objects in Cygnus and Serpens ($K = 14.8, d = 1.4 - 2$ kpc), then we would not detect them at distances $d > 3.32$ kpc. The complete sample of star forming complexes from Russeil (2003) shows that 83% of them are located beyond these distances. Correcting for this factor we then estimate a true source density of 41 deg^{-2}, though this figure does not include YSOs with low mass and luminosity that are too faint to be sampled by VVV due to the absence of nearby SFRs in the survey area. This figure of 41 deg^{-2} is three times larger than the one estimated from the UGPS analysis of Contreras Peña et al. (2014) (12.7 deg^{-2}).

Two effects can account for the larger source density in VVV than UGPS. (1) High luminosity YSOs are less common, but they can be observed at larger distances. The UGPS study would not find such objects at large distances

because the available dataset did not cover the mid-plane of the Galactic disc, in which all distant SFRs are located due to their small scale height. Since VVV does cover the midplane we are able to detect these rare higher luminosity YSOs. This seems to be supported by the slightly larger distances established for members of the spectroscopic subsample in paper II. (2) In the UGPS study, most (23/29) of the variables in SFRs were located in just 2 large SFRs: the Serpens OB2 association and portions of Cygnus X. The much smaller size of the UGPS sample (in number of SFRs and number of variables) meant that there was considerable statistical uncertainty in the area-averaged source density. Moreover, the incidence of high amplitude variability is greater at the earlier stages of YSO evolution (see Sect. 4.3) so the numbers in the UGPS study may have been reduced by a relative lack of YSOs at these stages in the two large SFRs surveyed.

The estimated highly variable YSO source density remains much larger than that estimated for Mira variables in Contreras Peña et al. (2014), indicating a higher average space density for the variable YSOs. The observed variables in SFRs also outnumber the EBs and unclassified variables in the magnitude range of this study. However, we are likely to miss a large part of the population of high amplitude EBs due to the sparse time sampling of VVV.

In Appendix A we attempt to calculate the source density and space density of high amplitude EBs from the OGLE-III Galactic disc sample of Pietrukowicz et al. (2013). In this we are aided by a recent analysis of the physical properties of the large sample of *Kepler* eclipsing binaries (Armstrong et al. 2014), which indicates that EBs with high amplitudes in the VVV $K_{\rm s}$ and OGLE I passbands are dominated by systems with F to G-type primaries. We use simple calculations to show that while EBs can have very high amplitudes at optical wavelengths, the eclipse depth should not exceed 1.6 mag in $K_{\rm s}$. Similarly, we find that eclipse depths should not exceed 3 mag in I. These results are supported by the VVV and OGLE-III datasets (Pietrukowicz et al. 2013) in which the distribution of EB amplitudes falls to zero by these limits. YSOs with $\Delta K_{\rm s} > 1.6$ mag are very numerous in our sample so we conclude that high amplitude YSOs greatly outnumber EBs above this limit. Below $\Delta K_{\rm s} = 1.6$ mag it is harder to reach a firm conclusion (see Appendix A). The space densities of EBs and those YSOs massive enough to be sampled by VVV may be comparable at $1 < \Delta K_{\rm s} < 1.6$ mag. High amplitude YSOs are likely to be more numerous if the variability extends down to the peak of the Initial Mass Function at low masses, given that high amplitude EB systems contain a giant with mass of order 1 $M_{\odot}$.

4 ANALYSIS OF VARIABLES IN STAR FORMATION REGIONS

The results presented here concern YSO variability in the $K_{\rm s}$ bandpass. At these wavelengths, variability in typical YSOs is produced by physical mechanisms (or a combination of them) affecting the stellar photosphere, the star-disc interface, the inner edge of the dust disc as well as spatial scales beyond 1 au (see e.g. Rice et al. 2015). These mechanisms include cold or hot spots on the stellar photosphere (e.g. Scholz 2012), changes in disc parameters such as the location of the inner disc boundary, variable disc inclination and changes in the accretion rate (as shown by Meyer et al. 1997). Variable extinction along the line of sight can also be responsible for the observed changes in the brightness of YSOs. Dust clumps that screen the stellar light have been invoked to explain the variability observed in Herbig Ae/Be stars and early-type Classical T Tauri stars (group also known as UX Ori stars, see e.g. Herbst & Shevchenko 1999; Eiroa et al. 2002). In other scenarios variable extinction can be produced by a warped inner disc, dust that is being uplifted at larger radii by a centrifugally driven wind, azimuthal disc asymmetry produced by the interaction of a planetary mass companion embedded within the disc or by occultations in a binary system with a circumbinary disc (see e.g., Romanova et al. 2013; Bans & Königl 2012; Bouvier et al. 2013; Windemuth & Herbst 2014, and references therein). Finally, sudden and abrupt increases in the accretion rate (of up to 3 orders of magnitude) explain the large changes observed in eruptive variable YSOs. The variability in these systems traces processes occurring at the inner disc (in EXors, see Lorenzetti et al. 2012) or at larger spatial scales beyond 1 au, such as instabilities leading to outbursts events (in FUors, see e.g. Audard et al. 2014).

The amplitude of the variability induced by most of these mechanisms is not expected to be larger than $\Delta K \sim 1$ magnitude. Table 6 of Wolk et al. (2013) shows the expected amplitude of the K-band variability that would be produced by these different mechanisms. Cold and hot spots, and changes in the size of the inner disc hole are not expected to show ΔK larger than 0.75 magnitudes. We do note that the variability produced by hot spots from accretion depends on the temperature of the spot and the percentage of the photosphere that is covered by such spots, thus sufficiently hot spots can produce larger changes in the magnitude of the system. The range in ΔK from variable extinction is effectively limitless as it depends on the amount of dust that obscures the star. Large changes (ΔK > 1 mag) have been observed from variable extinction in YSOs, e.g. AA Tau, V582 Mon (Bouvier et al. 2013; Windemuth & Herbst 2014). Nevertheless, variable extinction can be inferred from colour variability (see e.g. Sect. 4.2). Wolk et al. (2013) also estimate that a change in the accretion rate of a class II object of $\log \dot{M}(M_{\odot}\ yr^{-1})$ from -8.5 to -7 yields ΔK$\sim$0.75 magnitudes. Thus, larger changes as observed in eruptive variables will produce large amplitudes.

Given all of the above, it is reasonable to expect variability in our YSO sample to be dominated by accretion-related variability and/or events of obscuration by circumstellar dust.

4.1 Light curve morphologies

We have visually inspected the light curves of our 530 SFR-associated variables in order to gain insight into the physical mechanism causing the brightness variations. In addition, we used PDM in IRAF and LombScargleFast in GATSPY to search for periodicity in the light curves of our objects. We stress that this is a simple and preliminary classification that is highly influenced by the sparse sampling of VVV. A more detailed study is planned in future, with improved precision by applying the differential photometry method of

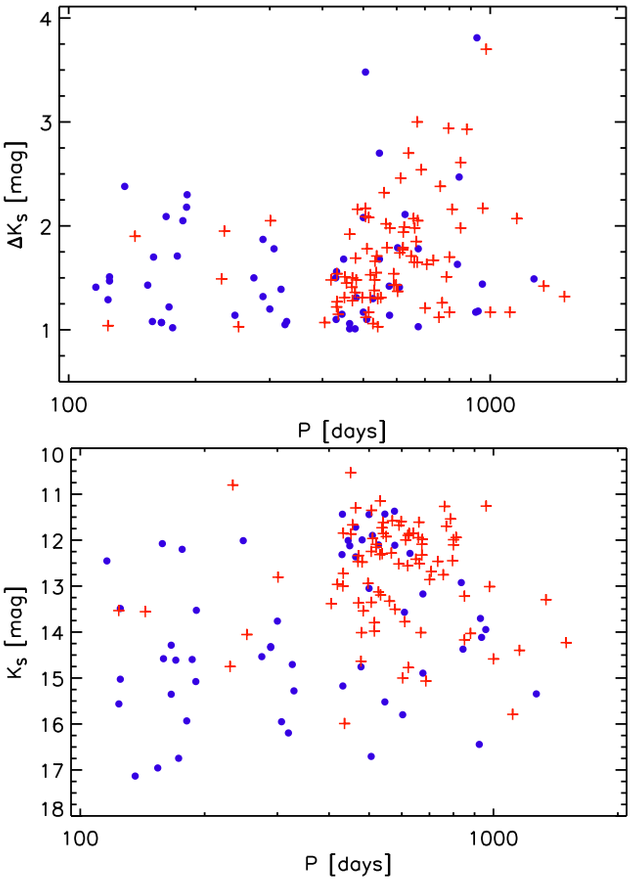

Figure 14. (top) K_s amplitude vs period for stars in SFRs with long-term periodic variability. LPVs that show Mira-like light curves are shown in red plus signs while other sources are shown as blue circles. (bottom) K_s magnitude (2010) vs period for the same sample of stars.

Huckvale et al. (2014) to the VVV images. We have divided the morphologies in the following classifications.

• **Long-term Periodic Variables.** Defined as objects showing periodic variability with $P > 100$ days. This limit is adopted for consistency with the limit used in the analysis of objects outside of SFRs, with the benefit that contamination by long period AGB stars will be confined to this group. We measure periods for most of these objects, albeit with some difficulty in phase-folding the data in many of them. In this subsample we find 154 stars, representing 29% of objects spatially associated with SFRs. In Sect. 3.4 we contended that field high-amplitude infrared variables with periodic light curves ($P > 100$ days) are very likely dust-enshrouded AGB stars, these being identifiable by their smooth, approximately sinusoidal light curves. We estimated that ∼27% of the 530 SFR-associated variables would be non-YSOs and up to 45% of these would be LPVs, implying that this subsample may contain ∼64 dusty Mira variables. Visual inspection of the 154 light curves indicates that while some have a smooth sinusoidal morphology (after allowing for long term trends due to variable extinction in the expanding circumstellar dust shell) others display short timescale scatter superimposed on the high amplitude long term periodicity. In Fig. 15, we show the examples of objects VVVv309 and VVVv411. The short timescale variability in their light curves is definitely not consistent with the typical light curves of Mira variables and their periods of 143.95 and 190.6 days, respectively, are shorter than those of the dusty Miras detected outside SFRs (see Fig. 12). This short timescale scatter is typical of the scatter observed in normal YSOs due to a combination of hot spots, cold spots, and small variations in accretion rate or extinction, so it is reasonable to think that most of the long period variables with short timescale scatter are in fact YSOs.

To support this interpretation, Fig. 14 shows the period vs ΔK_s and period vs K_s distributions, for objects where we are able to measure a period. The period vs ΔK_s distribution is similar to that observed in LPVs outside SFRs (Fig. 12) except that there is a larger number of "long-term" periodic variables found with periods, $100 < P < 350$ days. The 65 blue points are the objects with short timescale scatter and the red points are the remaining 89, categorised by careful inspection of the light curves of the 154 long-term periodic variables in SFRs. The blue points clearly dominate the group with $P < 350$ days and they also have a distinctly fainter distribution of K_s magnitudes, similar to that shown in the red histogram in Fig.13, which represents all objects in SFRs except those with Mira-like light curves. As expected, the red points with Mira-like light curves typically have $K_s \sim 12$, similar to the LPV distribution plotted in Fig. 10. We conclude that inspection of the light curves can separate the evolved star population of LPVs from the YSOs in SFRs with fair success, though we caution that this is an imperfect and somewhat subjective process that can be influenced by outlying data points and our limited knowledge of the time domain behaviour of circumstellar extinction in dusty Mira systems. The limitations are demonstrated by the presence of a number of blue points with $K_s \sim 12$ and $P > 350$ days in the lower panel of Fig. 14 and a hint of bimodality even in the "decontaminated" magnitude distribution in Fig. 13 (red histogram). In the subsequent discussion of YSOs from our sample we only include the 65 objects with short timescale scatter (called LPV-yso) and assume the other 89 sources are dusty AGB stars or other types of evolved star (or LPV-Mira).

This decontamination of AGB stars reduces the SFR-associated sample to 441 objects. The long term periodic YSOs represent 15% of this sample.

Periods, $P > 15$ days are longer than the stellar rotation period of YSOs, or the orbital period of their inner discs (Rice et al. 2015). Some YSOs have been observed to show variability with periods longer than even 100 days. WL 4 in ρ Oph shows periodic variability with $P = 130.87$ days (Plavchan et al. 2008), which can be explained by obscuration of the components of a binary system by a circumbinary disc. The K-band amplitude of the variability in that system is somewhat less than 1 magnitude. However, it is possible to think that a similar mechanism might be responsible for the variations in some of our objects. Hodapp et al. (2012) show that variable star V371 Ser, a class I object driving an H_2 outflow, has a periodic light curve with $P = 543$ days. The authors suggest that variability arises from variable accretion modulated by a binary companion. In view of this, the variability in some of the long term periodic variables might be driven by accretion and we discuss this in paper II, based on spectroscopic evidence for a sub-sample of them.

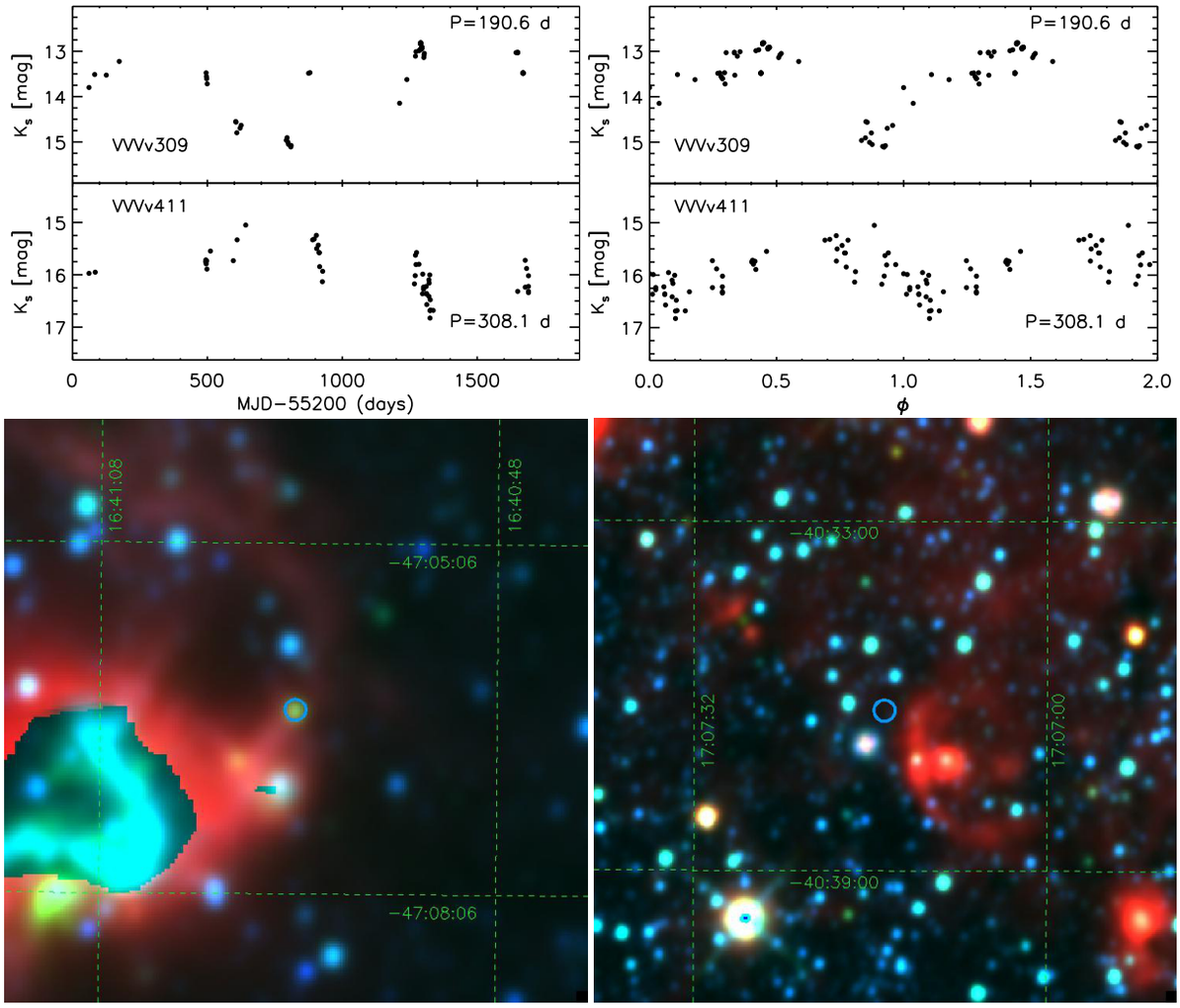

Figure 15. (top left) Examples of K_s light curves of the long-period variables VVVv309 and VVVv411, which are found in areas of star formation. (top right) Phased light curves for the same objects. (bottom) $10' \times 10'$ WISE false colour images (blue=3.5 μm, green=4.6 μm, red=12 μm) centred on VVVv309 (left) and VVVv411 (right). In both images the location of the variable star is marked by a ring around the location of the object. VVVv309 is 114″ from HII region GRS G337.90 -00.50 (see e.g. Culverhouse et al. 2011). The 12μm WISE image of VVVv309 saturates at the centre of the HII region creating the blue/green "inset" in the false colour image. VVVv411 is located 104″ from the infrared bubble [CPA2006] S10 (Simpson et al. 2012) as well as other indicators of ongoing star formation.

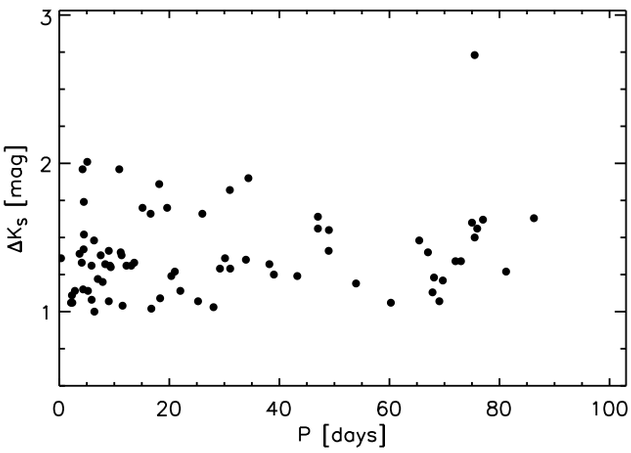

Figure 16. K_s amplitude vs period for stars with short-term variability and with a measured period.

• **Short-term Variability.** This group comprises objects that either have periodic variability and measured periods, $P < 100$ days, (75 objects) or else have light curves that appear to vary continuously over short timescales ($t <$ 100 days) but not with an apparent period (87 objects). Their light curves do not resemble those of detached EBs because they vary continuously and cannot be contact binaries (W UMa variables) because their periods are typically longer than 1 day. For objects in this classification that have measured periods, we observe a broad distribution from 1 to 100 days and the amplitudes are in the range ΔK_s=1 to 2 magnitudes (see Fig. 16). If we join together the long-term periodic variables and the short-term variables (STVs) with measured periods, we find that sources with periods, $P > 100$ days show higher amplitudes, on average, and sources with $P > 600$ days have redder SEDs (larger values of the spectral index α). There are no clear gaps in the period distribution, so the 100 day division between the

two groups that we adopted to aid decontamination is arbitrary. We find 162 stars in the STV group, which represents 37% of the decontaminated SFR-associated sample.

High-amplitude periodic variability has been observed in YSOs over a wide range of periods. RWA1 and RWA26 in Cygnus OB7 (Wolk et al. 2013) vary with periods of 9.11 and 5.8 days respectively. The variability has been explained as arising from extinction and inner disc changes. As mentioned before variability with $P > 15$ days is not expected to arise from the stellar photosphere or changes in the inner disc of YSOs. This instead could be related to obscuration events from a circumbinary disc, such as in V582 Mon (Windemuth & Herbst 2014), and YSOs ONCvar 149 and 479 in Rice et al. (2015). Variable accretion has been invoked to explain the observed periodic variability ($P \sim 30$ d) of L1634 IRS7 (Hodapp & Chini 2015). The shorter periods within this group may indicate rotational modulation by spots in objects with amplitudes not far above 1 magnitude, see below.

• **Aperiodic Long-term variability.** This category can be divided into three different subclasses: a) Faders. Here the light curves show a continuous decline in brightness or show a constant magnitude for the first epochs followed by a sudden drop in brightness that lasts for a long time ($\geqslant 1$ year), continuing until the end of the time series in 2014. This type of object might be related to either stars going back to quiescent states after an outburst or objects dominated by long-term extinction events similar to the long-lasting fading event in AA Tau (Bouvier et al. 2013), or some of the faders in Findeisen et al. (2013). b) Objects that show long-lasting fading events and then return to their normal brightness (such as VVVv504 in Fig. 17), which we refer to as dippers. These might also be related to extinction events. Examples of objects in groups (a) and (b) can be seen in Fig. 17.

Group (c) contains sources with outbursts, typically of long duration ($\geqslant 1$ yr). In a very small number of objects the outburst duration appears to be much shorter, on the order of weeks. The increases in brightness are also unique or happen no more than twice during the light curve of the object, thus not resembling the light curves of objects in the STV category. An exception is VVVv118, which shows four brief rises on timescales of weeks.

The light curves in this category typically have a monotonic rise of 1 magnitude or more, though sometimes a lower level scatter is present atop the rising trend. In a small number of cases the rise in the light curve is poorly sampled, starting at or before the beginning of the time series, but the subsequent drop exceeds 1 magnitude. Figure 18 shows four examples of objects falling in the eruptive classification. The examples have been selected in order to illustrate the different temporal behaviour observed in objects belonging to this class. As we have already mentioned, VVVv118 shows multiple short, high-amplitude rises. In general objects show outbursts which last between 1-4 years (see VVVv815 and VVVv322). We also detect a few cases where the outburst duration cannot be measured as it extends beyond 2014 data (e.g. VVVv270).

When comparing to the behaviour of known classes of eruptive variables, VVVv118 would resemble that of EXors and VVVv270 could potentially be an FUor object (based only on photometric data). However most of the objects have outburst durations that are in between the expected duration for EXors and FUors.

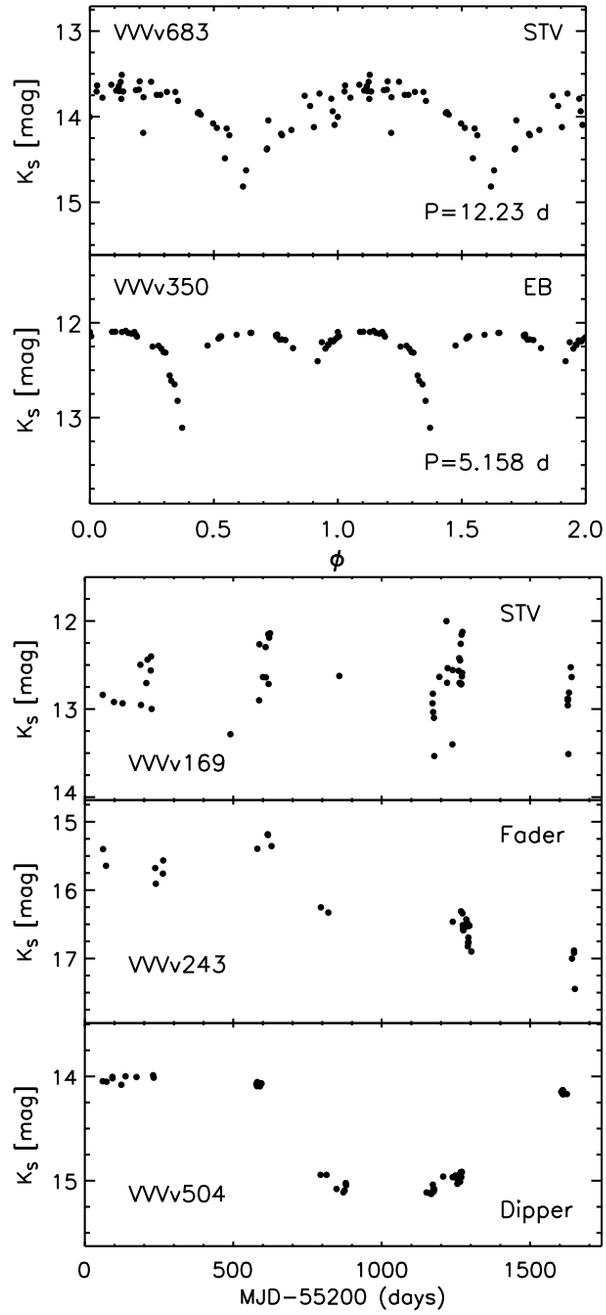

Figure 17. Examples of K_s light curves for the different classifications as explained in the text. (top) Phased light curves of short-term variable star with a measured period, VVVv683 and eclipsing binary VVVv350. (bottom) Light curves of short-term variable star, without a measured period, VVVv169, the fader VVVv243 and the dipper VVVv504.

Considering the outburst duration of the known subclasses of young eruptive variables, we are likely to miss detection of FUor outbursts if they went into outburst prior to 2010. In the case of EXors, which have outbursts that last from few weeks to several months, we would expect to detect more of these objects given the time baseline of

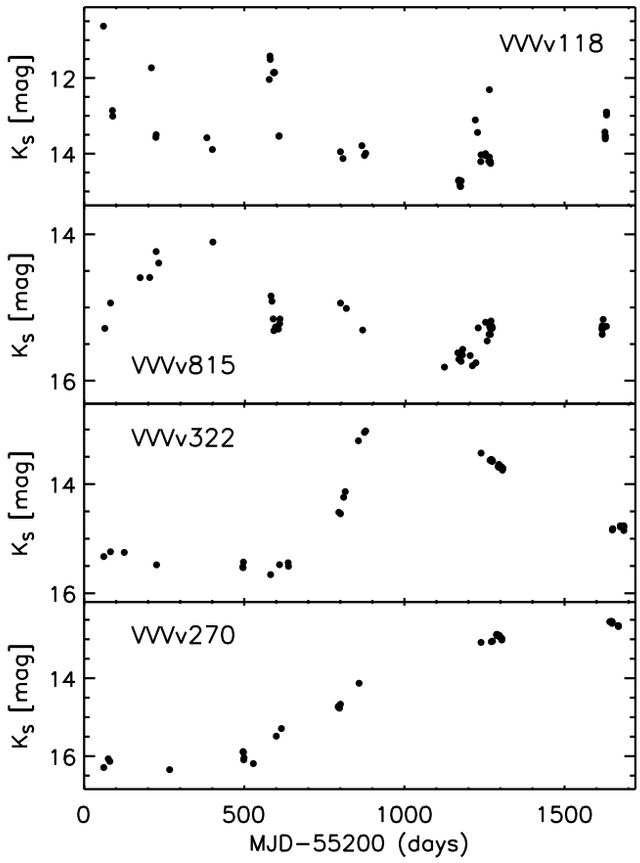

Figure 18. Examples of $K_{\rm s}$ light curves for different objects in the eruptive classification as explained in the text. From top to bottom we show objects VVVv118, VVVv815, VVVv322 and VVVv270.

VVV. However, our results show a lack of classical EXors, which could be a real feature or it could be related to the sparse VVV sampling. Thus, we need to test our sensitivity to short, EXor-like eruptions.

We simulate outbursts with timescales from 2 months to 3 yr. First we generate a very rough approximation of an eruptive light curve with outburst duration, T_o. The light curve consists of: 1) A quiescent phase of constant magnitude that lasts until the beginning of the outburst, which is set randomly at a point within the 2010-2012 period (between 0 and 1000 d). 2) A rise which is set arbitrarily to have a rate of 0.15 mag/day, lasting T_{rise} =10 d until reaching an outburst amplitude of 1.5 mag, which is a little below the median for the VVV eruptive variable candidates. 3) Plateau phase with a constant magnitude set to the peak of the outburst. This phase lasts for $T_o - T_{rise} - T_{decline} = T_o - 20$ d. 4) The decline, which lasts 10 days and has a rate of 0.15 mag/day. Finally, 5) A second quiescence phase. To every point in the light curve we add a randomly generated scatter of $\pm$0.2 mag. Once the light curve is generated, we measure the magnitude of the synthetic object at the observation dates of a particular VVV tile. If the synthetic object shows $\Delta K_{\rm s} \geqslant 1$ mag then it is marked as a detection. This procedure is repeated 1000 times for each outburst duration (which is set to be between 30 and 900 days). We also repeat this procedure for four different VVV tiles.

The simulation shows that the number of detections is very similar ($\sim$ 80%) for $T_o >$ 7 months and declines slowly as T_o is reduced, falling by a factor of 2 for $T_o = 2$ months. However, this is not enough to cause the apparent lack of eruptive variables with EXor-like outbursts in our sample. We conclude that the longer (1-4 yr) durations that we observe are typical values for infrared eruptive variables, rather than a a sampling effect.

The characteristics of our eruptive sample (see Paper II) agree with recent discoveries of eruptive variables that show a mixture of characteristics between the known subclasses of eruptive variables (see e.g. Aspin et al. 2009). We note that classification of our sample into the known subclasses becomes even more problematic when taking spectroscopic characteristics into account, as e.g. VVVv270, the potential FUor from its light curve, shows an emission line spectrum, or VVVv322 shows a classical FUor near-infrared spectrum. In Paper II we propose a new class of eruptive variable to describe these intermediate eruptive YSOs.

Sources classified as eruptive are very likely to be eruptive variables, where the changes are explained by an increase of the accretion rate onto the star due to instabilities in the disc of YSOs (see e.g. Audard et al. 2014). We find 39 objects in subgroup (a), 45 in (b) and 106 in (c). The whole class of faders/bursts represent 43% of the likely YSO sample.

• **Eclipsing Binaries.** We find 24 objects with this light curve morphology, representing 5% of the sample. We are able to measure a possible period in 15 of them. The remaining 9 objects are left with this classification given the resemblance of their light curves to the objects with measured periods. We expect that a number of them will be field EBs contaminating our YSO sample. However, inspection of the 2 to 23 μm spectral index for each object, α, (see Fig. 23), indicates that 12 objects are classified as either class II or flat-spectrum sources. If these are in fact YSOs, they would represent a significant discovery as YSO EBs are invaluable anchors for stellar evolutionary models, which generally lack empirical data on stellar radii. Figure 19 shows the light curve and location of one candidate YSO EB, VVVv317, with P= 6.85 d and $\alpha = -1.57$. The spectral index places it at the edge of the classification of class II YSOs.

In Fig. 20 we compare the amplitude distributions ($K_{\rm s,max} - K_{\rm s,min}$) of the different categories of variable YSO. We can see that the EBs and STVs typically have the smallest amplitudes (means of 1.18 mag and 1.33 mag, respectively), whereas the faders and eruptive variables have the highest amplitudes (means of 1.95 mag and 1.72 mag, and medians of 1.75 mag and 1.61 mag respectively). The dippers and long-term periodic variables have mean amplitudes of 1.64 mag and 1.57 mag respectively, which are similar to the mean amplitude of 1.56 mag for the full sample. The substantial number of STVs with amplitudes only a little over 1 magnitude is consistent with our suggestion that in the shorter period variables in this category variability may be explained by rotational modulation of dark or bright spots on the photosphere. The relatively high amplitudes of the eruptive variables are not unexpected, whilst the high amplitudes of the faders could be explained if some of these objects are eruptive variables returning to quiescent states.

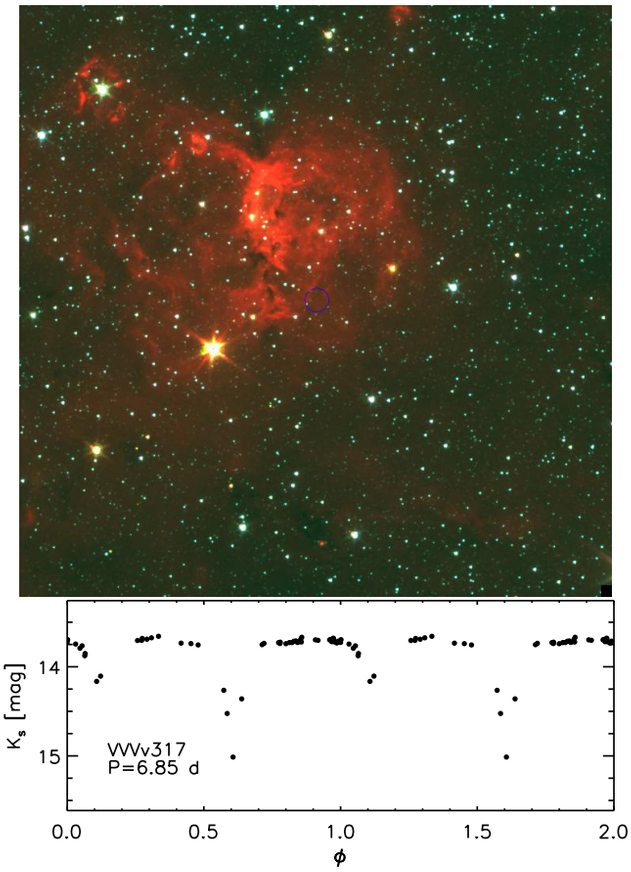

Figure 19. (top) False colour image (blue=3.6 μm, green=4.5 μm and red=8 μm) from GLIMPSE, showing the location of candidate YSO EB VVVv317 (blue ring). (bottom) Phased light curve of the object.

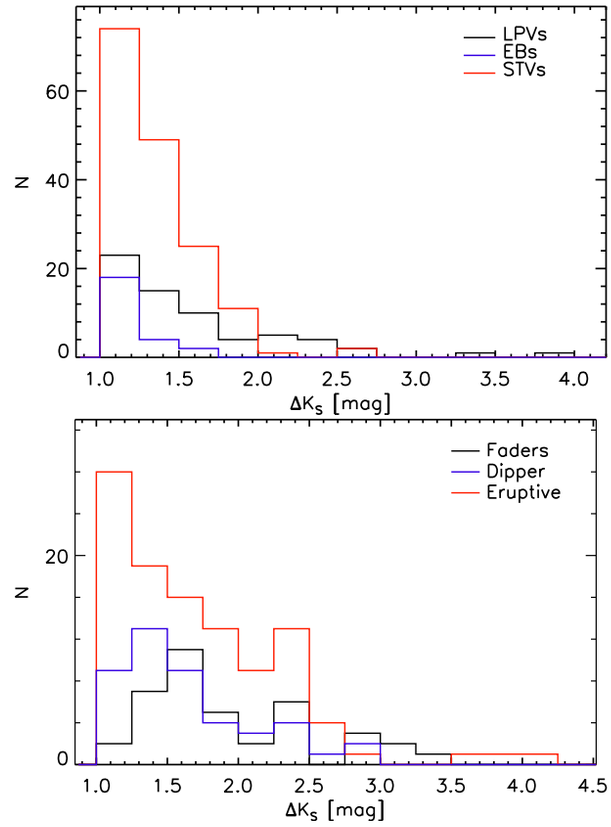

Figure 20. ΔK_s distribution for the different light curve morphology YSO classes. (top) Distribution for LPVs (black line), STVs (red line) and EBs (blue line). (bottom) Distribution for aperiodic variables, faders (black line), dippers (blue line) and eruptive objects (red line).

4.2 Near infrared colour variability

Considering the various classes of light curve defined above for SFR-associated variables, it is reasonable to expect that extinction causes the variability in dippers and perhaps some of the STVs. Extinction variability can be observed in eruptive objects. However, we do not expect the main cause of variability in this class to be due to this mechanism. It is less clear what to expect for faders and long-term periodic variables. We can test this by looking at colour variability data.

The VVV survey was initially designed with only 1 epoch of contemporaneous JHK$_s$ colour data but a 2nd such epoch was added to the programme for observation in 2015, both to benefit the YSO variability science and to help to understand VVV variables of unknown nature. We note that many objects in the SFR sample are not detected in J- and H-band (see Sect. 4.3), making a colour comparison impossible. Also, in many objects the two epochs do not span a large fraction of the full range of magnitudes in the light curve. E.g. in many eruptive objects we do not have direct comparison between quiescent and outburst states. Nevertheless, comparison of the change in colour vs magnitude still provides some valuable information on the mechanisms driving variability, particularly for those sources in which source magnitudes differ substantially at the 2 epochs.

Following a similar procedure to Lorenzetti et al. (2012) and Antoniucci et al. (2014) we compare the change in colour, $(H - K_s)$, vs magnitude, H, between 2010 and 2015 for the different classes of YSOs (see Fig. 21). In the figure we see that in most cases the changes in both colour and magnitude are small, thus objects cluster around the origin. This is especially true in EBs. The overall distribution of eruptive, dippers, LPVs and STVs on the other hand, seems to be elongated along an axis passing through the "bluer when brighter" and "redder when fainter" quadrants. This agrees with the behaviour expected from changes due to accretion or extinction in YSOs and resembles the near-infrared variability observed in EXors (Lorenzetti et al. 2009, 2012), the classical T Tauri sample of Lorenzetti et al. (2012), and the mid-infrared variability of candidate EXors from Antoniucci et al. (2014). It is interesting to see that many objects classified as faders fall in the bluer when fading quadrant. This behaviour is still consistent with YSO variability due to changes in disc parameters described by Meyer et al. (1997) and observed in some Cygnus OB7 YSOs (see e.g. Wolk et al. 2013). The different behaviour might also be caused by the different geometry (inclination) of the system with respect to the observer. Scattering of light by the circumsteller disc or envelope may also be contributing to the sources that are bluer when fainter.

Figure 21 also shows the observed change in both

$(J-H)$ and $(H-K_s)$ colours for YSOs detected in the three filters in both epochs. In there we also plot the expected change if the variability occurs parallel to the reddening line (independent of the direction of the change) as well as a linear fit to the different YSO classes. We would expect that variability similar to that observed in EXors (see e.g. fig. 1 in Lorenzetti et al. 2012) would show a behaviour that is not consistent with reddening. It is hard to say much from EBs as they do not show much variability. The overall change in STVs, faders and dippers appears to be different from the reddening path, although it appears to depend on the selection of objects from those samples. The path followed by LPVs is also different from the reddening line, but it does suggest a more similar behaviour to extinction compared to the other classes. Eruptive variables appear to follow a very different path from reddening. We would expect such behaviour if the variability is similar to that observed in EXors (see e.g. fig. 1 in Lorenzetti et al. 2012). Given that variable extinction and eruptive variability are the only known mechanisms to produce variability well in excess of 1 mag, the fact that colour variability disfavours the former in eruptive systems suggests that the latter is more likely.

We have checked the individual $(J-H)$ vs H, $(H-K_s)$ vs K_s and $(J-H)$ vs $(H-K_s)$ colour-magnitude (CMD) and colour-colour diagrams for the 15 eruptive variables that showed $\Delta K_s > 0.75$ mag between the two multi-wavelength epochs (this representing a significant fraction of the total amplitude in most systems). From 15 objects, 10 do not show changes consistent with extinction (e.g. they are bluer when fainter or show negligible colour change) and 5 were found to show variability approximately following the reddening vector. However, the colour behaviour in these 5 objects does not contradict the idea that accretion is the mechanism driving variability because: 1) we are not directly comparing quiescent vs outburst states, as the two near-infrared epochs cover random points in the light curve; 2) As previously mentioned, extinction does play a role in outburst variability. E.g. the near infrared colour variation of V1647 Ori follows the reddening path in fig. 13 of Aspin et al. (2008). Extinction might also be involved in the observed variability or the recent eruptive object V899 Mon (Ninan et al. 2015).

The same analysis of individual CMD and colour-colour diagrams for the remaining classes shows that 3/7 LPV-YSOs, 5/9 STVs, 1/4 dippers and 3/11 faders have colour changes consistent with variable extinction (again considering only systems with $\Delta K_s > 0.75$ between the 2 multi-colour epochs). No results can be derived from EBs as none of them show changes larger than 0.75 magnitudes between the two epochs. It is interesting to see that the changes in the majority of faders are not consistent with extinction. This supports the idea that variability in many of the objects in this class could be related to accretion changes.

In Appendix B we briefly summarise the colour and magnitude changes detected by the multi-epoch photometry from the WISE satellite. We note that this adds little to the preceding discussion of near-infrared colour changes, though large mid-infrared variability is observed in a minority of sources where the satellite happened to sample both a peak and a trough in the light curve.

4.3 Variability trends with SED class

In order to study the possible evolutionary stage of the variable stars in SFRs, we use the slope of the SEDs of the stars between $2 < \lambda < 24$ μm. Following Lada (1987), we define the parameter α as $\alpha = d(\log(\lambda F_\lambda))/d(log(\lambda))$. The value of α is determined from a linear fit to SED points between $2 < \lambda < 24$ μm. Objects are then classified according to their value of α following Greene et al. (1994), also shown in Table 3. We note that this class definition might not necessarily relate to the actual evolutionary stage of the object. As stated in e.g. Robitaille et al. (2006), parameters such as inclination or stellar temperature can affect the shape of the SED at the wavelengths used to classify YSOs. We have removed numerous objects that showed Mira-like characteristics from their light curves but there may still be some contamination by non-YSOs amongst the remaining objects projected close to an SFR.

We derive α using the photometry arising from VVV and WISE, given that these were taken in the same year (2010). When the objects are not detected in WISE, we use *Spitzer*/GLIMPSE photometry. The use of the latter is more likely to cause errors in the estimation of α due to the time difference between *Spitzer*/GLIMPSE and VVV measurements, but *Spitzer*/GLIMPSE benefits from higher spatial resolution. We find that if we use *Spitzer* instead of WISE the difference in α shows a random offset of 0.1-0.2 for the majority of the sample detected in both surveys.

The number of objects belonging to different classes are shown in Table 3. We find that the majority (67%) of objects in our sample are either class I or flat spectrum sources (45% and 22%, respectively). Objects belonging to different classes show some differences in their global properties. Figure 22 shows the near-infrared colours of objects in SFRs. As expected the vast majority of objects show colours consistent with them being YSOs. The $H-K_s$ colour tends to be redder for stars belonging to younger evolutionary stages. The fraction of objects detected at J and H bands also decreases with objects belonging to younger stages, as would be expected for typical deeply embedded class I objects. Table 3 shows that 66% of class I objects are not detected in the J band, whilst 23% of them are not detected in either the J nor H bands. These near IR colour trends confirm that, as with typical YSOs, highly variable YSOs whose spectral index indicates an earlier evolutionary stage also have higher extinction by circumstellar matter, along with more infrared emission from circumstellar matter.

It might be thought that the relatively high reddening of most of the YSOs in Fig. 22 is due to foreground extinction, given that in Paper II we derive typical distances of a few kpc for these sources. We measure foreground extinction for a sub-sample of VVV objects (the 28 variable YSOs in Paper II) by estimating the extinction of red clump giants found at distances similar to those of our objects. The red clump giants are identified in the local K_s vs $(J-K_s)$ colour-magnitude diagrams of the VVV objects ($6' \times 6'$ fields), and distances are estimated from their observed magnitudes K_s and mean $(J-K_s)$ colours using equation 1 in Minniti et al. (2011). The excess of the mean $(J-K_s)$ with respect to the intrinsic colour of red clump giants ($(J-K_s)_0$=0.70 mag Minniti et al. 2011), gives us a measure of the foreground extinction to the front of the molecular cloud containing each

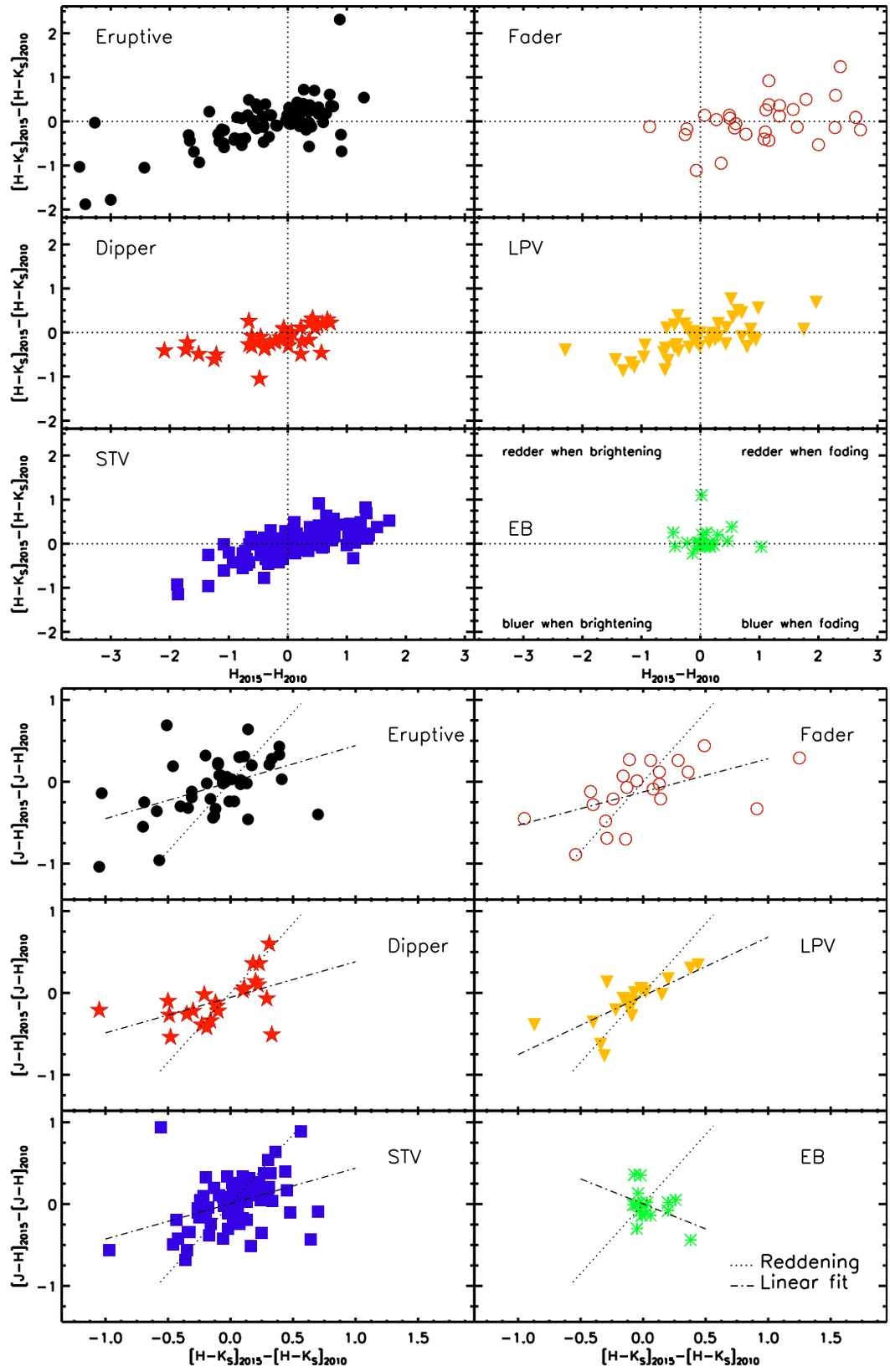

Figure 21. $\Delta(H-K_s)$ vs ΔH (top) and $\Delta(J-H)$ vs $\Delta(H-K_s)$ (bottom) for YSOs with an available second JHK_s epoch from VVV. In the plots we mark the different classes from light curve morphology. In the bottom plot we mark the expected changes which occur parallel to the reddening vector (dotted line) as well as the best fit to the observed change (dot-dashed line). In the bottom right of the upper panel we mark four distinct regions as explained in the text.

Class	α	N	N_{Jdrop}	N_{JHdrop}	$N_{\Delta K_s \geqslant 2}$
class I	$\alpha > 0.3$	198	130	45	49
flat	$-0.3 \leqslant \alpha \leqslant 0.3$	95	35	1	12
class II	$-1.6 < \alpha < -0.3$	83	19	1	6
class III	$\alpha \leqslant -1.6$	12	0	0	0
Undefined	n/a	53	10	2	3

Table 3. Number of VVV variable stars belonging to the different evolutionary classes of YSOs, as determined from their SEDs.

YSO. In most cases the YSO itself is redder than the red giant branch stars, due to extinction by matter within the cloud and by circumstellar matter. This method yields values of $A_{K_s} \sim 0.8$ to 1.4 mag (i.e. $A_V \sim 7$ to 12 mag) which is higher than the typically very low diffuse interstellar extinction between the sun and nearby molecular clouds. We infer that the optical faintness and steeply rising near-infrared SEDs of these objects are due not only to their early evolutionary stage but also to foreground extinction. Correcting our values of α accounting for $A_V = 11$ magnitudes, produces changes of 0.2-0.4 in this parameter. These changes would alter the classification of 1/3 of the sample where we can estimate α, mostly in objects where α has a value that is close to the limits set by Greene & Lada (1996). Despite this correction flat-spectrum and class I sources still dominate the sample of YSOs with a measured value of α: with no correction these represent 76% of the sample, whereas with a correction to α of 0.3 the proportion remains high, at 59%.

We choose not to apply a correction in Table 3 and our subsequent analysis because the extinctions and distances are uncertain (e.g. the red giant branch is not well defined in the CMDs for about a third of sources) and we cannot be sure this method is entirely correct. Our derived extinctions are a factor of ∼2 higher than indicated by the 3D extinction map of Marshall et al. (2006), which was also based on red clump giants but used 2MASS data on a coarser angular scale. Moreover, in Paper II we compare the ratio of 70 μm flux to 24 μm flux in the spectroscopic subsample with that found in a nearby sample of YSOs. At these far-infrared wavelengths, where extinction is very low, we find similar flux ratios for class I systems in both datasets, indicating that most VVV class I YSOs have been correctly classified. In the following discussion, we directly compare embedded (class I and flat spectrum) YSOs with sources in nearby SFRs. We simply ask the reader to note firstly that α may be slightly inflated by interstellar extinction and secondly that this more distant sample will be biased towards more luminous YSOs of intermediate mass (see Paper II).

The distribution of ΔK_s (Fig. 23, upper left panel) shows that peak of the distribution is found at larger ΔK_s for younger objects. We also observe a higher fraction of objects with $\Delta K_s > 2$ mag for class I objects (25%) than for flat-spectrum (13%) and class II (7%) objects. The comparison of α_{class} vs ΔK_s in the bottom panel of the same figure further illustrates the increase in amplitude at younger evolutionary stages, as well as the higher incidence of $\Delta K_s > 1$ variability at the younger stages. The class I and flat spectrum YSOs constitute 87% of the $\Delta K_s > 2$ subsample, dominating it even more than the full SFR-associated sample.

We note that 70 objects with $\Delta K_s > 2$ mag also have redder near infrared colours than the full sample: the proportions of J band non-detections and JH non-detections rises from 44% and 11% in the full SFR-associated sample to 56% and 24% in the $\Delta K_s > 2$ subsample. This further highlights the simple fact that efficient detection of the majority of YSOs with the most extreme variations requires observation at wavelengths $\lambda \geqslant 2$ μm. Most importantly, this further emphasises that younger objects have higher accretion variations. Eruptive variables are the largest component of the $\Delta K_s > 2$ sample, comprising 30/70 objects.

In Fig. 23 we also show the mean variability of YSOs belonging to different evolutionary classes as a function of time baseline. This is calculated by averaging the values of r.m.s. variability vs time interval computed using every possible pairing of two points within the light curve of each star. In the figure we show the variability over intervals up to 50 days (calculated with time bins of 1 day), and for intervals up to the full 1600 day baseline of the dataset (using time bins of 30 days). The r.m.s. variability over short timescales appears to be larger for more evolved objects than flat and class I sources. The variability increases with time for every YSO class and becomes flat at $t \sim 250 - 350$ days, although this is less clear for class III sources because of noise due to the lower number of objects in this class. Class I and flat sources have higher r.m.s. variability on these longer timescales.

The higher r.m.s variability in class II and III systems on timescales <25 days can be explained by the fact that in these more evolved YSOs the stellar photosphere contributes a greater proportion of the K-band luminosity of the system, whereas in less evolved YSOs the luminosity is more dominated by the accretion disc. Consequently we may expect a greater contribution to variability from cold and hot spots in the photosphere of class II and class III YSOs, which manifests itself on the timescale of stellar rotation. We note that variability on rotational timescales of a few days also contributes to the measured mean r.m.s. variability shown in Fig. 23 on all longer timescales, which is why the variation increases rapidly on baselines from zero to 3 days (a typical rotation timescale in YSOs, e.g Alencar et al. 2010) and then increases more slowly thereafter.

It is also very interesting to see that the 250-350 day timescale at which the maximum of mean r.m.s. variability is reached in all classes of YSO corresponds to variablity on spatial scales of 1-2 au, assuming the timescale is determined by Keplerian rotation about low to intermediate mass YSOs. Connelley & Greene (2014) found from a spectroscopic variability study that mass accretion tracers in their sample of class I YSOs, such as Brγ and CO emission, are highly variable over timescales of 1-3 yrs and they proposed the above explanation of the timescale.

Studies of the optical, near infrared and mid-infrared temporal behaviour of YSOs have shown that the great majority are variable at these wavelengths, with their light curves showing a diversity of amplitudes, timescales and morphologies (see e.g. Findeisen et al. 2013; Cody et al. 2014; Rebull et al. 2014; Rice et al. 2015; Wolk et al. 2015). These studies, and the earlier large scale study of Megeath et al. (2012) showed that the amplitude of the variability increases for younger embedded objects, though these works contained few if any YSOs with $\Delta K_s > 1$. Rice et al.

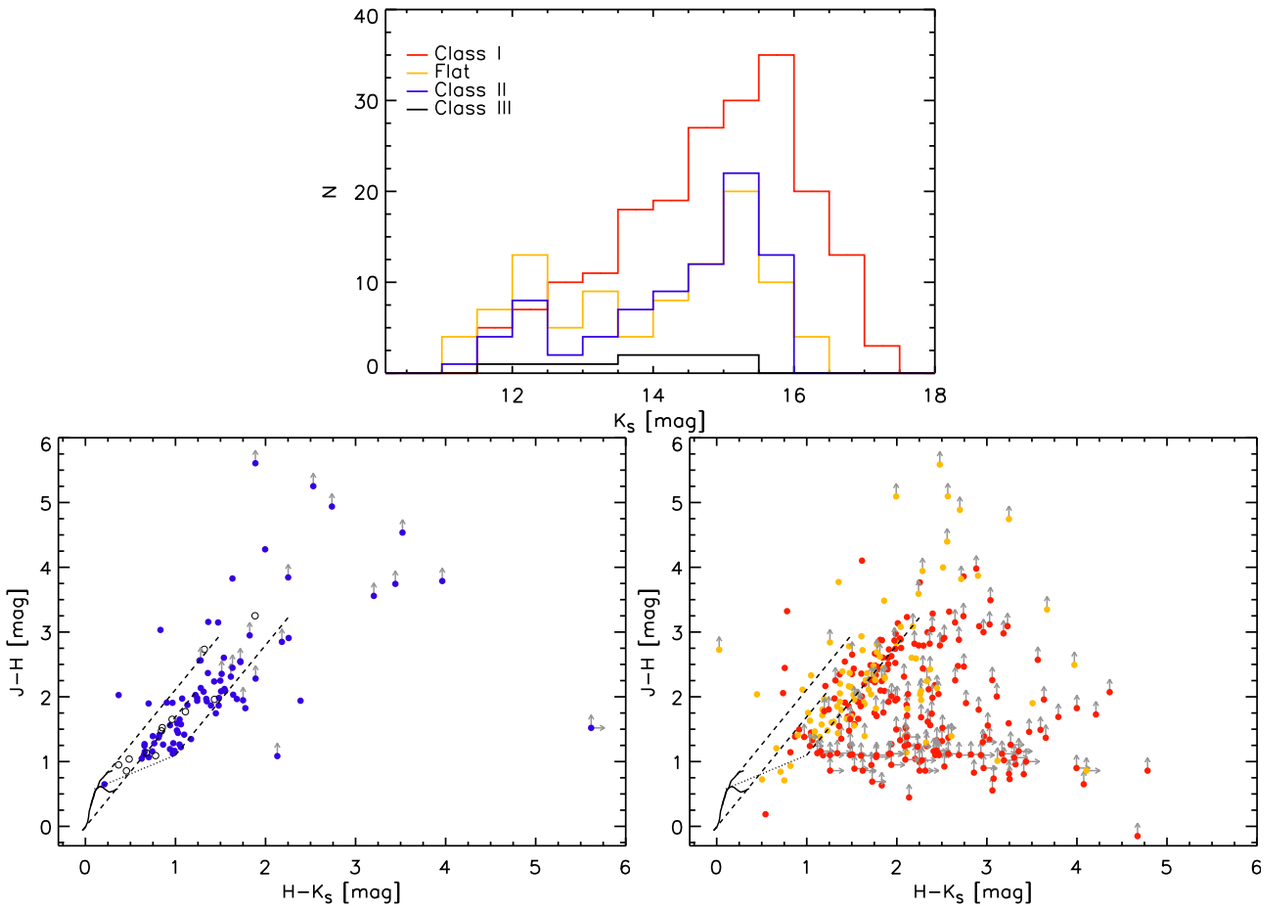

Figure 22. (top) K_s distribution (from 2010 data) of class I (red), flat-spectrum (orange), class II (blue) and class III (black) YSOs. (bottom left) Colour-colour diagram for class II (blue filled circles) and class III YSOs (black open circles) from VVV. In the figure, lower limits in colour are marked by arrows. The classical T Tauri locus of Meyer et al. (1997) is presented (long-dashed line) along with intrinsic colours of dwarfs and giants (solid lines) from Bessell & Brett (1988). Reddening vectors of $A_V = 20$ mag are shown as dotted lines. (bottom right) Colour-colour diagram for class I (red) and flat-spectrum (orange) YSOs.

(2012) found indications that amplitudes $\Delta K > 1$ mag are more common amongst class I systems ($13 \pm 7\%$, based on 2 high amplitude objects in a sample of 30 in the Braid Nebula within Cygnus OB7), whereas such high amplitudes are found to be less common in more evolved YSOs (see e.g. Carpenter et al. 2001).

4.4 Eruptive variability

We have found from the morphological classification that 106 of our SFR-associated high amplitude variables have light curves that show sudden and large increases in brightness. Our near infrared colour variability data, though limited, appears to verify that variability does not arise from changes in the extinction along the line of sight in most cases. As we have discussed previously, large magnitude changes in our sample are more likely explained by either changes in the accretion rate or in the extinction along the line of sight. Since we appear to discard the latter effect in our eruptive variables, we infer that large changes in the accretion rate are the most likely explanation for the observed variability in these objects.

In Fig. 23 (middle panels) we show histograms of the spectral index of the YSOs of each light curve type. We also see that the YSOs classified as eruptive have larger values of α (i.e. redder SEDs) than the other categories of YSO variables. The redder SEDs of the eruptive objects supports the idea that fluctuations in the accretion rates are larger and much more common at early stages of PMS evolution than in the class II stage. This is especially true given that class II YSOs typically outnumber class I YSOs in nearby SFRs by a factor of $\sim$ 3.7-4.8 (see e.g. table 1 in Dunham et al. 2014) due to the greater duration of the class II stage. We have 70 eruptive variables classified as class I YSOs and 5 classified as class II YSOs (the remainder being flat spectrum or class III systems). If we assume that the YSOs classified as eruptive are mainly genuine eruptive variables (which is supported by our spectroscopic follow up in paper II) this tells us that the incidence of eruptive variability is $\sim$50-70 times higher in class I YSOs than class II YSOs. If we consider the possible correction to α due to foreground extinction (see 4.3), then we have 52 class I YSOs and 15 class II YSOs in the eruptive category, so eruptive variability is still 13 to 17 times more common in class I YSOs. We conclude that the difference is at least an order of magnitude.

It is interesting to see that some of the theoretical mod-

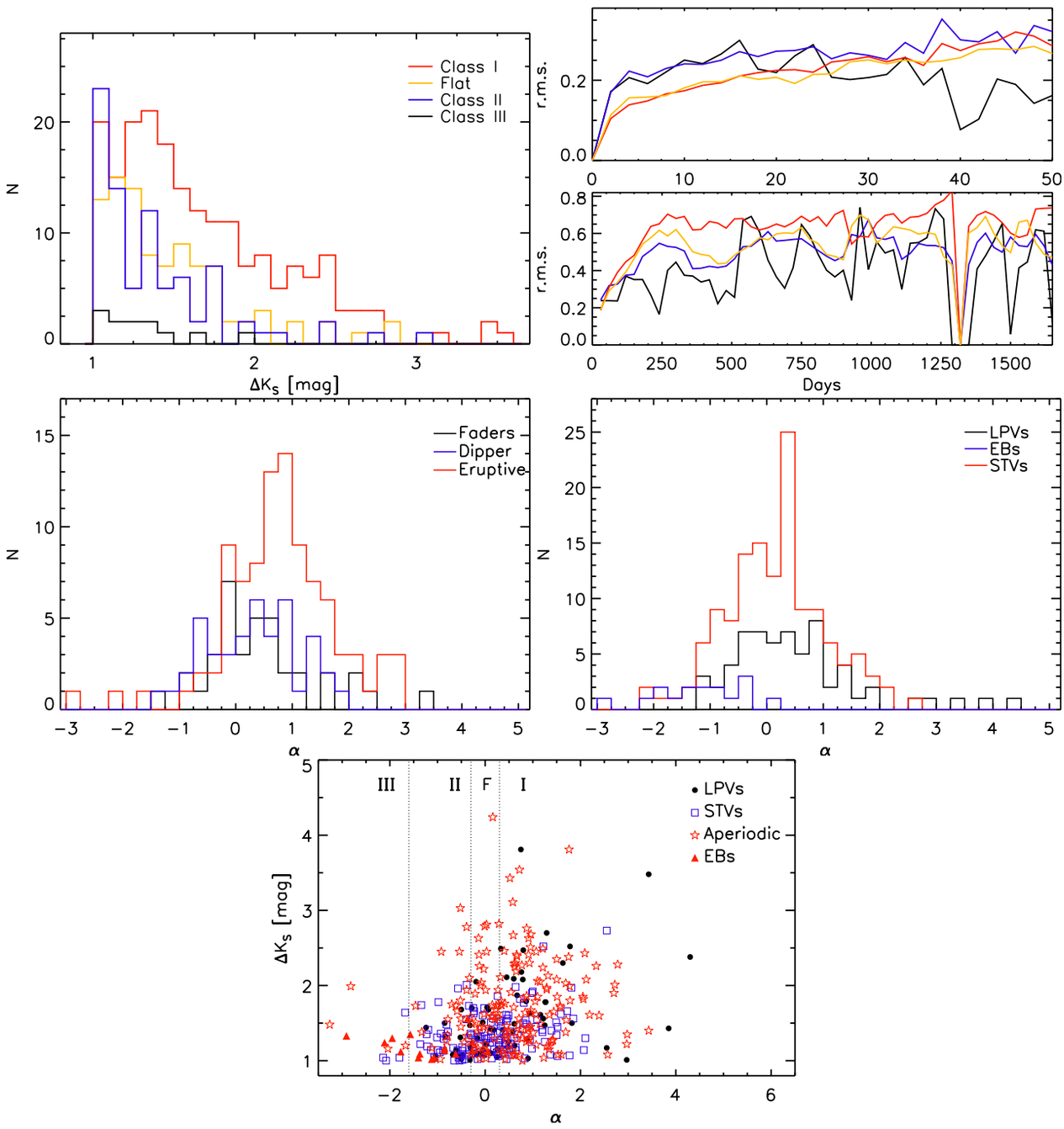

Figure 23. (top, left) ΔK_s distribution of the different YSO classes. (top, right) Mean r.m.s. variability for the different YSO classes in intervals up to 50 days (calculated with time bins of 1 day), and for intervals up to the full 1600 day baseline of the dataset (using time bins of 30 days). The colour coding in the top (left and right) figures is the same as in Fig.22. (middle, left) α distribution for fader (black line), dipper (blue line) and eruptive (red lines) objects. (middle, right) Same distribution but for long-term periodic objects (black lines), stars with short-term variability (red line) and EBs (blue line). (bottom) α vs ΔK_s for objects associated with SFRs. The limits for the different YSO classes are marked by dashed lines. Objects in this figure are divided according to the morphological light curve classification (Sect. 4.1). The different classifications are marked in the plot.

els that explain the outbursts observed in young stars, predict that luminosity bursts are more common in the class I stage compared to later stages of stellar evolution. These models mainly involve gravitational instability (GI) in the outer disc, which is most likely to occur during the embedded phase. GI can cause the outer disc to fragment, forming bound fragments that later migrate into the inner disc. The infall of these fragments can lead to mass accretion bursts. GI can also produce a persistent spiral structure which efficiently transfers mass to small radii. The continuous pile up of mass at lower radii can trigger magneto-rotational instabilities (MRI), which lead to sudden disc outbursts (see

e.g., Zhu et al. 2009; Audard et al. 2014; Vorobyov & Basu 2015, and references therein). Thus invoking these mechanisms might explain the higher occurrence of eruptive variables at younger stages. However, we note that most mechanisms that explain eruptive variability, such as bursts due to binary interaction (Bonnell & Bastien 1992), MRI activated by layered accretion (Zhu et al. 2009) or thermal instabilities (Hartmann & Kenyon 1996), predict outbursts during class I through class II stages of YSO evolution.

The classification as eruptive variables only comes from K_s light curves, and spectroscopic follow up is needed to confirm their YSO nature. However, we note that potentially adding 106 more objects to the YSO eruptive variable class would increase the known members by a factor of five. Moreover, our survey covers just a portion of the Galactic plane. Therefore eruptive variability in YSOs might be more common than previously thought, especially for the most embedded and young objects. Spectroscopic follow up of a subsample of the objects shows that a large fraction of them are indeed eruptive YSOs (see Paper II).

5 INCIDENCE OF ERUPTIVE VARIABILITY

To determine whether episodic accretion plays an important role in the assembly of stars it is essential to have an estimate of the incidence of the phenomenon. Hartmann & Kenyon (1996) estimate that stars must spend $\sim 5\%$ of their lifetime in high states of accretion to gain their final mass during the infall phase. Enoch et al. (2009) and Evans et al. (2009) find that 5-7% of class I stars in their sample are at high accretion states. In this section we attempt to derive an initial estimate of this number using our sample of eruptive variables from VVV and the intrinsically red *Spitzer* sources of Robitaille et al. (2008).

We investigated the intrinsically red *Spitzer* sources of Robitaille et al. (2008), specifically those objects classified by the authors as likely YSOs. The use of GLIMPSE and MIPSGAL (Carey et al. 2009) photometry allows us to study the SEDs of this sample, where we find 2059 class I YSOs in the Galactic disc area studied in our work. From these objects, 51 are found in our list of high amplitude variables in SFRs, 26 of them having the eruptive variable classification. These numbers would imply that approximately 2.5% of class I YSOs show large amplitude variability, and that eruptive variability is observed in 1.3% of YSOs at this evolutionary stage.

Once again we need to take into account the completeness of our sample due to our selection criteria. In Sect. 2.1 we showed that our strict selection criteria caused our sample of high amplitude variables to be only $\sim 50\%$ complete, down to $K_s = 15.5$ mag. In Sect. 2.1 we noted that at magnitudes fainter than $K_s = 15.5$ mag the completeness of our selection falls more steeply. Thus the incompleteness factor in the Robitaille et al. sample is likely to be higher.

We studied the completeness of the Robitaille et al. sample in four widely separated VVV tiles (d052, d065, d072 and d109) using 2010-2014 K_s data, where we found 138 counterparts in the VVV catalogues. If we only consider 2010-2012 data, 22 objects show high amplitude variability [2], are located in SFRs, and have light curves that do not resemble those of AGB stars. From these, 8 are part of the list of high amplitude variables presented in this work, which implies an incompleteness factor of 22/8 or 2.75, caused by the quality cuts that were required in Sect. 2.1 to reduce the number of false positives to a manageable level. This figure is higher than the factor of $\sim$2 (50% completeness) quoted above because many of the class I YSO variables from the Robitaille et al.(2008) list have mean $K_s > 15.5$ magnitudes. If we consider the whole period of 2010-2014, then the number of high amplitude variables increases to 29 raising the incidence by a further factor of 1.32.

We should also consider whether there is a bias towards erupting systems in the Robitaille et al. (2008) sample, which could in general be detected at greater distances, or lower down the mass function, than quiescent systems. Such a bias would only affect our calculation if erupting YSOs detected by GLIMPSE in $\sim$2003 also erupted a second time in 2010-2014. We tested for this by comparing the GLIMPSE $I2$ (4.5 μm) and WISE $W2$ (4.6 μm) magnitudes of the 26 systems from the Robitaille et al. (2008) sample that are included in our list of eruptive YSOs. $W2$ and $I2$ magnitudes for YSOs are typically similar (e.g. Antoniucci et al. 2014). Considering the 20/26 of these systems with $W2$ detections in the WISE AllSky catalogue (data from 2010, typically before the eruption) the median $I2 - W2$ is 0.02 mag. If we transform the *Spitzer* $I2$ magnitudes to the $W2$ passband using the equation given in Antoniucci et al. (2014) then the median difference between the *Spitzer* and WISE data is -0.14 mag. This small number indicates that any luminosity bias toward eruptive systems can be neglected in this initial estimate of their incidence.

After correcting for incompleteness, the incidence of high amplitude variability among class I YSOs rises to 6.8%, including only stars that varied in the 2010-2012 time period. This rises to 9% if we extend the time period to 2010-2014. More importantly the incidence of eruptive variables amongst class I YSOs reaches 3.4%(or 4.6% in the 2010-2014 data). The 4.6% figure has a statistical uncertainty of 40%, not including any biases arising from our use of the sample of Robitaille et al. (2008), so we should express the incidence of eruptive variability as about 3 to 6% over a 4 year timescale. These figures happen to agree with the incidence of outbursts inferred by Enoch et al. (2009) and Evans et al. (2009) from the observation of class I YSOs with high bolometric luminosities. However, their observations are perhaps more likely to trace long-duration, FUor-like outbursts than those detected by VVV.

If we assume that all class I YSOs go through episodes of enhanced accretion at the same average rate, then our estimate that $\sim 4\%$ of them burst over a 4 year period, would imply that roughly every source suffers at least one burst over 100 yr. Froebrich & Makin (2016) study the distribution of the separation between large H_2 knots in jets. The knots likely trace the accretion burst history of a particular source. Froebrich & Makin find that the bright knots have typical separations that correspond to about 1000 yr, which they conclude is too large to be EXor driven and too small to

[2] The true variability of these objects was confirmed via visual inspection of $1' \times 1'$images.

be FUor driven. This number is also larger than the 100 yr burst frequency of the VVV sample. However, further study needs to be done to obtain a more robust estimate, and the assumption of similar behaviour for all class I YSOs is of course questionable.

6 SUMMARY AND CONCLUSIONS

We have searched for high amplitude infrared variables in a 119 deg^2 area of the Galactic midplane covered by the VVV survey, using a method that tends to exclude transients and eruptive variables that saturated during outburst or very faint in quiescence, owing to our requirement for a high quality detection at every epoch. We discovered 816 bona fide variables in the 2010-2012 data with $\Delta K_{\rm s} > 1$ in that time interval. Nearly all of these were previously unknown as variable stars, though a significant minority had been identified as embedded YSO candidates in the Robitaille et al.(2008) catalogue of stars with very red [4.5]-[8.0] *Spitzer*/GLIMPSE colours.

We have presented a fairly simple analysis of the sample using the 2010-2014 VVV light curves, supplemented by a recently obtained 2nd epoch of multi-filter $JHK_{\rm s}$ data and photometry from WISE, and *Spitzer*. Our main conclusions are as follows.

- In agreement with the previous results from searches in the UKIDSS GPS (Contreras Peña et al. 2014), we observe a strong concentration of high-amplitude infrared variables towards areas of star formation. The two point correlation function and nearest neighbour distribution of VVV objects show evidence for clustering on angular scales typical of distant Galactic clusters and SFRs. The variable stars found in SFRs are characterized by having near-infrared colours and SEDs of YSOs.
- The most common types of variable outside SFRs are LPVs (typically dust-obscured Mira variables because other types are saturated in VVV) and EBs. By visual inspection of the light curves of the variables in SFRs we were able to identify and remove most of these contaminating systems and provide a reasonably clean sample of high amplitude YSOs. The YSOs make up about half of the full sample of 816 variables.
- We analysed the light curves of the variables in SFRs, after removal of likely Mira-types, and we classify them as 106 eruptive variables, 39 faders, 45 dippers, 162 short term variables, 65 long-term periodic variables ($P > 100$ days) and 24 eclipsing binaries (EBs) and EB candidates. Individual YSOs may display more than 1 type of variability and the low amplitude variation on short timescales seen in normal YSOs is common in every category.
- Spectroscopic follow up of a substantial subset of the variables with eruptive light curves is presented in the companion paper (Paper II), confirming that the great majority of systems with eruptive light curves are indeed eruptive variables with signatures of strong accretion similar to those seen in EXors or FUors, or a mixture of the two. The 2 epochs of VVV $JHK_{\rm s}$ multi-colour data indicate that extinction is not the main cause of the variability in systems with eruptive light curves, though there is a trend for the sources to become bluer when brighter, similar to EXors. The faders show a wider range of colour behaviour, with more examples of "bluer when fainter" than the other categories.
- Unsurprisingly, very few of the EBs showed significant magnitude or colour changes between the two multi-colour epochs. Amongst the STVs and dippers, we observe large colour and magnitude changes that appear to differ from the reddening vector, although this conclusion seems to depend on the selection of objects from these classes. We observed changes consistent with the reddening vector in a few systems. It is possible that the flux changes in some of the STVs are caused by extinction, e.g. as has been observed in some binary YSOs with a circumbinary disc (Windemuth & Herbst 2014; Rice et al. 2015).
- The STVs typically have lower amplitudes than any other category except the EBs and EB candidates. Moreover, the STVs have a bluer distribution of spectral indices than the full YSO sample, including a high proportion of class II YSOs with relatively low extinction. It is likely that in many of the STVs with periods P$<$ 15 days and $K_{\rm s}$ amplitudes not far above 1 magnitude the light curve is rotationally modulated by unusually prominent bright or dark spots on the photosphere.
- Variables in the eruptive and fader categories tend to have higher amplitudes than the full YSO sample over the 4 year period, with mean $\Delta K_{\rm s} = 1.72$ and 1.95 mag, respectively, compared to 1.56 mag for the full YSO sample.
- It is reasonable to suppose that variable accretion is the cause of photometric variability in a proportion of the faders and some of the long-term periodic variables and STVs, although spectroscopic confirmation is limited in these categories as yet. In the periodic variables the accretion rate would presumably be modulated by a companion body (Hodapp et al. 2012). Adding these together with the $\sim$100 YSOs with eruptive light curves suggests that the sample contains between 100 and 200 YSOs in which the variability is caused by large changes in accretion. If we take the lower end of this range, this increases the number of probable eruptive variable YSOs available for study by a factor of 5. Some of these systems have $K_{\rm s}$ amplitudes not far above the 1 mag level, below which variability due to spots and smaller changes in accretion rate and extinction becomes much more common. However, we see no clear argument for a higher threshold given that the amplitudes have a continuous distribution that can be be influenced in individual YSOs by the mass and luminosity of the central protostar as much as the change in accretion rate (Calvet et al. 1991).
- As a whole, the high amplitude variables are a very red sample, dominated by embedded YSOs (i.e. systems with Class I or flat spectrum SEDs that are typically not observable at optical wavelengths). This contrasts with the optical selection of the classical FUors and EXors, the majority of which have a class II or flat spectrum classification. While FUors are often discussed as systems with a remnant envelope, only 3 or 4 deeply embedded eruptive variables were known prior to this study and our recent UGPS 2-epoch study.
- Variables with eruptive light curves tend to have the reddest SEDs. The spectral indices in the eruptive category indicate that this type of variability is at least one order of magnitude more common among class I YSOs than class II YSOs. This demonstrates that eruptive variability is either much more common or recurs much more frequently

amongst YSOs at earlier stages of pre-MS evolution, when average accretion rates are higher. We hope this result will inform ongoing efforts to develop a theoretical framework for the phenomenon.

• For the full sample of YSOs, the r.m.s. variability is higher at earlier evolutionary (SED) classes for time intervals longer than 25 days, and reaches a maximum at 250-350 days for all SED classes. The full duration of the outbursts in eruptive systems is typically 1 to 4 years. Some variables with eruptive light curves show more than 1 outburst. If some of the faders are eruptive variables in decline then a similar or slightly longer duration would apply.

• At time intervals shorter than 25 days the evolutionary dependence is reversed, with class II YSOs showing higher amplitudes than flat spectrum and class I YSOs. This suggests that the shorter timescale variations are dominated by rotational modulation by spots on the photosphere (which are more readily observed in class II systems than embedded YSOs) whereas accretion variations usually take place on longer timescales.

• The 1 to 4 year duration of the eruptions is between that of FUors ($>$ 10 years) and EXors (weeks to months) A small but growing number of eruptive YSOs with these intermediate durations have been found in recent years, some of which have a mixture of the spectroscopic characteristics of FUors and EXors. This has led to the recent concept that FUor and EXors may simply be part of a range of different eruptive behaviours on different timescales, all driven by large variations in accretion rate. Until now it was unclear whether these recent discoveries were rare exceptions, but it now seems clear that they are not. In fact we find that YSOs with intermediate outburst durations outnumber short EXor-like outbursts and are now the majority of known eruptive systems, A much longer duration survey would be required to determine the incidence of FUor-like outbursts amongst embedded systems. In paper II we propose a new class of eruptive variable to describe YSOs with eruptive outbursts of intermediate duration, which are usually optically obscured class I or flat spectrum YSOs and display a variety of the EXor-like and/or FUor-like spectroscopic signatures of strong accretion.

• We investigated the intrinsically red *Spitzer* sources of Robitaille et al. (2008), specifically those objects classified by the authors as likely YSOs. We find 2059 such objects in the area covered by VVV. From these 51 are found in the list of high amplitude variables in SFRs from this work, with 26 of them being classified as eruptive variables. After correcting for incompleteness imposed by the strict selection criteria in the VVV sample, we estimate that high amplitude variability is observed from 6.8% (when considering 2010-2012 data) up to 9% (when considering 2010-2014 data) of class I YSOs. More importantly, the incidence of eruptive variability amongst class I YSOs rises to 3.4–4.6%. This estimate agrees with those inferred from observations of class I YSOs by Evans et al. (2009) and Enoch et al. (2009). However, the agreement might be a coincidence considering that their observations are likely tracing long-duration, FUor-like outbursts, rather than those detected in our study.

• YSOs are the commonest type of high amplitude infrared variable detected by the VVV survey. We estimate a completeness-corrected source density of 7 deg^{-2} in the mid-plane of quadrant 4, in the approximate mean magnitude range $11 < K_s < 16$. These YSOs are detected at typical distances of a few kpc, there being no very nearby SFRs in the area surveyed; they are therefore likely to be intermediate-mass YSOs. If we were able to detect such objects out to the far edge of the Galactic disc the source density would rise to perhaps $\sim$ 40 deg^{-2}. This confirms our previous suggestion in Contreras Peña et al. (2014) that high amplitude YSO variables have a higher source density and average space density than Mira variables. EBs are very common at low amplitudes and they may have a comparable space density to YSOs at K_s amplitudes of 1 to 1.6 mag (an approximate upper limit for EBs in *Kepler*). YSOs are more numerous at higher amplitudes and may well be more numerous for all amplitudes over 1 mag if the eruptive phenomenon extends to the lower part of the stellar Initial Mass Function.

ACKNOWLEDGMENTS

This work was supported by the UK's Science and Technology Facilities Council, grant numbers ST/J001333/1, ST/M001008/1 and ST/L001403/1.

We gratefully acknowledge the use of data from the ESO Public Survey program 179.B-2002 taken with the VISTA 4.1m telescope and data products from the Cambridge Astronomical Survey Unit. Support for DM, and CC is provided by the Ministry of Economy, Development, and Tourisms Millennium Science Initiative through grant IC120009, awarded to the Millennium Institute of Astrophysics, MAS. DM is also supported by the Center for Astrophysics and Associated Technologies PFB-06, and Fondecyt Project No. 1130196. This research has made use of the SIMBAD database, operated at CDS, Strasbourg, France; also the SAO/NASA Astrophysics data (ADS). A.C.G. was supported by the Science Foundation of Ireland, grant 13/ERC/I2907. We also acknowledge the support of CONICYT REDES project No. 140042 "Young variables and proper motion in the Galactic plane. Valparaiso-Hertfordshire collaboration"

C. Contreras Peña was supported by a University of Hertfordshire PhD studentship in the earlier stages of this research.

We thank Janet Drew for her helpful comments on the structure of the paper.

REFERENCES

Alencar, S. H. P., et al. 2010, A&A, 519, A88
Antoniucci, S., Giannini, T., Li Causi, G., & Lorenzetti, D. 2014, ApJ, 782, 51
Armstrong, D. J., Gómez Maqueo Chew, Y., Faedi, F., & Pollacco, D. 2014, MNRAS, 437, 3473
Aspin, C., Beck, T. L., & Reipurth, B. 2008, AJ, 135, 423
Aspin, C., Greene, T. P., & Reipurth, B. 2009, AJ, 137, 2968
Audard, M., et al. 2014, Protostars and Planets VI, 387
Avedisova, V. S. 2002, Astronomy Reports, 46, 193
Bans, A. & Königl, A. 2012, ApJ, 758, 100
Baraffe, I., Chabrier, G., & Gallardo, J. 2009, ApJ, 702, L27

Baraffe, I., Vorobyov, E., & Chabrier, G. 2012, ApJ, 756, 118
Bate, M. R., Clarke, C. J., & McCaughrean, M. J. 1998, MNRAS, 297, 1163
Benjamin, R. A., et al. 2003, PASP, 115, 953
Bessell, M. S. & Brett, J. M. 1988, PASP, 100, 1134
Bonnell, I. & Bastien, P. 1992, ApJL, 401, L31
Bouvier, J., Grankin, K., Ellerbroek, L. E., Bouy, H., & Barrado, D. 2013, A&A, 557, A77
Budding, E., Erdem, A., Çiçek, C., Bulut, I., Soydugan, F., Soydugan, E., Bakiş, V., & Demircan, O. 2004, A&A, 417, 263
Calvet, N., Patino, A., Magris, G. C., & D'Alessio, P. 1991, ApJ, 380, 617
Caratti o Garatti, A., et al. 2012, A&A, 538, A64
Caratti o Garatti, A., et al. 2011, A&A, 526, L1
Carey, S. J., et al. 2009, PASP, 121, 76
Carpenter, J. M., Hillenbrand, L. A., & Skrutskie, M. F. 2001, AJ, 121, 3160
Catelan, M., et al. 2013, ArXiv:1310.1996
Chen, C.-H. R., Chu, Y.-H., Gruendl, R. A., Gordon, K. D., & Heitsch, F. 2009, ApJ, 695, 511
Cioni, M.-R. L., et al. 2011, A&A, 527, A116
Cody, A. M., et al. 2014, AJ, 147, 82
Connelley, M. S. & Greene, T. P. 2014, AJ, 147, 125
Contreras Peña, C., et al. 2014, MNRAS, 439, 1829
Culverhouse, T., et al. 2011, ApJS, 195, 8
Derue, F., et al. 2002, A&A, 389, 149
Drew, J. E., et al. 2014, MNRAS, 440, 2036
Dunham, M. M., et al. 2014, Protostars and Planets VI, 195
Eiroa, C., et al. 2002, A&A, 384, 1038
Enoch, M. L., Evans, II, N. J., Sargent, A. I., & Glenn, J. 2009, ApJ, 692, 973
Epchtein, N., et al. 1994, A&SS, 217, 3
Evans, II, N. J., et al. 2009, ApJS, 181, 321
Findeisen, K., Hillenbrand, L., Ofek, E., Levitan, D., Sesar, B., Laher, R., & Surace, J. 2013, ApJ, 768, 93
Froebrich, D. & Makin, S. V. 2016, MNRAS, 462, 1444
Gonzalez, O. A., Rejkuba, M., Zoccali, M., Valenti, E., & Minniti, D. 2011, A&A, 534, A3
Greene, T. P. & Lada, C. J. 1996, AJ, 112, 2184
Greene, T. P., Wilking, B. A., Andre, P., Young, E. T., & Lada, C. J. 1994, ApJ, 434, 614
Hartmann, L. & Kenyon, S. J. 1996, ARA&A, 34, 207
Herbst, W. & Shevchenko, V. S. 1999, AJ, 118, 1043
Hodapp, K. W. & Chini, R. 2015, ApJ, 813, 107
Hodapp, K. W., Chini, R., Watermann, R., & Lemke, R. 2012, ApJ, 744, 56
Hodapp, K.-W., Hora, J. L., Rayner, J. T., Pickles, A. J., & Ladd, E. F. 1996, ApJ, 468, 861
Huckvale, L., Kerins, E., & Sale, S. E. 2014, MNRAS, 442, 259
Hughes, J. P., Slane, P., Posselt, B., Charles, P., Rajoelimanana, A., Sefako, R., Halpern, J., & Steeghs, D. 2010, The Astronomer's Telegram, 2771, 1
Irwin, M. 2009, UKIRT Newsletter, 25, 15
Ishihara, D., Kaneda, H., Onaka, T., Ita, Y., Matsuura, M., & Matsunaga, N. 2011, A&A, 534, A79
Javadi, A., Saberi, M., van Loon, J. T., Khosroshahi, H., Golabatooni, N., & Mirtorabi, M. T. 2015, MNRAS, 447, 3973
Jiménez-Esteban, F. M., García-Lario, P., Engels, D., & Manchado, A. 2006a, A&A, 458, 533
Jiménez-Esteban, F. M., García-Lario, P., Engels, D., & Perea Calderón, J. V. 2006b, A&A, 446, 773
Kenyon, S. J., Hartmann, L. W., Strom, K. M., & Strom, S. E. 1990, AJ, 99, 869
Koenig, X. P. & Leisawitz, D. T. 2014, ApJ, 791, 131
Kóspál, Á., Ábrahám, P., Prusti, T., Acosta-Pulido, J., Hony, S., Moór, A., & Siebenmorgen, R. 2007, A&A, 470, 211
Lada, C. J. 1987, in IAU Symposium, Vol. 115, Star Forming Regions, ed. M. Peimbert & J. Jugaku, 1
Lawrence, A., et al. 2007, MNRAS, 379, 1599
López-Morales, M. & Clemens, J. C. 2004, PASP, 116, 22
Lorenzetti, D., et al. 2012, ApJ, 749, 188
Lorenzetti, D., Larionov, V. M., Giannini, T., Arkharov, A. A., Antoniucci, S., Nisini, B., & Di Paola, A. 2009, ApJ, 693, 1056
Lucas, P. W., et al. 2008, MNRAS, 391, 136
Marshall, D. J., Robin, A. C., Reylé, C., Schultheis, M., & Picaud, S. 2006, A&A, 453, 635
Megeath, S. T., et al. 2012, AJ, 144, 192
Meyer, M. R., Calvet, N., & Hillenbrand, L. A. 1997, AJ, 114, 288
Minniti, D., et al. 2010, NewA, 15, 433
Minniti, D., Saito, R. K., Alonso-García, J., Lucas, P. W., & Hempel, M. 2011, ApJL, 733, L43
Murakami, H., et al. 2007, PASJ, 59, 369
Ninan, J. P., et al. 2015, ApJ, 815, 4
Ochsenbein, F., Bauer, P., & Marcout, J. 2000, A&AS, 143, 23
Paczyński, B., Szczygieł, D. M., Pilecki, B., & Pojmański, G. 2006, MNRAS, 368, 1311
Persi, P., Tapia, M., Gòmez, M., Whitney, B. A., Marenzi, A. R., & Roth, M. 2007, AJ, 133, 1690
Pietrukowicz, P., et al. 2013, AcA, 63, 115
Plavchan, P., Gee, A. H., Stapelfeldt, K., & Becker, A. 2008, ApJL, 684, L37
Price, S. D., Egan, M. P., Carey, S. J., Mizuno, D. R., & Kuchar, T. A. 2001, AJ, 121, 2819
Rebull, L. M., et al. 2014, AJ, 148, 92
Reipurth, B. & Aspin, C. 2010, in Evolution of Cosmic Objects through their Physical Activity, ed. H. A. Harutyunian, A. M. Mickaelian, & Y. Terzian, 19
Rice, T. S., Reipurth, B., Wolk, S. J., Vaz, L. P., & Cross, N. J. G. 2015, AJ, 150, 132
Rice, T. S., Wolk, S. J., & Aspin, C. 2012, ApJ, 755, 65
Robitaille, T. P., et al. 2008, AJ, 136, 2413
Robitaille, T. P., Whitney, B. A., Indebetouw, R., Wood, K., & Denzmore, P. 2006, ApJS, 167, 256
Romanova, M. M., Ustyugova, G. V., Koldoba, A. V., & Lovelace, R. V. E. 2013, MNRAS, 430, 699
Russeil, D. 2003, A&A, 397, 133
Safron, E. J., et al. 2015, ApJL, 800, L5
Saito, R. K., et al. 2012, A&A, 537, A107
Saito, R. K., et al. 2013, A&A, 554, A123
Schechter, P. L., Mateo, M., & Saha, A. 1993, PASP, 105, 1342
Schlafly, E. F. & Finkbeiner, D. P. 2011, ApJ, 737, 103
Schlegel, D. J., Finkbeiner, D. P., & Davis, M. 1998, ApJ, 500, 525
Scholz, A. 2012, MNRAS, 420, 1495

Scholz, A., Froebrich, D., & Wood, K. 2013, MNRAS, 430, 2910
Simpson, R. J., et al. 2012, MNRAS, 424, 2442
Skrutskie, M. F., et al. 2006, AJ, 131, 1163
Stellingwerf, R. F. 1978, ApJ, 224, 953
Tudose, V., Fender, R. P., Tzioumis, A. K., Spencer, R. E., & van der Klis, M. 2008, MNRAS, 390, 447
van Loon, J. T., Cohen, M., Oliveira, J. M., Matsuura, M., McDonald, I., Sloan, G. C., Wood, P. R., & Zijlstra, A. A. 2008, A&A, 487, 1055
Vijh, U. P., et al. 2009, AJ, 137, 3139
Vorobyov, E. I. & Basu, S. 2015, ApJ, 805, 115
Ward, J. L., Oliveira, J. M., van Loon, J. T., & Sewiło, M. 2016, MNRAS, 455, 2345
Wenger, M., et al. 2000, A&AS, 143, 9
Whitelock, P. A., Feast, M. W., & van Leeuwen, F. 2008, MNRAS, 386, 313
Windemuth, D. & Herbst, W. 2014, AJ, 147, 9
Wolk, S. J., et al. 2015, AJ, 150, 145
Wolk, S. J., Rice, T. S., & Aspin, C. 2013, ApJ, 773, 145
Wright, E. L., et al. 2010, AJ, 140, 1868
Zhu, Z., Hartmann, L., & Gammie, C. 2009, ApJ, 694, 1045

APPENDIX A: ECLIPSING BINARIES

In order to compare the YSO and EB space densities, we look at the measured source density of EBs detected in Galactic disc fields by OGLE-III (Pietrukowicz et al. 2013) and estimate their distances with the help of a recent analysis of the physical properties of *Kepler* eclipsing binaries (Armstrong et al. 2014).

Shallow surveys such as the Automated All-Sky Survey (ASAS Paczyński et al. 2006) are sensitive only to the more luminous high amplitude EBs, which are mainly early type Algol systems, similar to the high amplitude EBs in the General Catalogue of Variable Stars (Samus et al.2010). However, simulations by López-Morales & Clemens (2004) find that EBs seen by deeper surveys such as OGLE-III will be dominated by later type systems. Armstrong et al. (2014) analysed the large sample of EBs discovered by *Kepler*, providing temperature and radius estimates for the full sample. They note that their results are most accurate for cases where the temperatures of the primary and the secondary are very different, which is fortunate because this is characteristic of high amplitude EBs, in which a hotter main sequence star is eclipsed by a cooler giant star. Inspection of their results shows that high amplitude EBs fall into 2 groups: EBs with early type primaries and EBs with F or early G-type primaries. Simple calculations assuming Planckian SEDs indicate that only the latter group can produce eclipses deeper than 1 magnitude in the $K_{\rm s}$ passband (and this group also dominates in the OGLE I passband) because early type stars emit little of their total flux in the infrared. The same calculations indicate that no systems with $K_{\rm s}$ amplitudes above 1.6 mag exist in the *Kepler* sample, whereas YSOs with higher amplitudes are common in our sample, see Sect. 4. Applying this approach in the optical indicates that EBs should exist with amplitudes up to 3 mag in the I passband. This limit is confirmed by the OGLE-III sample of Pietrukowicz et al. (2013), thereby giving confidence that our limit of 1.6 mag at $K_{\rm s}$ is robust. Indeed our VVV sample of 72 EBs contains no systems with higher amplitude than this. We can assume that the EBs from Pietrukowicz et al. (2013) are mainly composed of F or early G-type stars, based on the *Kepler* results, together with the fact that later type primaries are not expected given the need for these systems to have produced a post-main sequence star within the lifetime of the Galactic disc. Pietrukowicz et al. (2013) reports the discovery of 11589 EBs in area of 7.21 deg^2 across different fields on the Galactic midplane. The catalogue of EBs is reported to be 75% complete to I=18. Correcting for the 75% completeness indicates a source density of 2143 EBs deg^{-2}, from which only $\sim$ 1.6% display $\Delta I > 1$ magnitude. Our earlier calculation (assuming Planckian SEDs) from the results of Armstrong et al. (2014) suggests that this drops to 0.6% at $K_{\rm s}$. This implies $\sim$12 high amplitude EBs per deg^2. We can estimate the extinction to the EBs from their observed $V-I$ colours and then roughly estimate their typical distances either using the absolute I magnitudes of F to early G-stars or by converting extinction to distance using the red clump giant branch (as in Sect. 4.3). Both approaches indicate that the EBs from Pietrukowicz et al. (2013) are typically at heliocentric distances of a few kpc, which is similar to the estimated distances to our YSOs based on radial velocities, literature distances to the SFRs and SED fitting (see paper II). Given that the surface density of EBs ($\sim$12 deg^{-2}) is similar to the surface density of the VVV YSO population sampled in this study ($\sim$7 deg^{-2}), the similar distances suggest that the high amplitude EB and YSO populations may have similar average space densities, within an order of magnitude. The YSO population is certainly more numerous at $K_{\rm s}$ amplitudes over 1.6 mag. If the high amplitude YSO population extends well below a solar mass, which is very possible, then they would probably be more numerous even at our $\Delta K_{\rm s}$=1 mag threshold. However, the VVV and OGLE-III data tell us only that both populations are substantial. The number of YSOs rises steeply up to the sensitivity limit and a similar trend is obtained in EBs if we assume that a significant fraction of the unclassified variables shown in Fig. 10 are EBs.

APPENDIX B: MID-INFRARED COLOUR AND MAGNITUDE VARIABILITY

Photometry from the WISE and NEOWISE missions in the W1 (3.4 μm) and W2 (4.6 μm) passbands are available at 4 epochs for the whole sky, with simultaneous photometry in the two filters. The WISE satellite scanned the whole sky twice in 2010, at epochs separated by 6 months, and the extended mission, NEOWISE, has repeated the process in 2014. For any given sky location, each epoch is composed of multiple scans taken over a period of several days. For all the high amplitude variables, we downloaded photometry for all these scans from the AllWISE Multiepoch Photometry table (for the 2010 data) and NEOWISE-R Single Exposure L1b Source Table (for the 2014 data), both of which are archived in IRSA.

Inspection of the W1 and W2 photometry indicated that the uncertainties typically become larger for saturated stars and for faint stars in crowded Galactic fields. For this analysis we therefore considered only sources with

Category	Median $\Delta W1$	Median $\Delta W2$	Median $\Delta(W1-W2)$	No. in sample
Faders	1.33	0.93	0.37	12
Eruptive	0.72	0.56	0.26	21
LPV-YSOs	0.62	0.67	0.13	23
STVs	0.50	0.38	0.10	11
Dippers	0.59	0.62	0.27	9

Table B1. Colour and megnitude changes measured by WISE.

$7 < W1 < 11$, and $6 < W2 < 11$ (defining these cuts with the AllWISE Source Catalog). We combined the data from the multiple scans into the 4 widely separated epochs by binning the scans into groups (epochs) with a maximum baseline of 20 days and computing the medians of $W1$, $W2$ and $(W1-W2)$ at each epoch.

In most cases the WISE data do not sample the full peak to trough variation in the VVV light curves, so changes in W1 and W2 fluxes are often small. We define $\Delta W1$, $\Delta W2$ and $\Delta(W1-W2)$ for each source as the largest difference observed at any two epochs (not necessarily the same pair of epochs for each quantity). Then considering each type of VVV light curve category, we present the median of these quantities in Table B1. We see that both magnitude and colour variability are typically larger for faders than the other categories, as is the case in $K_{\rm s}$. Eruptive sources, dippers and lpv-YSOs have similar magnitude changes, while STVs have smaller changes (as in $K_{\rm s}$). EBs typically show negligible changes since the eclipses are very rarely sampled.

The WISE data are less useful than the $JHK_{\rm s}$ data for investigating the physical cause of the photometric variability in $K_{\rm s}$ because the extinction vs wavelength relation appears to depend strongly on environment (Koenig & Leisawitz 2014). Also, extinction is lower in the WISE passbands than at $K_{\rm s}$ so extinction may have less effect on the $W1-W2$ colour than even a modest change in accretion rate.

In most STVs and LPV-YSOs we can confidently state the extinction is not the main cause of the measured W1-W2 colour changes because the trend over the 4 epochs is "bluer when fainter", or a negligible colour change, or there is no clear trend. In the eruptive and fader categories about half the variables (10/21 and 7/12) have a "redder when fainter" trend that might be due to variable accretion, variable extinction, or a combination of the two (in some sources, 1 of the 4 epochs does not follow the trend of the other 3 epochs). The remainder of the eruptive variables and faders show a different trend or no clear result. In some sources with a "redder when fainter" trend in the WISE data, the 2 epochs of $JHK_{\rm s}$ data appear to rule out extinction as the cause of variability. In dippers, the majority (5/9) sources have a "redder when fainter" trend that might be consistent with extinction.

These results are not very informative because of the limited sampling of the WISE data. In most cases $K_{\rm s}-W1$, $K_{\rm s}-W2$ changes cannot be investigated because there are very few sources for which two of the WISE epochs are contemporaneous with VVV $K_{\rm s}$ epochs.

Fortunately, there are some sources with clear long term trends in the 2010-2014 VVV light curves for which we can usefully compare WISE data from 2010 and 2014. Four examples of such sources are VVVv270, VVVv631, VVV118 and VVVv562, all of which are members of the spectroscopic sub-sample that are discussed individually in Paper II. To bring together those sources here, we note that all four have unusually large amplitudes in $K_{\rm s}$, $W1$ and $W2$ ($2.6 < \Delta K_{\rm s} < 4.2$ mag). The first two show a rising trend (classed as eruptive light curves) whereas the other two show a declining trend: VVVv562 is a fader but VVVv118 is an eruptive variable with several brief eruptions superimposed on a long-term decline. In every case the trend is similar in the 3 wavelengths but the amplitude is larger in $K_{\rm s}$ than in $W1$ and $W2$, typically by a factor between 1 and 2. Three sources have $\Delta W1 \approx \Delta W2$ (VVVv118, VVVv562, VVVv631), whereas in VVVv270 $\Delta W1 \approx 2\Delta W2$.

The spectroscopic evidence in paper II indicates that these four variables are all bona fide eruptive variables driven by episodic accretion, so the different amplitudes in the different filters presumably reflect differing changes in the luminosity of the different regions of the accretion disc responsible for most of the emission at each wavelength, as well as the effect of temperature changes on the flux emitted by each region at different wavelengths.

APPENDIX C: TABLE 2

In here we present the full version of Table 2.

Table C1: Parameters of the high-amplitude variables from VVV.

Object ID	VVV Designation	α (J2000)	δ (J2000)	l (degrees)	b (degrees)	Z (mag)	Z_{err} (mag)	Y (mag)	Y_{err} (mag)	J (mag)	J_{err} (mag)	H (mag)	H_{err} (mag)	$K_{\rm s}$ (mag)	$K_{\rm s,err}$ (mag)	$\Delta K_{\rm s}$ (mag)	α_{class}	SFR	Class	Period (days)
VVVv1	VVV J114135.16-622055.51	11:41:35.16	-62:20:55.51	294.92603	-0.56770	–	–	–	–	17.99	0.06	15.95	0.02	14.44	0.01	1.34	-0.29	y	STV	72
VVVv2	VVV J114412.94-623449.09	11:44:12.94	-62:34:49.09	295.28005	-0.71146	–	–	–	–	–	–	18.78	0.23	15.71	0.03	2.52	1.22	y	STV	–
VVVv3	VVV J115113.03-623729.29	11:51:13.03	-62:37:29.29	296.07199	-0.55784	13.17	0.01	12.93	0.01	12.90	0.01	12.70	0.01	12.24	0.01	2.21	–	n	Known	–
VVVv4	VVV J115808.69-630708.60	11:58:08.69	-63:07:08.60	296.95057	-0.86785	–	–	–	–	18.23	0.08	16.62	0.04	15.32	0.02	1.10	-0.24	y	STV	–
VVVv5	VVV J115959.68-622613.20	11:59:59.68	-62:26:13.20	297.02026	-0.15716	17.69	0.02	16.62	0.01	15.87	0.01	15.25	0.01	13.53	0.01	1.30	–	n	LPV	–
VVVv6	VVV J115937.81-631109.77	11:59:37.81	-63:11:09.77	297.12836	-0.89953	19.02	0.05	18.08	0.04	16.80	0.02	15.95	0.02	15.50	0.02	1.02	–	n	EB	1.64
VVVv7	VVV J120202.67-623615.60	12:02:02.67	-62:36:15.60	297.28472	-0.27538	–	–	–	–	–	–	–	–	17.22	0.12	1.60	2.39	y	Eruptive	–
VVVv8	VVV J120059.11-631636.18	12:00:59.11	-63:16:36.18	297.29582	-0.95838	–	–	–	–	–	–	–	–	16.86	0.09	1.38	0.64	y	Eruptive	–
VVVv9	VVV J120217.23-623647.83	12:02:17.23	-62:36:47.83	297.31381	-0.27888	–	–	–	–	18.29	0.08	16.33	0.03	14.64	0.01	2.78	-0.39	y	Dipper	–
VVVv10	VVV J120250.85-622437.62	12:02:50.85	-62:24:37.62	297.33912	-0.06749	18.57	0.04	18.23	0.05	16.97	0.03	16.35	0.03	16.07	0.04	1.19	–	n	STV	–
VVVv11	VVV J120436.62-625704.60	12:04:36.62	-62:57:04.60	297.63741	-0.56188	20.20	0.19	19.01	0.13	17.87	0.07	16.79	0.05	16.08	0.08	1.10	–	n	STV	–
VVVv12	VVV J121033.19-630755.71	12:10:33.19	-63:07:55.71	298.33185	-0.62611	–	–	–	–	–	–	16.30	0.03	15.04	0.03	1.74	0.28	y	Fader	–
VVVv13	VVV J121216.83-624838.32	12:12:16.83	-62:48:38.32	298.47603	-0.27814	–	–	–	–	–	–	–	–	16.72	0.14	1.40	1.39	y	STV	–
VVVv14	VVV J121218.13-624904.48	12:12:18.13	-62:49:04.48	298.47958	-0.28495	19.48	0.10	18.88	0.12	17.84	0.06	16.74	0.05	15.56	0.05	1.29	0.88	y	LPV-YSO	124
VVVv15	VVV J121226.09-624416.97	12:12:26.09	-62:44:16.97	298.48252	-0.20371	19.00	0.07	17.72	0.04	16.57	0.02	15.60	0.02	15.04	0.03	1.09	–	y	EB	2.27
VVVv16	VVV J121329.76-624107.74	12:13:29.76	-62:41:07.74	298.59498	-0.13364	18.01	0.03	17.13	0.02	16.06	0.01	14.72	0.01	13.66	0.01	1.29	0.92	y	Eruptive	–
VVVv17	VVV J121352.08-625549.90	12:13:52.08	-62:55:49.90	298.67278	-0.36986	–	–	–	–	–	–	17.79	0.12	16.41	0.10	1.22	0.44	y	STV	–
VVVv18	VVV J121950.31-632142.24	12:19:50.31	-63:21:42.24	299.39868	-0.70695	17.82	0.02	17.29	0.02	16.20	0.01	15.52	0.01	15.32	0.02	1.04	–	n	STV	–
VVVv19	VVV J122255.30-632352.56	12:22:55.30	-63:23:52.56	299.74594	-0.70270	19.56	0.08	18.67	0.06	17.55	0.04	16.40	0.03	15.61	0.03	1.82	–	n	EB	16.88
VVVv20	VVV J122827.97-625713.97	12:28:27.97	-62:57:13.97	300.32402	-0.19849	–	–	–	–	17.38	0.04	14.10	0.01	11.70	0.01	1.71	0.60	y	Eruptive	–
VVVv21	VVV J122902.24-625234.10	12:29:02.24	-62:52:34.10	300.38193	-0.11533	–	–	–	–	–	–	17.12	0.05	15.80	0.03	1.79	0.86	y	LPV-YSO	603
VVVv22	VVV J123105.60-624457.34	12:31:05.60	-62:44:57.34	300.60547	0.03057	–	–	–	–	18.81	0.14	16.94	0.05	15.55	0.03	1.73	-0.34	y	STV	–
VVVv23	VVV J123128.53-624433.10	12:31:28.53	-62:44:33.10	300.64855	0.04070	19.44	0.07	18.37	0.05	17.14	0.03	15.57	0.02	14.40	0.01	1.51	-0.20	y	Fader	–
VVVv24	VVV J123235.68-634319.61	12:32:35.68	-63:43:19.61	300.84794	-0.92662	17.17	0.01	16.13	0.01	14.05	0.01	12.95	0.01	12.23	0.01	1.20	–	n	LPV	430
VVVv25	VVV J123514.37-624715.63	12:35:14.37	-62:47:15.63	301.08129	0.02587	–	–	–	–	–	–	16.01	0.02	12.34	0.01	1.68	0.22	y	Eruptive	–
VVVv26	VVV J123845.66-631136.03	12:38:45.66	-63:11:36.03	301.50320	-0.35674	–	–	–	–	19.67	0.29	16.70	0.04	14.71	0.01	2.45	1.07	y	Eruptive	–
VVVv27	VVV J123848.33-633939.15	12:38:48.33	-63:39:39.15	301.53114	-0.82347	–	–	–	–	–	–	–	–	12.04	0.01	2.73	–	n	LPV	1329.00
VVVv28	VVV J123911.54-630524.76	12:39:11.54	-63:05:24.76	301.54688	-0.25138	–	–	–	–	–	–	18.91	0.32	16.78	0.09	1.39	0.54	y	STV	3.68
VVVv29	VVV J123931.48-630720.38	12:39:31.48	-63:07:20.38	301.58593	-0.28170	–	–	–	–	–	–	–	–	16.94	0.10	2.13	1.32	y	Eruptive	–
VVVv30	VVV J124140.56-635033.57	12:41:40.56	-63:50:33.57	301.85616	-0.99128	17.92	0.02	17.22	0.02	16.40	0.02	15.66	0.02	15.23	0.02	1.22	–	n	EB	1.91
VVVv31	VVV J124140.15-635918.05	12:41:40.15	-63:59:18.05	301.86093	-1.13689	13.91	0.01	13.27	0.01	12.46	0.01	12.08	0.01	11.69	0.01	1.15	–	n	LPV	760
VVVv32	VVV J124357.15-625445.09	12:43:57.15	-62:54:45.09	302.07991	-0.05314	19.58	0.07	18.08	0.04	16.07	0.01	14.07	0.01	12.45	0.01	2.49	0.33	y	LPV-YSO	–
VVVv33	VVV J124425.05-631355.76	12:44:25.05	-63:13:55.76	302.14153	-0.37116	–	–	–	–	–	–	18.10	0.16	16.43	0.07	1.37	–	n	STV	–
VVVv34	VVV J125029.87-625124.93	12:50:29.87	-62:51:24.93	302.82470	0.01465	19.22	0.05	18.32	0.05	17.86	0.06	16.70	0.04	15.71	0.03	1.30	-0.34	y	STV	–
VVVv35	VVV J125206.52-635711.52	12:52:06.52	-63:57:11.52	303.00557	-1.08152	17.62	0.01	16.85	0.01	17.13	0.03	16.21	0.03	15.97	0.04	1.24	–	n	EB	1.12
VVVv36	VVV J125917.72-633008.44	12:59:17.72	-63:30:08.44	303.80825	-0.64394	14.38	0.01	13.84	0.01	13.27	0.01	12.56	0.01	11.81	0.01	1.03	-0.11	y	Eruptive	–
VVVv37	VVV J130243.05-631130.00	13:02:43.05	-63:11:30.00	304.20331	-0.34774	18.80	0.03	17.75	0.03	16.74	0.02	15.89	0.02	15.38	0.03	1.34	–	n	STV	–
VVVv38	VVV J130311.38-631439.09	13:03:11.38	-63:14:39.09	304.25411	-0.40259	–	–	–	–	–	–	17.79	0.13	16.32	0.07	1.41	1.20	y	STV	48.96
VVVv39	VVV J130440.98-635313.45	13:04:40.98	-63:53:13.45	304.38893	-1.05277	18.67	0.03	17.89	0.03	17.57	0.05	16.38	0.04	15.49	0.03	1.51	–	n	STV	–
VVVv40	VVV J130600.43-630144.40	13:06:00.43	-63:01:44.40	304.58298	-0.20394	20.71	0.20	19.49	0.14	16.52	0.02	15.42	0.02	14.69	0.01	1.24	–	n	EB	10.29
VVVv41	VVV J130944.05-634431.38	13:09:44.05	-63:44:31.38	304.95408	-0.94214	18.09	0.02	17.50	0.03	15.83	0.01	15.22	0.01	14.90	0.02	1.20	–	n	EB	20.33

Continued on next page

Table C1 – *Continued from previous page*

Object ID	VVV Designation	α (J2000)	δ (J2000)	l (degrees)	b (degrees)	Z (mag)	Z_{err} (mag)	Y (mag)	Y_{err} (mag)	J (mag)	J_{err} (mag)	H (mag)	H_{err} (mag)	$K_{\rm s}$ (mag)	$K_{\rm s,err}$ (mag)	$\Delta K_{\rm s}$ (mag)	α_{class}	SFR	Class	Period (days)
VVVv42	VVV J130934.64-624932.52	13:09:34.64	-62:49:32.52	305.00126	-0.02683	–	–	–	–	18.45	0.10	14.26	0.01	11.94	0.01	2.16	–	y	LPV-Mira	812
VVVv43	VVV J131044.06-625541.32	13:10:44.06	-62:55:41.32	305.12535	-0.13858	–	–	–	–	–	–	17.62	0.11	16.14	0.06	1.23	0.53	y	STV	68.10
VVVv44	VVV J131054.29-625604.36	13:10:54.29	-62:56:04.36	305.14420	-0.14642	–	–	–	–	19.34	0.23	16.83	0.05	15.15	0.02	1.27	–	y	STV	81.20
VVVv45	VVV J131143.07-624854.77	13:11:43.07	-62:48:54.77	305.24579	-0.03459	–	–	–	–	–	–	–	–	13.33	0.01	2.32	1.27	y	LPV-Mira	560
VVVv46	VVV J131246.62-625628.58	13:12:46.62	-62:56:28.58	305.35595	-0.16998	–	–	–	–	–	–	17.32	0.09	15.80	0.04	1.31	0.12	y	STV	5.86
VVVv47	VVV J131313.97-624429.31	13:13:13.97	-62:44:29.31	305.42449	0.02477	–	–	–	–	19.12	0.19	17.27	0.08	15.93	0.05	1.71	0.04	y	LPV-YSO	181
VVVv48	VVV J131545.37-625244.45	13:15:45.37	-62:52:44.45	305.69929	-0.13798	–	–	–	–	19.53	0.28	17.39	0.09	16.09	0.05	1.30	–	y	Dipper	–
VVVv49	VVV J131816.29-633743.65	13:18:16.29	-63:37:43.65	305.90658	-0.91211	19.98	0.13	–	–	18.35	0.09	–	–	12.48	0.01	1.76	–	n	LPV	701
VVVv50	VVV J131843.99-632716.96	13:18:43.99	-63:27:16.96	305.97598	-0.74438	17.60	0.02	17.30	0.02	16.24	0.01	15.81	0.02	15.60	0.03	1.14	–	n	STV	–
VVVv51	VVV J131942.87-630101.88	13:19:42.87	-63:01:01.88	306.13293	-0.32129	–	–	–	–	–	–	16.86	0.05	14.49	0.01	2.82	0.29	y	Dipper	–
VVVv52	VVV J132308.94-624835.13	13:23:08.94	-62:48:35.13	306.54533	-0.16068	14.49	0.01	13.64	0.01	12.75	0.01	12.66	0.01	12.16	0.01	1.11	–	n	EB	3.98
VVVv53	VVV J132702.40-630622.47	13:27:02.40	-63:06:22.47	306.94521	-0.51222	–	–	–	–	–	–	16.61	0.06	14.53	0.02	2.41	0.66	y	Eruptive	–
VVVv54	VVV J132758.65-631448.97	13:27:58.65	-63:14:48.97	307.03032	-0.66629	12.89	0.01	12.51	0.01	–	–	12.49	0.01	12.12	0.01	1.02	–	n	Known	5.51
VVVv55	VVV J133403.43-625325.69	13:34:03.43	-62:53:25.69	307.76515	-0.41933	20.11	0.21	18.92	0.15	16.87	0.03	15.93	0.03	15.39	0.03	1.15	–	n	STV	–
VVVv56	VVV J133746.01-622807.54	13:37:46.01	-62:28:07.54	308.25687	-0.07694	19.21	0.08	17.48	0.03	15.52	0.01	13.41	0.01	12.45	0.01	1.41	0.18	y	LPV-YSO	116
VVVv57	VVV J134041.89-631440.96	13:40:41.89	-63:14:40.96	308.44250	-0.90120	–	–	–	–	18.10	0.06	16.69	0.04	15.85	0.04	1.62	–	n	EB	2.81
VVVv58	VVV J134213.00-621825.35	13:42:13.00	-62:18:25.35	308.79362	-0.01457	17.48	0.02	16.46	0.01	15.04	0.01	13.79	0.01	12.61	0.01	1.20	–	n	LPV	205
VVVv59	VVV J134330.94-623719.95	13:43:30.94	-62:37:19.95	308.87836	-0.35323	–	–	–	–	17.64	0.04	14.68	0.01	12.62	0.01	1.11	–	n	LPV	230
VVVv60	VVV J134452.75-631740.41	13:44:52.75	-63:17:40.41	308.89356	-1.04304	–	–	18.78	0.09	16.98	0.02	15.82	0.02	15.15	0.02	1.13	–	n	EB	3.62
VVVv61	VVV J134406.00-624932.88	13:44:06.00	-62:49:32.88	308.90289	-0.56614	–	–	–	–	–	–	18.27	0.17	15.54	0.03	1.04	–	n	STV	–
VVVv62	VVV J134550.28-622827.70	13:45:50.28	-62:28:27.70	309.17062	-0.26336	–	–	–	–	–	–	–	–	14.01	0.01	1.85	1.13	y	LPV-Mira	667
VVVv63	VVV J134620.48-622530.81	13:46:20.48	-62:25:30.81	309.23785	-0.22755	–	–	–	–	18.53	0.09	15.79	0.02	13.81	0.01	1.44	0.90	y	Eruptive	–
VVVv64	VVV J134623.81-622003.09	13:46:23.81	-62:20:03.09	309.26338	-0.13994	–	–	–	–	–	–	14.96	0.01	11.44	0.01	1.17	-0.31	y	LPV-YSO	500
VVVv65	VVV J134751.09-624237.46	13:47:51.09	-62:42:37.46	309.34673	-0.54335	–	–	–	–	18.75	0.10	15.85	0.02	13.59	0.01	1.36	-0.31	y	STV	30.12
VVVv66	VVV J134820.90-624309.74	13:48:20.90	-62:43:09.74	309.40035	-0.56451	–	–	–	–	18.12	0.06	16.64	0.03	15.41	0.03	1.24	0.02	y	STV	–
VVVv67	VVV J134838.70-624627.31	13:48:38.70	-62:46:27.31	309.42145	-0.62550	–	–	–	–	19.33	0.17	16.98	0.05	15.61	0.03	1.08	0.40	y	Eruptive	–
VVVv68	VVV J134843.51-624549.42	13:48:43.51	-62:45:49.42	309.43271	-0.61725	–	–	–	–	19.90	0.28	16.42	0.03	14.56	0.01	1.03	0.14	y	STV	–
VVVv69	VVV J134759.94-622011.92	13:47:59.94	-62:20:11.92	309.44451	-0.18221	–	–	–	–	19.69	0.24	17.55	0.08	16.34	0.06	1.36	–	n	LPV	–
VVVv70	VVV J135020.05-624524.09	13:50:20.05	-62:45:24.09	309.61377	-0.65149	–	–	20.14	0.21	18.05	0.05	16.35	0.03	15.31	0.02	1.15	–	n	EB	4.23
VVVv71	VVV J135332.54-623724.91	13:53:32.54	-62:37:24.91	310.00262	-0.60748	–	–	–	–	19.15	0.14	16.79	0.04	15.23	0.02	1.15	–	n	LPV	120
VVVv72	VVV J135328.30-623001.48	13:53:28.30	-62:30:01.48	310.02404	-0.48591	21.20	0.33	19.39	0.11	17.77	0.04	16.53	0.03	15.83	0.04	1.03	–	n	EB	4.41
VVVv73	VVV J135517.97-630055.44	13:55:17.97	-63:00:55.44	310.10271	-1.03615	16.43	0.01	15.27	0.01	15.21	0.01	14.29	0.01	13.64	0.01	1.02	–	n	EB	4.54
VVVv74	VVV J135625.78-630003.44	13:56:25.78	-63:00:03.44	310.23056	-1.05383	17.69	0.02	17.21	0.02	16.50	0.01	15.91	0.02	15.57	0.03	1.04	–	n	STV	–
VVVv75	VVV J135613.31-623609.30	13:56:13.31	-62:36:09.30	310.30662	-0.66206	–	–	–	–	18.81	0.10	17.09	0.05	15.86	0.04	1.17	–	n	Rare	–
VVVv76	VVV J135547.01-621233.21	13:55:47.01	-62:12:33.21	310.35477	-0.26837	–	–	–	–	19.88	0.28	15.35	0.01	11.94	0.01	1.65	–	n	LPV	632.36
VVVv77	VVV J135706.18-620016.61	13:57:06.18	-62:00:16.61	310.55520	-0.10865	–	–	19.74	0.16	18.83	0.11	17.63	0.08	16.87	0.10	1.06	–	y	STV	60.26
VVVv78	VVV J135733.86-615736.39	13:57:33.86	-61:57:36.39	310.61885	-0.07926	20.79	0.23	19.14	0.09	17.59	0.04	16.04	0.02	15.13	0.02	1.01	–	n	LPV	–
VVVv79	VVV J135935.30-621036.12	13:59:35.30	-62:10:36.12	310.79224	-0.34949	–	–	–	–	–	–	18.68	0.25	16.75	0.15	1.12	–	y	Eruptive	–
VVVv80	VVV J135903.61-614733.53	13:59:03.61	-61:47:33.53	310.83213	0.03749	–	–	–	–	18.87	0.12	16.74	0.04	15.45	0.05	1.14	-0.99	y	STV	22
VVVv81	VVV J140700.55-615115.98	14:07:00.55	-61:51:15.98	311.71777	-0.27860	–	–	–	–	–	–	17.32	0.07	13.20	0.01	1.66	0.67	y	LPV-Mira	533
VVVv82	VVV J140719.19-613717.46	14:07:19.19	-61:37:17.46	311.82022	-0.06621	–	–	–	–	–	–	15.71	0.02	11.75	0.01	1.47	-0.32	y	LPV-YSO	–
VVVv83	VVV J141056.71-622513.45	14:10:56.71	-62:25:13.45	311.98995	-0.95514	–	–	17.99	0.03	16.39	0.01	14.44	0.01	12.75	0.01	1.12	0.22	y	LPV-Mira	756

Continued on next page

Table C1 – *Continued from previous page*

Object ID	VVV Designation	α (J2000)	δ (J2000)	l (degrees)	b (degrees)	Z (mag)	Z_{err} (mag)	Y (mag)	Y_{err} (mag)	J (mag)	J_{err} (mag)	H (mag)	H_{err} (mag)	$K_{\rm s}$ (mag)	$K_{\rm s,err}$ (mag)	$\Delta K_{\rm s}$ (mag)	α_{class}	SFR	Class	Period (days)
VVVv84	VVV J140911.55-613224.31	14:09:11.55	-61:32:24.31	312.05712	-0.05358	20.05	0.13	19.33	0.11	17.10	0.03	14.02	0.01	11.97	0.01	2.81	0.03	y	Fader	–
VVVv85	VVV J141046.67-615734.01	14:10:46.67	-61:57:34.01	312.11070	-0.50985	19.81	0.10	18.86	0.07	17.68	0.04	16.20	0.03	15.39	0.04	1.32	–	n	LPV	–
VVVv86	VVV J141028.74-614946.06	14:10:28.74	-61:49:46.06	312.11632	-0.37530	–	–	–	–	18.34	0.08	13.78	0.01	10.78	0.01	2.10	–	n	LPV	560
VVVv87	VVV J141254.98-614527.53	14:12:54.98	-61:45:27.53	312.41250	-0.39486	–	–	–	–	–	–	18.52	0.22	15.40	0.04	1.73	0.23	y	Fader	–
VVVv88	VVV J141227.76-613027.81	14:12:27.76	-61:30:27.81	312.43848	-0.14052	–	–	–	–	18.42	0.08	16.68	0.04	15.71	0.06	1.52	–	y	STV	4.48
VVVv89	VVV J141534.31-621945.07	14:15:34.31	-62:19:45.07	312.52810	-1.03528	–	–	–	–	–	–	15.71	0.02	12.28	0.01	2.52	–	n	LPV	660
VVVv90	VVV J141730.13-615054.83	14:17:30.13	-61:50:54.83	312.89716	-0.65337	–	–	–	–	–	–	17.68	0.10	16.08	0.08	2.05	1.15	y	Eruptive	–
VVVv91	VVV J141649.12-611516.58	14:16:49.12	-61:15:16.58	313.01334	-0.06523	–	–	–	–	–	–	17.82	0.11	15.71	0.06	1.97	1.29	y	Dipper	–
VVVv92	VVV J141848.92-614133.03	14:18:48.92	-61:41:33.03	313.09512	-0.55705	19.94	0.09	18.67	0.05	17.28	0.03	16.11	0.02	15.60	0.05	1.16	–	n	EB	1.24
VVVv93	VVV J142239.35-620248.52	14:22:39.35	-62:02:48.52	313.40139	-1.04353	21.05	0.25	20.11	0.21	18.77	0.11	17.10	0.06	15.98	0.07	2.10	–	n	Rare	–
VVVv94	VVV J142257.76-610547.03	14:22:57.76	-61:05:47.03	313.76407	-0.16427	–	–	–	–	–	–	16.42	0.03	13.39	0.01	1.91	0.54	y	Eruptive	–
VVVv95	VVV J142517.08-613042.02	14:25:17.08	-61:30:42.02	313.87973	-0.65086	–	–	20.11	0.25	18.07	0.06	16.66	0.04	15.98	0.04	1.09	–	n	STV	–
VVVv96	VVV J142634.45-613900.61	14:26:34.45	-61:39:00.61	313.97367	-0.83496	–	–	19.91	0.21	18.48	0.08	16.78	0.04	15.92	0.04	1.05	–	n	EB	4.73
VVVv97	VVV J142422.62-605320.62	14:24:22.62	-60:53:20.62	313.99705	-0.02970	–	–	–	–	19.21	0.16	17.04	0.05	15.71	0.03	1.09	–	y	STV	–
VVVv98	VVV J142500.68-605448.20	14:25:00.68	-60:54:48.20	314.06065	-0.07963	–	–	–	–	–	–	18.08	0.14	14.61	0.01	2.09	0.60	y	LPV-YSO	170.27
VVVv99	VVV J142701.20-612525.27	14:27:01.20	-61:25:25.27	314.10472	-0.64275	13.48	0.01	13.04	0.01	12.74	0.01	12.78	0.01	12.39	0.01	1.03	–	n	EB	4.17
VVVv100	VVV J142807.13-613816.91	14:28:07.13	-61:38:16.91	314.14907	-0.88999	18.30	0.03	17.51	0.02	16.63	0.02	15.71	0.02	15.33	0.02	1.12	–	n	Rare	–
VVVv101	VVV J142538.25-604811.19	14:25:38.25	-60:48:11.19	314.17103	-0.00354	–	–	–	–	–	–	17.60	0.09	15.61	0.03	1.32	0.43	y	STV	38.18
VVVv102	VVV J142852.17-612217.27	14:28:52.17	-61:22:17.27	314.32991	-0.67464	–	–	–	–	19.05	0.14	15.27	0.01	12.37	0.01	2.17	–	n	LPV	636
VVVv103	VVV J143227.49-603942.58	14:32:27.49	-60:39:42.58	314.99820	-0.17868	–	–	–	–	19.78	0.28	16.83	0.04	14.75	0.01	1.49	0.94	y	LPV-Mira	230.44
VVVv104	VVV J143404.67-610609.65	14:34:04.67	-61:06:09.65	315.01158	-0.66137	18.20	0.02	17.57	0.03	16.64	0.02	15.64	0.01	14.77	0.01	1.06	–	n	STV	–
VVVv105	VVV J143437.21-611023.13	14:34:37.21	-61:10:23.13	315.04474	-0.75160	18.29	0.03	17.92	0.03	16.94	0.02	16.29	0.03	15.99	0.04	1.15	–	n	STV	–
VVVv106	VVV J143357.09-604737.87	14:33:57.09	-60:47:37.87	315.11639	-0.37046	–	–	–	–	–	–	14.88	0.01	11.91	0.01	2.35	–	n	LPV	665
VVVv107	VVV J144044.97-610704.39	14:40:44.97	-61:07:04.39	315.74517	-0.99527	–	–	–	–	16.35	0.02	12.93	0.01	11.32	0.01	1.54	–	n	LPV	616
VVVv108	VVV J143853.29-601007.32	14:38:53.29	-60:10:07.32	315.92142	-0.03511	–	–	–	–	17.74	0.05	15.05	0.01	13.44	0.01	1.12	–	n	LPV	1830
VVVv109	VVV J144212.43-604125.50	14:42:12.43	-60:41:25.50	316.08250	-0.67847	–	–	19.33	0.11	16.66	0.02	14.21	0.01	12.36	0.01	1.35	0.12	y	STV	–
VVVv110	VVV J144351.27-602150.93	14:43:51.27	-60:21:50.93	316.40259	-0.46621	–	–	–	–	19.44	0.26	16.64	0.05	14.40	0.01	1.19	1.29	y	Eruptive	–
VVVv111	VVV J144444.70-602616.44	14:44:44.70	-60:26:16.44	316.47132	-0.57939	–	–	–	–	–	–	–	–	13.22	0.01	1.98	1.23	y	LPV-Mira	851
VVVv112	VVV J144427.29-595924.99	14:44:27.29	-59:59:24.99	316.62747	-0.15834	–	–	–	–	18.79	0.13	14.92	0.01	12.02	0.01	1.32	-0.10	y	STV	–
VVVv113	VVV J144523.82-595209.70	14:45:23.82	-59:52:09.70	316.78555	-0.09868	–	–	–	–	–	–	18.58	0.27	15.72	0.04	1.56	1.85	y	STV	47
VVVv114	VVV J144906.82-604557.11	14:49:06.82	-60:45:57.11	316.81448	-1.10592	–	–	–	–	–	–	–	–	15.78	0.04	3.02	–	n	LPV	860
VVVv115	VVV J144802.41-600427.26	14:48:02.41	-60:04:27.26	316.99634	-0.42561	20.02	0.11	18.86	0.07	17.71	0.05	16.40	0.04	15.47	0.03	1.26	–	n	STV	–
VVVv116	VVV J144812.64-600310.10	14:48:12.64	-60:03:10.10	317.02482	-0.41553	19.66	0.08	18.49	0.05	17.41	0.04	16.50	0.04	15.96	0.05	1.39	–	n	STV	–
VVVv117	VVV J145003.98-594734.18	14:50:03.98	-59:47:34.18	317.34758	-0.28338	–	–	20.39	0.27	18.14	0.07	16.55	0.04	15.49	0.03	1.15	–	y	STV	–
VVVv118	VVV J145120.97-600027.40	14:51:20.97	-60:00:27.40	317.39680	-0.54718	16.61	0.01	15.98	0.01	16.09	0.01	14.54	0.01	13.01	0.01	4.24	0.16	y	Eruptive	–
VVVv119	VVV J145253.28-600452.73	14:52:53.28	-60:04:52.73	317.53562	-0.69901	–	–	–	–	18.30	0.08	15.49	0.02	13.71	0.01	1.22	0.02	y	LPV-YSO	–
VVVv120	VVV J145300.70-591443.50	14:53:00.70	-59:14:43.50	317.92578	0.04041	17.94	0.02	17.71	0.02	17.37	0.04	16.55	0.04	15.94	0.05	1.50	–	n	STV	–
VVVv121	VVV J145521.85-593709.11	14:55:21.85	-59:37:09.11	318.02247	-0.42844	18.58	0.03	16.84	0.01	15.06	0.01	13.65	0.01	12.76	0.01	1.11	–	n	LPV	1830
VVVv122	VVV J145630.67-594925.77	14:56:30.67	-59:49:25.77	318.05670	-0.67663	–	–	–	–	19.39	0.19	17.03	0.05	15.42	0.03	1.08	0.55	y	STV	–
VVVv123	VVV J145731.64-593810.86	14:57:31.64	-59:38:10.86	318.25710	-0.56991	–	–	–	–	–	–	14.17	0.01	11.27	0.01	2.38	0.78	y	LPV-Mira	761
VVVv124	VVV J145531.30-590703.08	14:55:31.30	-59:07:03.08	318.27027	0.00823	20.32	0.16	19.24	0.11	17.59	0.04	15.89	0.02	14.12	0.01	1.18	0.47	y	LPV-YSO	936
VVVv125	VVV J145940.19-595943.02	14:59:40.19	-59:59:43.02	318.32666	-1.01321	–	–	–	–	18.32	0.07	16.83	0.04	16.04	0.05	1.20	–	n	STV	–

Continued on next page

Table C1 – *Continued from previous page*

Object ID	VVV Designation	α (J2000)	δ (J2000)	l (degrees)	b (degrees)	Z (mag)	Z_{err} (mag)	Y (mag)	Y_{err} (mag)	J (mag)	J_{err} (mag)	H (mag)	H_{err} (mag)	$K_{\rm s}$ (mag)	$K_{\rm s,err}$ (mag)	$\Delta K_{\rm s}$ (mag)	α_{class}	SFR	Class	Period (days)
VVVv126	VVV J150007.69-595334.83	15:00:07.69	-59:53:34.83	318.42562	-0.95026	–	–	19.24	0.11	16.50	0.01	14.04	0.01	12.18	0.01	1.70	–	n	LPV	429
VVVv127	VVV J145747.25-591424.34	14:57:47.25	-59:14:24.34	318.47092	-0.23466	–	–	–	–	–	–	–	–	16.93	0.11	1.13	2.03	y	LPV-Mira	–
VVVv128	VVV J145829.67-590940.29	14:58:29.67	-59:09:40.29	318.58781	-0.20720	–	–	–	–	19.62	0.24	17.15	0.06	14.47	0.01	2.51	0.95	y	Eruptive	–
VVVv129	VVV J150213.13-595904.80	15:02:13.13	-59:59:04.80	318.61195	-1.15579	16.90	0.01	16.49	0.01	15.92	0.01	15.25	0.01	15.00	0.02	1.39	–	n	Rare	–
VVVv130	VVV J150043.33-592229.68	15:00:43.33	-59:22:29.68	318.73777	-0.52997	–	–	20.34	0.31	17.07	0.02	14.40	0.01	12.65	0.01	1.02	0.42	y	Eruptive	–
VVVv131	VVV J150310.44-595120.55	15:03:10.44	-59:51:20.55	318.77903	-1.10056	19.84	0.10	18.72	0.07	18.30	0.07	17.40	0.07	16.78	0.09	1.31	–	n	EB	1.41
VVVv132	VVV J150201.88-584927.58	15:02:01.88	-58:49:27.58	319.14859	-0.12671	–	–	–	–	19.08	0.15	17.31	0.07	16.38	0.06	1.02	–	n	STV	–
VVVv133	VVV J150620.36-592544.52	15:06:20.36	-59:25:44.52	319.33663	-0.92401	19.89	0.11	19.01	0.10	17.88	0.05	16.61	0.04	15.78	0.04	1.11	–	n	STV	–
VVVv134	VVV J150738.24-585138.25	15:07:38.24	-58:51:38.25	319.76324	-0.51313	–	–	–	–	18.57	0.11	16.04	0.03	14.32	0.01	1.32	-0.83	y	LPV-YSO	289
VVVv135	VVV J150738.65-582404.65	15:07:38.65	-58:24:04.65	319.99291	-0.11534	–	–	–	–	–	–	17.57	0.11	15.18	0.02	1.06	1.52	y	STV	–
VVVv136	VVV J151216.89-590331.54	15:12:16.89	-59:03:31.54	320.17950	-0.98686	19.05	0.05	18.04	0.04	17.15	0.03	16.36	0.04	15.97	0.05	1.39	–	n	STV	–
VVVv137	VVV J151252.81-591036.72	15:12:52.81	-59:10:36.72	320.18465	-1.12765	17.29	0.01	16.34	0.01	15.04	0.01	13.95	0.01	13.06	0.01	1.27	–	n	Rare	–
VVVv138	VVV J151007.47-582209.73	15:10:07.47	-58:22:09.73	320.29002	-0.25102	17.81	0.02	16.83	0.01	15.92	0.01	15.03	0.01	14.60	0.01	1.22	–	n	EB	1.67
VVVv139	VVV J150932.71-581345.47	15:09:32.71	-58:13:45.47	320.29513	-0.09169	–	–	–	–	–	–	18.17	0.19	16.06	0.05	2.22	-0.03	y	Eruptive	–
VVVv140	VVV J151338.45-585243.48	15:13:38.45	-58:52:43.48	320.42244	-0.92288	–	–	–	–	–	–	16.06	0.03	13.32	0.01	2.30	0.63	y	Dipper	–
VVVv141	VVV J151120.96-582222.07	15:11:20.96	-58:22:22.07	320.42657	-0.33559	18.01	0.02	17.19	0.02	17.28	0.03	15.54	0.02	14.09	0.01	1.01	-0.48	y	STV	–
VVVv142	VVV J151430.54-585847.00	15:14:30.54	-58:58:47.00	320.46581	-1.06733	–	–	–	–	–	–	17.99	0.16	16.23	0.06	1.24	–	n	LPV	1470
VVVv143	VVV J151523.39-585404.60	15:15:23.39	-58:54:04.60	320.60367	-1.05966	20.83	0.25	19.81	0.19	18.15	0.08	15.62	0.02	12.63	0.01	1.98	–	n	LPV	744
VVVv144	VVV J151636.38-580912.14	15:16:36.38	-58:09:12.14	321.13146	-0.50643	–	–	18.88	0.09	17.80	0.07	16.62	0.06	16.00	0.07	1.19	–	n	STV	–
VVVv145	VVV J151656.42-580326.30	15:16:56.42	-58:03:26.30	321.21961	-0.44808	–	–	–	–	–	–	16.94	0.08	14.59	0.02	1.04	1.23	y	Eruptive	–
VVVv146	VVV J152110.72-582125.91	15:21:10.72	-58:21:25.91	321.53117	-0.99990	18.06	0.02	17.44	0.03	16.93	0.03	16.39	0.05	15.87	0.06	1.12	–	n	STV	–
VVVv147	VVV J151837.80-574504.85	15:18:37.80	-57:45:04.85	321.57219	-0.30779	–	–	–	–	–	–	18.65	0.40	15.90	0.06	1.95	–	n	Rare	–
VVVv148	VVV J151906.61-573927.84	15:19:06.61	-57:39:27.84	321.67639	-0.26286	–	–	–	–	–	–	–	–	16.23	0.08	1.70	–	n	STV	–
VVVv149	VVV J152100.25-575153.34	15:21:00.25	-57:51:53.34	321.77808	-0.57327	–	–	–	–	–	–	–	–	15.53	0.04	2.03	1.69	y	Eruptive	–
VVVv150	VVV J151958.89-571807.48	15:19:58.89	-57:18:07.48	321.96587	-0.02536	–	–	–	–	18.52	0.13	16.44	0.05	15.13	0.03	1.14	-0.58	y	STV	5.21
VVVv151	VVV J152447.81-580940.66	15:24:47.81	-58:09:40.66	322.03681	-1.09599	–	–	–	–	–	–	–	–	16.19	0.07	1.07	1.77	y	STV	69.07
VVVv152	VVV J152040.85-571000.26	15:20:40.85	-57:10:00.26	322.11848	0.03774	15.65	0.01	14.44	0.01	13.46	0.01	12.50	0.01	11.82	0.01	2.21	–	n	Known	16.55
VVVv153	VVV J152128.41-571847.88	15:21:28.41	-57:18:47.88	322.12944	-0.14352	–	–	–	–	–	–	–	–	16.70	0.13	1.27	0.30	y	STV	21
VVVv154	VVV J152405.24-574954.21	15:24:05.24	-57:49:54.21	322.13999	-0.76917	18.33	0.03	17.19	0.02	16.27	0.02	16.07	0.04	14.94	0.03	1.08	–	n	EB	2.23
VVVv155	VVV J152308.09-571712.94	15:23:08.09	-57:17:12.94	322.33200	-0.24357	–	–	–	–	–	–	17.10	0.10	14.99	0.03	2.13	–	n	LPV	252
VVVv156	VVV J152511.24-571946.17	15:25:11.24	-57:19:46.17	322.54002	-0.43158	18.96	0.05	17.81	0.03	16.69	0.02	15.61	0.02	14.99	0.02	1.30	–	n	Rare	–
VVVv157	VVV J152548.43-565949.91	15:25:48.43	-56:59:49.91	322.79413	-0.20156	–	–	19.32	0.12	17.70	0.05	16.32	0.04	15.37	0.03	1.05	–	n	STV	–
VVVv158	VVV J152542.31-564529.64	15:25:42.31	-56:45:29.64	322.91517	0.00496	–	–	19.12	0.10	16.70	0.02	15.28	0.01	14.52	0.01	1.15	–	n	EB	5.28
VVVv159	VVV J152729.60-565854.70	15:27:29.60	-56:58:54.70	322.99331	-0.31691	–	–	–	–	18.82	0.14	17.09	0.08	16.04	0.06	1.02	–	n	STV	–
VVVv160	VVV J152734.81-565811.76	15:27:34.81	-56:58:11.76	323.00980	-0.31367	16.66	0.01	15.19	0.01	13.74	0.01	12.91	0.01	12.32	0.01	1.09	–	n	EB	4.14
VVVv161	VVV J152939.43-571119.22	15:29:39.43	-57:11:19.22	323.11960	-0.65341	–	–	–	–	–	–	18.35	0.24	16.64	0.10	1.42	0.90	y	Eruptive	–
VVVv162	VVV J152917.51-565411.95	15:29:17.51	-56:54:11.95	323.24023	-0.39007	–	–	–	–	–	–	–	–	14.01	0.01	1.69	0.31	y	LPV-Mira	479
VVVv163	VVV J152934.08-565225.52	15:29:34.08	-56:52:25.52	323.28806	-0.38705	–	–	–	–	18.71	0.13	16.17	0.03	14.74	0.02	1.79	0.34	y	Fader	–
VVVv164	VVV J152921.67-563902.13	15:29:21.67	-56:39:02.13	323.39104	-0.18706	19.50	0.09	18.25	0.05	17.19	0.03	16.02	0.03	15.55	0.04	1.06	–	n	STV	–
VVVv165	VVV J152941.48-564020.33	15:29:41.48	-56:40:20.33	323.41614	-0.23066	–	–	–	–	17.99	0.07	15.56	0.02	13.78	0.01	1.08	1.53	y	Eruptive	–
VVVv166	VVV J152940.33-563823.01	15:29:40.33	-56:38:23.01	323.43245	-0.20232	–	–	–	–	18.87	0.15	17.00	0.07	16.10	0.06	1.12	–	n	EB	2.09
VVVv167	VVV J153021.60-563844.55	15:30:21.60	-56:38:44.55	323.50687	-0.26093	20.18	0.16	18.26	0.05	15.70	0.01	13.34	0.01	11.84	0.01	1.33	0.46	y	Eruptive	–

Continued on next page

Table C1 – *Continued from previous page*

Object ID	VVV Designation	α (J2000)	δ (J2000)	l (degrees)	b (degrees)	Z (mag)	Z_{err} (mag)	Y (mag)	Y_{err} (mag)	J (mag)	J_{err} (mag)	H (mag)	H_{err} (mag)	$K_{\rm s}$ (mag)	$K_{\rm s,err}$ (mag)	$\Delta K_{\rm s}$ (mag)	α_{class}	SFR	Class	Period (days)
VVVv168	VVV J153200.86-563842.58	15:32:00.86	-56:38:42.58	323.69382	-0.39040	–	–	–	–	–	–	16.45	0.04	14.27	0.01	1.96	-0.57	y	STV	4.23
VVVv169	VVV J153157.36-563609.37	15:31:57.36	-56:36:09.37	323.71166	-0.35094	–	–	–	–	–	–	15.32	0.02	12.44	0.01	1.53	0.33	y	STV	–
VVVv170	VVV J153647.49-565210.20	15:36:47.49	-56:52:10.20	324.09644	-0.95330	–	–	–	–	–	–	17.67	0.17	15.17	0.03	1.56	1.22	y	LPV-YSO	432
VVVv171	VVV J153706.12-563233.54	15:37:06.12	-56:32:33.54	324.32323	-0.71408	–	–	19.42	0.15	17.33	0.05	16.24	0.04	15.61	0.05	1.30	–	n	EB	1.98
VVVv172	VVV J153640.80-555258.91	15:36:40.80	-55:52:58.91	324.66374	-0.14610	20.61	0.23	18.66	0.07	18.03	0.09	16.60	0.06	15.86	0.06	1.04	–	n	EB	2.06
VVVv173	VVV J153746.87-560415.21	15:37:46.87	-56:04:15.21	324.67753	-0.38864	–	–	–	–	18.23	0.10	17.26	0.11	16.10	0.07	1.11	–	n	STV	–
VVVv174	VVV J153815.79-553951.62	15:38:15.79	-55:39:51.62	324.97249	-0.10080	–	–	–	–	19.19	0.26	17.11	0.10	16.03	0.07	1.22	–	n	STV	–
VVVv175	VVV J153939.81-555046.92	15:39:39.81	-55:50:46.92	325.02281	-0.36427	–	–	–	–	19.40	0.31	17.16	0.10	15.73	0.05	1.55	-0.40	y	STV	49
VVVv176	VVV J153837.25-552821.44	15:38:37.25	-55:28:21.44	325.12683	0.02366	–	–	–	–	–	–	–	–	14.56	0.02	1.22	2.97	y	Eruptive	–
VVVv177	VVV J154007.59-553015.85	15:40:07.59	-55:30:15.85	325.27927	-0.12884	–	–	19.58	0.17	18.22	0.11	17.22	0.11	16.75	0.13	1.47	–	n	STV	–
VVVv178	VVV J154249.38-560011.63	15:42:49.38	-56:00:11.63	325.28237	-0.75552	19.84	0.11	18.92	0.10	17.76	0.07	16.91	0.08	16.43	0.10	1.21	–	n	EB	1.81
VVVv179	VVV J154502.34-555807.95	15:45:02.34	-55:58:07.95	325.54925	-0.91681	–	–	–	–	18.45	0.11	16.58	0.05	15.45	0.04	1.56	-0.51	y	Dipper	–
VVVv180	VVV J154252.38-552311.07	15:42:52.38	-55:23:11.07	325.66138	-0.26881	–	–	–	–	–	–	–	–	12.18	0.01	1.74	–	n	LPV	550
VVVv181	VVV J154639.17-555028.27	15:46:39.17	-55:50:28.27	325.80621	-0.95485	20.42	0.17	19.40	0.14	17.81	0.06	15.02	0.01	12.72	0.01	3.54	0.72	y	Eruptive	–
VVVv182	VVV J154309.19-550153.01	15:43:09.19	-55:01:53.01	325.90823	-0.01055	–	–	–	–	19.08	0.19	16.98	0.08	15.16	0.03	1.56	0.47	y	STV	75.95
VVVv183	VVV J154307.07-550119.87	15:43:07.07	-55:01:19.87	325.90979	-0.00017	–	–	–	–	–	–	16.80	0.07	14.51	0.02	1.42	0.76	y	Dipper	–
VVVv184	VVV J154513.00-552251.04	15:45:13.00	-55:22:51.04	325.92885	-0.46700	–	–	19.84	0.23	17.35	0.04	15.58	0.02	14.54	0.02	1.07	–	n	EB	3.36
VVVv185	VVV J154605.44-551957.68	15:46:05.44	-55:19:57.68	326.05649	-0.50513	–	–	–	–	19.42	0.26	17.33	0.11	15.46	0.04	1.50	0.80	y	STV	75.49
VVVv186	VVV J154758.12-552938.44	15:47:58.12	-55:29:38.44	326.16666	-0.79655	14.57	0.01	13.99	0.01	13.43	0.01	12.91	0.01	12.55	0.01	1.26	–	n	EB	1.12
VVVv187	VVV J154617.80-550439.61	15:46:17.80	-55:04:39.61	326.23646	-0.32207	–	–	–	–	–	–	–	–	12.88	0.01	1.77	–	n	LPV	907
VVVv188	VVV J154635.47-545846.03	15:46:35.47	-54:58:46.03	326.33016	-0.27062	–	–	–	–	–	–	14.19	0.01	11.68	0.01	1.43	0.11	y	LPV-Mira	591
VVVv189	VVV J154905.50-552236.60	15:49:05.50	-55:22:36.60	326.36429	-0.80370	19.67	0.08	18.92	0.10	18.80	0.15	17.60	0.14	16.65	0.11	1.49	–	n	LPV	–
VVVv190	VVV J154703.56-544310.15	15:47:03.56	-54:43:10.15	326.54350	-0.10750	–	–	–	–	18.83	0.15	15.60	0.02	13.49	0.01	1.47	1.25	y	LPV-YSO	125
VVVv191	VVV J154707.98-544302.68	15:47:07.98	-54:43:02.68	326.55314	-0.11242	–	–	–	–	–	–	–	–	15.63	0.04	1.08	2.57	y	Eruptive	–
VVVv192	VVV J155121.51-545723.34	15:51:21.51	-54:57:23.34	326.87990	-0.67856	–	–	–	–	–	–	18.10	0.17	14.45	0.01	1.18	0.64	y	STV	–
VVVv193	VVV J154914.34-543423.66	15:49:14.34	-54:34:23.66	326.88153	-0.18832	–	–	–	–	–	–	16.59	0.04	13.90	0.01	1.25	0.86	y	Eruptive	–
VVVv194	VVV J154957.50-543838.27	15:49:57.50	-54:38:38.27	326.91875	-0.30860	–	–	–	–	–	–	–	–	15.54	0.04	1.16	0.98	y	STV	–
VVVv195	VVV J155314.61-551333.40	15:53:14.61	-55:13:33.40	326.91871	-1.05781	19.67	0.11	18.83	0.09	18.55	0.10	16.97	0.06	15.91	0.05	2.10	-0.33	y	Fader	–
VVVv196	VVV J154932.40-542534.67	15:49:32.40	-54:25:34.67	327.00734	-0.10072	–	–	–	–	–	–	18.14	0.18	16.10	0.06	1.14	2.07	y	STV	–
VVVv197	VVV J155122.71-542010.52	15:51:22.71	-54:20:10.52	327.27238	-0.19829	–	–	–	–	–	–	16.78	0.05	12.50	0.01	1.37	0.56	y	LPV-Mira	–
VVVv198	VVV J155307.15-543639.89	15:53:07.15	-54:36:39.89	327.29485	-0.57106	20.53	0.23	19.49	0.16	19.11	0.16	17.72	0.12	14.75	0.02	1.82	2.06	y	Fader	–
VVVv199	VVV J155256.17-542852.83	15:52:56.17	-54:28:52.83	327.35655	-0.45388	–	–	–	–	19.24	0.18	16.80	0.05	15.28	0.03	1.08	0.72	y	Eruptive	–
VVVv200	VVV J155302.80-542708.40	15:53:02.80	-54:27:08.40	327.38735	-0.44161	–	–	–	–	–	–	–	–	12.68	0.01	1.63	1.00	y	LPV-Mira	707
VVVv201	VVV J155211.02-541051.16	15:52:11.02	-54:10:51.16	327.46158	-0.15176	–	–	–	–	–	–	–	–	14.62	0.02	2.54	–	n	LPV	853
VVVv202	VVV J155426.41-540829.40	15:54:26.41	-54:08:29.40	327.74188	-0.33087	–	–	–	–	17.38	0.03	13.28	0.01	11.66	0.01	1.61	1.16	y	LPV-YSO	–
VVVv203	VVV J155643.05-542945.28	15:56:43.05	-54:29:45.28	327.76983	-0.81574	–	–	18.26	0.05	16.65	0.02	15.19	0.01	14.39	0.01	1.09	–	n	EB	4.84
VVVv204	VVV J155450.66-540315.87	15:54:50.66	-54:03:15.87	327.84307	-0.30161	–	–	–	–	–	–	–	–	14.17	0.01	2.61	2.39	y	LPV-Mira	851
VVVv205	VVV J155628.83-541406.86	15:56:28.83	-54:14:06.86	327.91112	-0.59397	19.69	0.11	18.78	0.09	16.31	0.01	14.97	0.01	13.79	0.01	1.78	-0.98	y	STV	–
VVVv206	VVV J155608.75-535525.81	15:56:08.75	-53:55:25.81	328.07362	-0.32383	–	–	–	–	–	–	16.24	0.03	11.62	0.01	1.30	-0.25	y	LPV-Mira	541
VVVv207	VVV J155544.14-533732.94	15:55:44.14	-53:37:32.94	328.21834	-0.05636	–	–	–	–	–	–	16.12	0.03	12.28	0.01	2.02	0.18	y	LPV-Mira	566
VVVv208	VVV J155641.55-534553.75	15:56:41.55	-53:45:53.75	328.23755	-0.25395	–	–	19.61	0.18	–	–	16.79	0.05	12.52	0.01	1.54	0.20	y	LPV-Mira	590
VVVv209	VVV J155758.41-535807.08	15:57:58.41	-53:58:07.08	328.25034	-0.53142	–	–	–	–	19.17	0.17	16.68	0.05	15.34	0.03	1.31	–	y	LPV-YSO	–

Continued on next page

Table C1 – *Continued from previous page*

Object ID	VVV Designation	α (J2000)	δ (J2000)	l (degrees)	b (degrees)	Z (mag)	Z_{err} (mag)	Y (mag)	Y_{err} (mag)	J (mag)	J_{err} (mag)	H (mag)	H_{err} (mag)	$K_{\rm s}$ (mag)	$K_{\rm s,err}$ (mag)	$\Delta K_{\rm s}$ (mag)	α_{class}	SFR	Class	Period (days)
VVVv210	VVV J155819.39-540133.97	15:58:19.39	-54:01:33.97	328.25230	-0.60849	–	–	–	–	–	–	15.47	0.02	11.67	0.01	1.45	-0.37	y	LPV-Mira	456
VVVv211	VVV J155807.52-535714.66	15:58:07.52	-53:57:14.66	328.27680	-0.53478	–	–	–	–	–	–	–	–	15.51	0.04	1.40	3.43	y	Fader	–
VVVv212	VVV J155558.91-533219.30	15:55:58.91	-53:32:19.30	328.30224	-0.01294	–	–	19.38	0.15	16.56	0.02	14.07	0.01	12.36	0.01	3.11	0.58	y	Fader	–
VVVv213	VVV J155617.48-532950.20	15:56:17.48	-53:29:50.20	328.36411	-0.01074	–	–	–	–	17.79	0.07	14.54	0.01	12.65	0.01	1.99	-2.82	y	Eruptive	–
VVVv214	VVV J155741.02-534347.63	15:57:41.02	-53:43:47.63	328.37212	-0.32167	–	–	–	–	–	–	16.26	0.05	14.06	0.01	1.02	0.45	y	STV	–
VVVv215	VVV J155916.48-540006.12	15:59:16.48	-54:00:06.12	328.37445	-0.68067	–	–	–	–	19.15	0.23	14.52	0.01	11.65	0.01	2.36	–	n	LPV	469
VVVv216	VVV J155844.58-535337.80	15:58:44.58	-53:53:37.80	328.38508	-0.54785	–	–	–	–	18.88	0.18	16.95	0.09	15.60	0.05	1.73	-0.61	y	Eruptive	–
VVVv217	VVV J155902.40-534116.97	15:59:02.40	-53:41:16.97	328.55209	-0.41986	17.70	0.02	16.69	0.01	15.30	0.01	14.04	0.01	12.99	0.01	3.03	-0.52	y	Fader	–
VVVv218	VVV J155807.87-532943.96	15:58:07.87	-53:29:43.96	328.57433	-0.18588	–	–	19.25	0.14	17.54	0.06	15.48	0.02	12.12	0.01	1.55	–	n	LPV	–
VVVv219	VVV J155938.19-533959.95	15:59:38.19	-53:39:59.95	328.63309	-0.46109	–	–	–	–	–	–	16.95	0.08	14.50	0.02	1.49	-0.28	y	Dipper	–
VVVv220	VVV J155954.74-534027.71	15:59:54.74	-53:40:27.71	328.65906	-0.49357	–	–	–	–	–	–	17.79	0.18	15.46	0.04	1.30	0.07	y	STV	–
VVVv221	VVV J160046.60-534036.32	16:00:46.60	-53:40:36.32	328.75440	-0.57900	–	–	–	–	–	–	15.93	0.03	12.29	0.01	2.22	–	n	LPV	–
VVVv222	VVV J160448.76-535412.84	16:04:48.76	-53:54:12.84	329.05271	-1.14271	–	–	–	–	18.39	0.11	14.95	0.01	12.21	0.01	1.78	–	n	LPV	593
VVVv223	VVV J160202.72-532218.87	16:02:02.72	-53:22:18.87	329.09671	-0.47265	–	–	–	–	17.53	0.05	13.46	0.01	11.69	0.01	1.15	–	n	LPV	393
VVVv224	VVV J160347.48-533418.99	16:03:47.48	-53:34:18.99	329.15985	-0.79441	–	–	–	–	–	–	16.64	0.06	13.31	0.01	2.46	–	n	LPV	486.00
VVVv225	VVV J160528.47-534420.45	16:05:28.47	-53:44:20.45	329.23518	-1.08499	17.16	0.01	16.09	0.01	14.89	0.01	13.99	0.01	13.31	0.01	1.14	–	n	LPV	–
VVVv226	VVV J160206.29-530850.39	16:02:06.29	-53:08:50.39	329.25116	-0.30937	–	–	–	–	–	–	16.82	0.08	14.18	0.01	1.82	0.73	y	STV	–
VVVv227	VVV J160133.14-525521.83	16:01:33.14	-52:55:21.83	329.33616	-0.08550	18.05	0.02	17.13	0.02	17.38	0.05	16.44	0.06	15.68	0.05	1.23	–	n	EB	1.53
VVVv228	VVV J160335.44-531414.20	16:03:35.44	-53:14:14.20	329.35903	-0.52381	–	–	–	–	–	–	16.82	0.08	13.76	0.01	1.20	0.62	y	LPV-YSO	300
VVVv229	VVV J160424.48-530114.01	16:04:24.48	-53:01:14.01	329.59450	-0.44282	–	–	–	–	–	–	–	–	13.01	0.01	3.70	–	y	LPV-Mira	978
VVVv230	VVV J161006.42-525119.46	16:10:06.42	-52:51:19.46	330.34185	-0.89679	–	–	–	–	17.43	0.05	15.94	0.03	14.93	0.03	1.30	–	n	EB	5.61
VVVv231	VVV J160825.89-521333.77	16:08:25.89	-52:13:33.77	330.57989	-0.26091	–	–	–	–	–	–	15.52	0.02	12.81	0.01	2.05	-0.21	y	LPV-Mira	301
VVVv232	VVV J161004.42-521301.46	16:10:04.42	-52:13:01.46	330.77123	-0.42439	–	–	–	–	–	–	16.75	0.07	14.81	0.02	2.49	1.21	y	Eruptive	–
VVVv233	VVV J161240.47-523302.72	16:12:40.47	-52:33:02.72	330.83416	-0.93907	–	–	–	–	19.04	0.23	17.09	0.10	15.76	0.06	1.18	–	n	LPV	225
VVVv234	VVV J161146.65-521915.53	16:11:46.65	-52:19:15.53	330.89153	-0.67793	18.15	0.03	17.73	0.04	17.15	0.04	15.68	0.03	11.95	0.01	1.20	–	n	LPV	–
VVVv235	VVV J160935.53-515414.08	16:09:35.53	-51:54:14.08	330.92907	-0.14398	–	–	–	–	–	–	17.95	0.22	11.70	0.01	1.26	1.15	y	LPV-Mira	769
VVVv236	VVV J160937.74-514027.52	16:09:37.74	-51:40:27.52	331.08873	0.02112	19.43	0.08	17.88	0.04	16.45	0.02	15.36	0.02	14.58	0.02	1.04	-1.80	y	STV	–
VVVv237	VVV J161048.22-514245.01	16:10:48.22	-51:42:45.01	331.19651	-0.13049	–	–	19.46	0.21	18.44	0.15	16.25	0.05	13.83	0.01	1.85	1.10	y	Eruptive	–
VVVv238	VVV J161210.99-515417.23	16:12:10.99	-51:54:17.23	331.22135	-0.41654	–	–	–	–	19.20	0.31	16.71	0.07	14.95	0.03	2.11	0.32	y	Eruptive	–
VVVv239	VVV J161153.85-513059.51	16:11:53.85	-51:30:59.51	331.45432	-0.10280	–	–	–	–	–	–	–	–	15.71	0.06	1.27	1.42	y	Dipper	–
VVVv240	VVV J161303.44-514151.91	16:13:03.44	-51:41:51.91	331.46161	-0.35819	–	–	–	–	–	–	16.35	0.05	12.10	0.01	1.17	0.74	y	LPV-Mira	800
VVVv241	VVV J161706.22-511730.81	16:17:06.22	-51:17:30.81	332.19736	-0.49979	18.35	0.04	16.72	0.02	15.33	0.01	14.19	0.01	13.51	0.01	1.24	-2.11	y	EB	55
VVVv242	VVV J161703.71-510640.99	16:17:03.71	-51:06:40.99	332.31823	-0.36556	–	–	–	–	–	–	15.26	0.02	12.06	0.01	2.45	-0.54	y	Dipper	–
VVVv243	VVV J161802.02-511439.85	16:18:02.02	-51:14:39.85	332.33479	-0.56710	–	–	–	–	–	–	–	–	15.64	0.05	2.26	2.33	y	Fader	–
VVVv244	VVV J162001.99-512602.11	16:20:01.99	-51:26:02.11	332.42494	-0.92108	–	–	–	–	17.62	0.07	14.99	0.01	13.05	0.01	2.08	0.79	y	LPV-YSO	500
VVVv245	VVV J161920.93-511107.06	16:19:20.93	-51:11:07.06	332.52333	-0.66895	–	–	–	–	–	–	17.48	0.14	15.61	0.05	1.08	–	n	STV	–
VVVv246	VVV J161841.84-505702.76	16:18:41.84	-50:57:02.76	332.61452	-0.42986	–	–	–	–	–	–	17.76	0.18	16.27	0.10	1.23	–	n	LPV	1800
VVVv247	VVV J161713.24-503845.65	16:17:13.24	-50:38:45.65	332.66002	-0.04874	17.47	0.01	16.71	0.01	15.93	0.01	14.87	0.01	12.46	0.01	1.67	0.84	y	LPV-Mira	733
VVVv248	VVV J162051.74-511336.09	16:20:51.74	-51:13:36.09	332.66283	-0.86504	–	–	–	–	19.68	0.30	17.17	0.08	15.27	0.03	1.54	0.85	y	STV	–
VVVv249	VVV J161724.00-503658.01	16:17:24.00	-50:36:58.01	332.70127	-0.04709	–	–	20.04	0.22	18.10	0.07	15.86	0.02	14.83	0.02	1.27	–	y	Eruptive	–
VVVv250	VVV J161819.35-503227.95	16:18:19.35	-50:32:27.95	332.85853	-0.09549	–	–	–	–	–	–	15.79	0.02	12.30	0.01	1.71	0.47	y	LPV-Mira	538
VVVv251	VVV J162034.52-505106.31	16:20:34.52	-50:51:06.31	332.89495	-0.56713	–	–	–	–	–	–	17.29	0.09	15.03	0.02	1.51	-0.05	y	LPV-YSO	125

Continued on next page

Table C1 – *Continued from previous page*

Object ID	VVV Designation	α (J2000)	δ (J2000)	l (degrees)	b (degrees)	Z (mag)	Z_{err} (mag)	Y (mag)	Y_{err} (mag)	J (mag)	J_{err} (mag)	H (mag)	H_{err} (mag)	K_s (mag)	$K_{s,err}$ (mag)	ΔK_s (mag)	α_{class}	SFR	Class	Period (days)
VVVv252	VVV J161920.52-502317.47	16:19:20.52	-50:23:17.47	333.08142	-0.09980	–	–	–	–	–	–	–	–	17.13	0.17	2.38	4.30	y	LPV-YSO	135.81
VVVv253	VVV J162115.82-504027.98	16:21:15.82	-50:40:27.98	333.09714	-0.51808	–	–	–	–	19.72	0.30	17.97	0.16	13.77	0.01	1.74	2.16	y	LPV-Mira	610
VVVv254	VVV J161943.16-502401.84	16:19:43.16	-50:24:01.84	333.11563	-0.15078	–	–	–	–	18.62	0.11	16.36	0.04	14.71	0.02	1.05	0.25	y	LPV-YSO	326
VVVv255	VVV J162122.89-503514.65	16:21:22.89	-50:35:14.65	333.17183	-0.46962	–	–	–	–	–	–	18.05	0.18	15.61	0.04	1.38	1.20	y	STV	7.53
VVVv256	VVV J161935.14-501640.86	16:19:35.14	-50:16:40.86	333.18641	-0.04855	–	–	–	–	–	–	18.57	0.29	15.16	0.03	1.12	0.37	y	Dipper	–
VVVv257	VVV J162101.87-502912.99	16:21:01.87	-50:29:12.99	333.20324	-0.35914	–	–	–	–	–	–	17.76	0.13	15.42	0.04	1.66	1.72	y	STV	26
VVVv258	VVV J162153.24-503407.34	16:21:53.24	-50:34:07.34	333.24186	-0.51312	–	–	–	–	–	–	17.70	0.13	15.43	0.04	1.62	1.59	y	STV	77
VVVv259	VVV J162141.05-502857.12	16:21:41.05	-50:28:57.12	333.27994	-0.42935	–	–	–	–	–	–	–	–	16.91	0.14	2.08	2.12	y	Eruptive	–
VVVv260	VVV J162105.71-501916.41	16:21:05.71	-50:19:16.41	333.32734	-0.24884	14.41	0.01	13.52	0.01	13.20	0.01	13.02	0.01	12.47	0.01	1.37	1.01	y	Eruptive	–
VVVv261	VVV J162136.83-502407.96	16:21:36.83	-50:24:07.96	333.32877	-0.36459	–	–	–	–	–	–	17.38	0.09	14.27	0.01	1.61	2.19	y	Fader	–
VVVv262	VVV J162159.58-502620.59	16:21:59.58	-50:26:20.59	333.34544	-0.43335	19.02	0.05	18.23	0.04	17.30	0.03	16.32	0.04	15.67	0.05	1.03	–	y	Eruptive	–
VVVv263	VVV J162144.17-502041.41	16:21:44.17	-50:20:41.41	333.38312	-0.33779	–	–	–	–	–	–	16.81	0.06	13.24	0.01	2.24	1.21	y	Eruptive	–
VVVv264	VVV J162120.67-501547.33	16:21:20.67	-50:15:47.33	333.39653	-0.23577	–	–	–	–	–	–	–	–	15.07	0.03	2.54	1.31	y	LPV-Mira	686
VVVv265	VVV J162047.39-500359.42	16:20:47.39	-50:03:59.42	333.47223	-0.03372	–	–	–	–	17.09	0.03	14.72	0.01	13.05	0.01	1.13	-0.02	y	Eruptive	–
VVVv266	VVV J162052.46-500415.80	16:20:52.46	-50:04:15.80	333.47864	-0.04650	–	–	20.13	0.25	18.13	0.07	16.15	0.03	15.08	0.03	1.13	-0.88	y	STV	67
VVVv267	VVV J162217.53-501402.98	16:22:17.53	-50:14:02.98	333.52419	-0.32240	–	–	–	–	–	–	–	–	14.77	0.02	1.94	2.41	y	LPV-Mira	622
VVVv268	VVV J162255.11-495757.37	16:22:55.11	-49:57:57.37	333.78515	-0.20438	–	–	–	–	–	–	17.99	0.17	15.38	0.04	1.29	-0.11	y	STV	–
VVVv269	VVV J162330.97-495006.51	16:23:30.97	-49:50:06.51	333.94581	-0.18068	–	–	–	–	–	–	16.89	0.06	12.92	0.01	2.00	-0.10	y	Dipper	–
VVVv270	VVV J162327.14-494443.96	16:23:27.14	-49:44:43.96	334.00225	-0.11033	–	–	–	–	–	–	18.34	0.23	16.14	0.07	3.81	1.76	y	Eruptive	–
VVVv271	VVV J162733.92-495537.61	16:27:33.92	-49:55:37.61	334.33558	-0.71174	–	–	–	–	18.25	0.08	16.58	0.05	15.47	0.04	1.06	–	n	STV	–
VVVv272	VVV J162841.05-495311.78	16:28:41.05	-49:53:11.78	334.48953	-0.81370	18.97	0.05	18.14	0.04	16.85	0.02	15.78	0.02	15.08	0.03	1.22	-1.36	y	STV	7
VVVv273	VVV J163010.37-495319.51	16:30:10.37	-49:53:19.51	334.65324	-0.98893	17.95	0.02	17.07	0.02	15.63	0.01	14.35	0.01	13.37	0.01	1.00	-0.65	y	STV	–
VVVv274	VVV J162618.97-491433.07	16:26:18.97	-49:14:33.07	334.68700	-0.09031	–	–	–	–	–	–	17.05	0.08	13.38	0.01	1.07	0.99	y	LPV-Mira	405
VVVv275	VVV J162951.29-493754.93	16:29:51.29	-49:37:54.93	334.80437	-0.77501	20.31	0.16	18.71	0.07	17.26	0.03	16.14	0.03	15.47	0.04	1.00	–	n	STV	–
VVVv276	VVV J162917.42-492231.45	16:29:17.42	-49:22:31.45	334.92721	-0.53187	–	–	–	–	–	–	17.97	0.17	13.81	0.01	1.25	–	n	LPV	519
VVVv277	VVV J162708.30-490019.80	16:27:08.30	-49:00:19.80	334.95085	-0.02207	–	–	–	–	–	–	–	–	15.95	0.06	1.80	1.78	y	Eruptive	–
VVVv278	VVV J162856.75-491343.89	16:28:56.75	-49:13:43.89	334.99454	-0.39010	–	–	19.73	0.17	17.67	0.05	16.02	0.03	15.06	0.03	1.00	-2.08	y	STV	–
VVVv279	VVV J162939.57-492006.48	16:29:39.57	-49:20:06.48	334.99782	-0.54768	–	–	–	–	–	–	17.97	0.17	15.40	0.04	1.92	1.00	y	STV	–
VVVv280	VVV J162952.41-491102.80	16:29:52.41	-49:11:02.80	335.13140	-0.46904	–	–	–	–	19.11	0.18	16.24	0.04	14.42	0.02	2.30	0.93	y	Dipper	–
VVVv281	VVV J162749.92-485144.00	16:27:49.92	-48:51:44.00	335.13307	-0.00469	–	–	–	–	17.08	0.03	15.61	0.02	14.52	0.02	1.23	-0.23	y	Eruptive	–
VVVv282	VVV J162953.95-490948.69	16:29:53.95	-49:09:48.69	335.14921	-0.45791	–	–	–	–	19.92	0.38	17.14	0.08	15.67	0.05	1.39	-0.16	y	Eruptive	–
VVVv283	VVV J162904.28-485908.99	16:29:04.28	-48:59:08.99	335.18456	-0.23722	–	–	–	–	–	–	–	–	13.37	0.01	1.28	-0.09	y	LPV-Mira	471
VVVv284	VVV J162820.68-484917.24	16:28:20.68	-48:49:17.24	335.22089	-0.03732	–	–	–	–	–	–	15.07	0.01	12.09	0.01	1.53	0.76	y	LPV-Mira	520
VVVv285	VVV J162959.38-484955.29	16:29:59.38	-48:49:55.29	335.40001	-0.24062	–	–	20.24	0.27	18.15	0.08	15.26	0.01	12.75	0.01	1.76	0.41	y	Eruptive	–
VVVv286	VVV J163051.43-484356.65	16:30:51.43	-48:43:56.65	335.57057	-0.27605	18.21	0.04	17.23	0.03	17.29	0.04	15.60	0.03	14.15	0.02	1.07	0.64	y	Dipper	–
VVVv287	VVV J163317.78-490138.74	16:33:17.78	-49:01:38.74	335.62893	-0.77046	–	–	–	–	17.51	0.05	16.07	0.04	15.04	0.03	1.19	-1.22	y	STV	53.93
VVVv288	VVV J163058.02-482220.40	16:30:58.02	-48:22:20.40	335.84512	-0.04237	–	–	19.02	0.14	17.18	0.04	16.00	0.04	15.20	0.04	1.21	–	y	EB	–
VVVv289	VVV J163232.83-483609.97	16:32:32.83	-48:36:09.97	335.85597	-0.39099	–	–	–	–	17.82	0.07	15.51	0.02	14.23	0.02	1.32	-0.87	y	LPV-Mira	1500
VVVv290	VVV J163231.47-480227.03	16:32:31.47	-48:02:27.03	336.26444	-0.00508	–	–	–	–	–	–	15.39	0.02	12.56	0.01	1.77	1.10	y	LPV-Mira	520
VVVv291	VVV J163441.08-482000.21	16:34:41.08	-48:20:00.21	336.29434	-0.46802	–	–	18.49	0.08	16.28	0.02	13.56	0.01	12.04	0.01	1.19	–	n	LPV	180
VVVv292	VVV J163252.77-475717.93	16:32:52.77	-47:57:17.93	336.36776	0.00997	–	–	–	–	16.62	0.02	14.66	0.01	13.23	0.01	1.64	-1.68	y	STV	47
VVVv293	VVV J163455.76-481324.47	16:34:55.76	-48:13:24.47	336.40284	-0.42364	18.78	0.06	18.31	0.07	17.54	0.06	16.80	0.08	16.33	0.11	1.60	–	n	STV	–

Continued on next page

Table C1 – *Continued from previous page*

Object ID	VVV Designation	α (J2000)	δ (J2000)	l (degrees)	b (degrees)	Z (mag)	Z_{err} (mag)	Y (mag)	Y_{err} (mag)	J (mag)	J_{err} (mag)	H (mag)	H_{err} (mag)	$K_{\rm s}$ (mag)	$K_{\rm s,err}$ (mag)	$\Delta K_{\rm s}$ (mag)	α_{class}	SFR	Class	Period (days)
VVVv294	VVV J163257.43-475355.83	16:32:57.43	-47:53:55.83	336.41772	0.03868	–	–	–	–	–	–	17.13	0.11	15.22	0.04	1.60	0.49	y	STV	75
VVVv295	VVV J163657.31-482731.22	16:36:57.31	-48:27:31.22	336.45585	-0.83088	–	–	–	–	16.45	0.02	13.15	0.01	11.67	0.01	2.51	–	n	LPV	–
VVVv296	VVV J163559.12-475138.62	16:35:59.12	-47:51:38.62	336.78964	-0.30906	–	–	–	–	17.80	0.08	16.18	0.04	15.25	0.04	1.10	–	y	EB	5.7
VVVv297	VVV J163510.88-473943.17	16:35:10.88	-47:39:43.17	336.84518	-0.07525	17.74	0.03	17.20	0.03	16.97	0.03	16.49	0.06	16.06	0.09	1.12	–	y	STV	–
VVVv298	VVV J163506.52-473750.51	16:35:06.52	-47:37:50.51	336.85998	-0.04508	19.92	0.18	18.40	0.08	17.07	0.04	16.17	0.04	15.43	0.05	1.04	–	y	STV	–
VVVv299	VVV J163549.32-474139.27	16:35:49.32	-47:41:39.27	336.89416	-0.17660	–	–	19.65	0.25	17.36	0.05	16.07	0.04	15.29	0.05	1.06	–	y	STV	2.13
VVVv300	VVV J163520.86-473509.87	16:35:20.86	-47:35:09.87	336.92010	-0.04465	–	–	–	–	–	–	16.79	0.08	12.72	0.01	1.54	0.27	y	LPV-Mira	433
VVVv301	VVV J163815.13-474825.10	16:38:15.13	-47:48:25.10	337.08476	-0.55507	–	–	–	–	16.50	0.02	13.82	0.01	11.90	0.01	1.79	0.77	y	LPV-Mira	621
VVVv302	VVV J163716.53-473816.00	16:37:16.53	-47:38:16.00	337.10049	-0.31979	–	–	–	–	18.75	0.18	16.58	0.07	15.37	0.05	1.61	1.07	y	Fader	–
VVVv303	VVV J163909.57-473235.02	16:39:09.57	-47:32:35.02	337.38326	-0.49277	–	–	–	–	–	–	15.59	0.03	12.47	0.01	1.41	-0.07	y	LPV-Mira	470
VVVv304	VVV J164056.68-474302.70	16:40:56.68	-47:43:02.70	337.45259	-0.83342	–	–	18.90	0.10	17.32	0.05	14.86	0.01	13.06	0.01	1.09	0.37	y	STV	–
VVVv305	VVV J163942.31-473033.43	16:39:42.31	-47:30:33.43	337.46978	-0.53905	–	–	–	–	–	–	15.97	0.04	13.57	0.01	1.48	0.87	y	STV	65.42
VVVv306	VVV J164057.54-471531.45	16:40:57.54	-47:15:31.45	337.79806	-0.53166	–	–	–	–	–	–	17.51	0.17	15.52	0.06	1.21	0.42	y	STV	–
VVVv307	VVV J164113.16-471747.09	16:41:13.16	-47:17:47.09	337.79902	-0.58970	–	–	–	–	–	–	16.28	0.05	16.26	0.11	1.12	0.06	y	EB	–
VVVv308	VVV J164220.97-471911.31	16:42:20.97	-47:19:11.31	337.90787	-0.74909	–	–	–	–	16.95	0.03	14.45	0.01	12.36	0.01	1.62	–	n	LPV	466
VVVv309	VVV J164058.19-470631.93	16:40:58.19	-47:06:31.93	337.91164	-0.43387	–	–	–	–	–	–	17.32	0.14	13.53	0.01	2.30	1.63	y	LPV-YSO	191
VVVv310	VVV J164118.44-470744.80	16:41:18.44	-47:07:44.80	337.93443	-0.49032	–	–	–	–	–	–	–	–	15.55	0.06	1.51	1.49	y	STV	–
VVVv311	VVV J164222.77-463204.23	16:42:22.77	-46:32:04.23	338.50224	-0.23581	–	–	–	–	18.84	0.18	16.87	0.08	15.53	0.05	1.07	-0.51	y	STV	–
VVVv312	VVV J164336.63-463555.56	16:43:36.63	-46:35:55.56	338.59283	-0.43754	–	–	–	–	–	–	16.26	0.05	11.86	0.01	1.99	0.50	y	LPV-Mira	625
VVVv313	VVV J164322.08-463031.47	16:43:22.08	-46:30:31.47	338.63345	-0.34702	–	–	–	–	–	–	–	–	16.44	0.11	1.17	2.55	y	LPV-YSO	924
VVVv314	VVV J164436.13-462642.81	16:44:36.13	-46:26:42.81	338.82057	-0.46604	19.29	0.08	19.03	0.11	16.14	0.02	14.11	0.01	12.39	0.01	1.29	0.03	y	STV	31.06
VVVv315	VVV J164319.07-460818.16	16:43:19.07	-46:08:18.16	338.90723	-0.09744	–	–	–	–	16.91	0.03	14.88	0.01	13.66	0.01	1.35	-1.57	y	EB	6.85
VVVv316	VVV J164517.96-462415.96	16:45:17.96	-46:24:15.96	338.92986	-0.53047	–	–	–	–	19.38	0.29	16.64	0.07	14.73	0.02	2.25	0.62	y	Fader	–
VVVv317	VVV J164447.36-461634.12	16:44:47.36	-46:16:34.12	338.96971	-0.38009	–	–	–	–	–	–	15.91	0.03	13.27	0.01	1.77	0.81	y	STV	–
VVVv318	VVV J164542.89-461737.70	16:45:42.89	-46:17:37.70	339.06053	-0.51288	–	–	–	–	–	–	14.66	0.01	12.10	0.01	1.30	-0.16	y	LPV-YSO	527
VVVv319	VVV J164517.04-460555.44	16:45:17.04	-46:05:55.44	339.16005	-0.32929	–	–	–	–	17.35	0.05	14.75	0.01	12.58	0.01	1.94	0.01	y	Eruptive	–
VVVv320	VVV J164541.05-460645.91	16:45:41.05	-46:06:45.91	339.19456	-0.39105	20.04	0.16	19.33	0.14	18.33	0.11	16.88	0.08	15.84	0.06	1.39	0.31	y	STV	–
VVVv321	VVV J164703.25-461214.67	16:47:03.25	-46:12:14.67	339.27907	-0.63080	18.01	0.03	17.58	0.03	17.67	0.06	16.09	0.04	14.56	0.02	1.30	0.61	y	STV	9.36
VVVv322	VVV J164624.57-455921.04	16:46:24.57	-45:59:21.04	339.37029	-0.40641	–	–	–	–	18.48	0.13	16.82	0.08	15.25	0.04	2.63	0.91	y	Eruptive	–
VVVv323	VVV J164925.09-461955.83	16:49:25.09	-46:19:55.83	339.44450	-1.02573	–	–	–	–	–	–	16.19	0.04	14.22	0.01	1.28	0.94	y	STV	–
VVVv324	VVV J164711.61-455737.06	16:47:11.61	-45:57:37.06	339.48056	-0.49144	–	–	–	–	17.83	0.07	15.98	0.03	14.51	0.02	1.47	0.70	y	Fader	–
VVVv325	VVV J164916.71-461417.94	16:49:16.71	-46:14:17.94	339.50098	-0.94697	15.95	0.01	15.38	0.01	13.46	0.01	12.62	0.01	11.91	0.01	1.24	0.28	y	STV	20.36
VVVv326	VVV J164528.77-453801.97	16:45:28.77	-45:38:01.97	339.53491	-0.05229	–	–	–	–	–	–	17.89	0.20	13.35	0.01	2.09	1.04	y	LPV-Mira	506
VVVv327	VVV J164746.43-455444.92	16:47:46.43	-45:54:44.92	339.58225	-0.53750	–	–	–	–	17.29	0.04	15.42	0.02	13.94	0.01	1.02	-0.94	y	Eruptive	–
VVVv328	VVV J164737.86-453948.08	16:47:37.86	-45:39:48.08	339.75637	-0.35759	–	–	–	–	18.32	0.11	15.59	0.03	14.27	0.02	1.16	-2.04	y	Eruptive	–
VVVv329	VVV J164623.58-452459.68	16:46:23.58	-45:24:59.68	339.80405	-0.03261	–	–	–	–	–	–	13.38	0.01	10.66	0.01	2.16	–	n	LPV	528
VVVv330	VVV J164925.34-454635.09	16:49:25.34	-45:46:35.09	339.87121	-0.66959	–	–	–	–	–	–	16.35	0.05	12.57	0.01	2.43	–	n	LPV	780
VVVv331	VVV J164654.11-451521.92	16:46:54.11	-45:15:21.92	339.98421	0.00338	–	–	–	–	19.84	0.30	16.52	0.06	15.74	0.07	2.67	0.59	y	Eruptive	–
VVVv332	VVV J165142.03-455238.00	16:51:42.03	-45:52:38.00	340.04734	-1.03927	–	–	–	–	–	–	16.85	0.08	15.35	0.05	1.49	0.61	y	LPV-YSO	1270
VVVv333	VVV J164815.42-452141.77	16:48:15.42	-45:21:41.77	340.05765	-0.24663	–	–	–	–	–	–	–	–	15.99	0.09	1.15	6.22	y	LPV-Mira	436
VVVv334	VVV J164809.91-451905.07	16:48:09.91	-45:19:05.07	340.08052	-0.20624	–	–	–	–	–	–	15.21	0.02	12.16	0.01	1.31	0.42	y	LPV-Mira	520
VVVv335	VVV J165209.73-455249.55	16:52:09.73	-45:52:49.55	340.09595	-1.10332	17.20	0.01	16.11	0.01	14.61	0.01	12.55	0.01	11.82	0.01	3.43	0.52	y	Fader	–

Continued on next page

Table C1 – *Continued from previous page*

Object ID	VVV Designation	α (J2000)	δ (J2000)	l (degrees)	b (degrees)	Z (mag)	Z_{err} (mag)	Y (mag)	Y_{err} (mag)	J (mag)	J_{err} (mag)	H (mag)	H_{err} (mag)	$K_{\rm s}$ (mag)	$K_{\rm s,err}$ (mag)	$\Delta K_{\rm s}$ (mag)	α_{class}	SFR	Class	Period (days)
VVVv336	VVV J165106.53-454324.24	16:51:06.53	-45:43:24.24	340.10021	-0.86179	–	–	–	–	–	–	–	–	15.47	0.06	2.27	0.77	y	Eruptive	–
VVVv337	VVV J165207.12-454634.45	16:52:07.12	-45:46:34.45	340.17162	-1.03128	–	–	–	–	18.55	0.09	14.78	0.01	13.43	0.01	1.66	-0.23	y	STV	16.6
VVVv338	VVV J164900.46-451559.95	16:49:00.46	-45:15:59.95	340.21527	-0.28650	–	–	19.42	0.20	17.99	0.06	12.88	0.01	10.53	0.01	1.31	-0.27	y	LPV-Mira	451
VVVv339	VVV J164856.73-451230.02	16:48:56.73	-45:12:30.02	340.25289	-0.24062	–	–	–	–	–	–	16.88	0.08	15.07	0.04	1.06	0.28	y	STV	2.37
VVVv340	VVV J164831.39-450636.17	16:48:31.39	-45:06:36.17	340.28023	-0.12039	18.31	0.03	17.56	0.04	17.33	0.03	15.72	0.03	12.86	0.01	1.21	0.02	y	LPV-Mira	700.5
VVVv341	VVV J164936.97-451216.30	16:49:36.97	-45:12:16.30	340.33168	-0.32873	–	–	–	–	–	–	15.76	0.03	12.31	0.01	1.50	-0.85	y	LPV-YSO	430
VVVv342	VVV J165400.57-452249.43	16:54:00.57	-45:22:49.43	340.68757	-1.03674	20.10	0.17	18.46	0.09	17.58	0.04	15.68	0.03	14.98	0.04	1.29	-0.87	y	STV	29.2
VVVv343	VVV J165207.50-450636.51	16:52:07.50	-45:06:36.51	340.68672	-0.60889	17.01	0.01	15.91	0.01	15.60	0.01	14.42	0.01	14.43	0.02	1.17	–	n	EB	1.24
VVVv344	VVV J165408.46-451939.80	16:54:08.46	-45:19:39.80	340.74304	-1.02144	20.70	0.30	18.73	0.11	17.96	0.06	15.93	0.03	15.48	0.06	1.15	-0.22	y	Eruptive	–
VVVv345	VVV J165128.98-445511.43	16:51:28.98	-44:55:11.43	340.76133	-0.40026	–	–	–	–	–	–	17.12	0.10	12.97	0.01	3.69	–	n	LPV	681
VVVv346	VVV J165412.34-451756.95	16:54:12.34	-45:17:56.95	340.77239	-1.01226	–	–	19.58	0.24	18.05	0.06	15.73	0.03	14.95	0.04	1.55	–	y	Dipper	–
VVVv347	VVV J164957.30-443856.10	16:49:57.30	-44:38:56.10	340.79657	-0.01860	–	–	–	–	–	–	–	–	12.36	0.01	1.06	-1.04	y	LPV-YSO	464
VVVv348	VVV J165357.35-451050.19	16:53:57.35	-45:10:50.19	340.83662	-0.90334	–	–	–	–	–	–	14.76	0.01	11.60	0.01	1.43	0.41	y	LPV-Mira	598
VVVv349	VVV J165453.41-451345.52	16:54:53.41	-45:13:45.52	340.90250	-1.06184	19.43	0.09	17.57	0.04	16.20	0.01	–	–	13.38	0.01	1.02	-0.16	y	STV	–
VVVv350	VVV J165030.84-442939.22	16:50:30.84	-44:29:39.22	340.97914	0.00390	–	–	19.03	0.14	15.96	0.01	12.93	0.01	12.10	0.01	1.02	-1.12	y	EB	5.16
VVVv351	VVV J165149.25-444006.46	16:51:49.25	-44:40:06.46	340.99336	-0.28646	–	–	–	–	–	–	14.25	0.01	11.72	0.01	1.01	-0.32	y	LPV-YSO	464
VVVv352	VVV J165153.69-443850.98	16:51:53.69	-44:38:50.98	341.01790	-0.28327	–	–	–	–	–	–	16.94	0.08	15.66	0.07	1.33	-0.38	y	Eruptive	–
VVVv353	VVV J165209.03-444046.25	16:52:09.03	-44:40:46.25	341.02208	-0.33871	–	–	–	–	–	–	14.41	0.01	11.35	0.01	1.12	-0.47	y	LPV-Mira	507
VVVv354	VVV J165049.33-442228.30	16:50:49.33	-44:22:28.30	341.10638	0.03805	18.16	0.03	17.42	0.03	16.97	0.02	15.62	0.03	14.77	0.03	2.25	–	y	Eruptive	–
VVVv355	VVV J165113.82-442732.78	16:51:13.82	-44:27:32.78	341.08776	-0.07202	–	–	–	–	–	–	13.91	0.01	11.44	0.01	1.10	0.12	y	LPV-YSO	431
VVVv356	VVV J165240.98-443802.07	16:52:40.98	-44:38:02.07	341.11746	-0.38295	–	–	–	–	–	–	16.13	0.04	12.00	0.01	2.46	1.00	y	LPV-Mira	613
VVVv357	VVV J165238.49-443632.52	16:52:38.49	-44:36:32.52	341.13199	-0.36144	–	–	18.44	0.08	17.19	0.03	15.16	0.02	14.79	0.03	1.13	-0.47	y	STV	–
VVVv358	VVV J165433.46-445023.87	16:54:33.46	-44:50:23.87	341.16816	-0.77117	–	–	–	–	–	–	14.04	0.01	11.84	0.01	1.22	–	n	LPV	224
VVVv359	VVV J165329.81-443421.75	16:53:29.81	-44:34:21.75	341.25655	-0.45631	–	–	19.22	0.17	17.54	0.04	15.09	0.02	14.33	0.02	1.21	1.07	y	Fader	–
VVVv360	VVV J165643.64-445641.92	16:56:43.64	-44:56:41.92	341.32737	-1.13632	–	–	–	–	–	–	–	–	16.81	0.20	3.71	–	n	LPV	806
VVVv361	VVV J165454.74-443841.67	16:54:54.74	-44:38:41.67	341.35939	-0.69735	–	–	–	–	–	–	15.48	0.02	12.65	0.01	1.38	–	n	LPV	624
VVVv362	VVV J165304.23-442234.26	16:53:04.23	-44:22:34.26	341.36060	-0.27305	–	–	–	–	–	–	17.46	0.13	15.33	0.05	1.61	1.35	y	Eruptive	–
VVVv363	VVV J165300.74-441028.62	16:53:00.74	-44:10:28.62	341.50999	-0.13733	–	–	–	–	18.32	0.09	15.47	0.02	12.17	0.01	1.85	–	n	LPV	654
VVVv364	VVV J165432.55-440446.80	16:54:32.55	-44:04:46.80	341.75703	-0.29022	–	–	–	–	18.40	0.10	14.12	0.01	12.12	0.01	1.68	-0.50	y	LPV-YSO	449
VVVv365	VVV J165521.41-440217.92	16:55:21.41	-44:02:17.92	341.88120	-0.37796	17.33	0.01	16.61	0.01	15.83	0.01	15.08	0.01	14.65	0.02	1.08	–	n	EB	0.68
VVVv366	VVV J165644.69-433017.90	16:56:44.69	-43:30:17.90	342.45393	-0.23927	–	–	–	–	18.10	0.07	15.84	0.03	14.59	0.02	1.17	0.03	y	LPV-Mira	1000
VVVv367	VVV J170029.61-435300.34	17:00:29.61	-43:53:00.34	342.57740	-1.00550	–	–	–	–	–	–	17.32	0.11	13.69	0.01	2.35	1.50	y	Fader	–
VVVv368	VVV J165755.54-432803.82	16:57:55.54	-43:28:03.82	342.61656	-0.38353	–	–	–	–	–	–	17.72	0.16	16.09	0.08	1.23	–	n	STV	–
VVVv369	VVV J165641.41-431129.86	16:56:41.41	-43:11:29.86	342.69237	-0.03573	–	–	18.66	0.08	17.41	0.04	16.33	0.04	15.79	0.06	1.07	–	n	STV	–
VVVv370	VVV J165748.65-430442.53	16:57:48.65	-43:04:42.53	342.90831	-0.12502	–	–	–	–	–	–	14.57	0.01	12.01	0.01	1.15	0.25	y	LPV-YSO	445
VVVv371	VVV J165950.04-431721.62	16:59:50.04	-43:17:21.62	342.97146	-0.54512	–	–	19.26	0.11	17.75	0.04	15.79	0.02	14.60	0.01	2.05	-0.19	y	LPV-YSO	186.6
VVVv372	VVV J165834.31-425647.04	16:58:34.31	-42:56:47.04	343.09823	-0.15194	–	–	–	–	–	–	14.73	0.01	11.99	0.01	1.31	-0.52	y	LPV-YSO	481
VVVv373	VVV J170242.77-432514.46	17:02:42.77	-43:25:14.46	343.18920	-1.03878	–	–	–	–	–	–	14.23	0.01	11.66	0.01	1.63	–	n	LPV	659
VVVv374	VVV J165833.99-424955.25	16:58:33.99	-42:49:55.25	343.18734	-0.08021	–	–	–	–	17.12	0.02	13.99	0.01	11.98	0.01	2.41	0.91	y	Eruptive	–
VVVv375	VVV J165916.71-425325.43	16:59:16.71	-42:53:25.43	343.22235	-0.21877	–	–	–	–	17.47	0.03	13.64	0.01	12.01	0.01	1.14	-0.61	y	LPV-YSO	248
VVVv376	VVV J165844.44-424736.58	16:58:44.44	-42:47:36.58	343.23737	-0.08137	–	–	–	–	17.28	0.03	14.67	0.01	12.83	0.01	1.74	0.34	y	Fader	–
VVVv377	VVV J170123.56-430945.16	17:01:23.56	-43:09:45.16	343.24620	-0.69078	–	–	–	–	20.17	0.34	16.56	0.03	14.40	0.01	2.07	0.13	y	LPV-Mira	1156

Continued on next page

Table C1 – *Continued from previous page*

Object ID	VVV Designation	α (J2000)	δ (J2000)	l (degrees)	b (degrees)	Z (mag)	Z_{err} (mag)	Y (mag)	Y_{err} (mag)	J (mag)	J_{err} (mag)	H (mag)	H_{err} (mag)	$K_{\rm s}$ (mag)	$K_{\rm s,err}$ (mag)	$\Delta K_{\rm s}$ (mag)	α_{class}	SFR	Class	Period (days)
VVVv378	VVV J165846.18-424637.73	16:58:46.18	-42:46:37.73	343.25349	-0.07541	–	–	–	–	–	–	15.94	0.02	12.32	0.01	1.65	0.82	y	LPV-Mira	671
VVVv379	VVV J170043.40-430219.08	17:00:43.40	-43:02:19.08	343.26885	-0.51826	–	–	–	–	–	–	–	–	17.09	0.14	1.79	1.05	y	Eruptive	–
VVVv380	VVV J170128.15-430612.43	17:01:28.15	-43:06:12.43	343.30142	-0.66553	14.12	0.01	14.11	0.01	12.84	0.01	12.79	0.01	12.46	0.01	1.04	–	n	STV	–
VVVv381	VVV J170056.90-425637.41	17:00:56.90	-42:56:37.41	343.36899	-0.49231	–	–	–	–	–	–	16.67	0.04	13.71	0.01	2.76	0.87	y	Fader	–
VVVv382	VVV J170206.05-425926.64	17:02:06.05	-42:59:26.64	343.46124	-0.68763	19.48	0.08	19.13	0.10	18.62	0.09	17.83	0.11	14.32	0.01	3.29	–	n	LPV	1414
VVVv383	VVV J170340.88-431135.78	17:03:40.88	-43:11:35.78	343.47692	-1.03981	–	–	19.97	0.21	16.54	0.01	12.98	0.01	11.24	0.01	2.02	–	n	LPV	640
VVVv384	VVV J170024.90-423701.24	17:00:24.90	-42:37:01.24	343.56623	-0.21407	–	–	–	–	19.28	0.16	14.46	0.01	11.96	0.01	1.78	0.48	y	LPV-Mira	510
VVVv385	VVV J165952.37-422429.44	16:59:52.37	-42:24:29.44	343.66897	-0.00661	17.24	0.01	16.78	0.01	16.25	0.01	15.70	0.02	15.50	0.03	1.30	–	n	STV	–
VVVv386	VVV J170105.37-423008.44	17:01:05.37	-42:30:08.44	343.73305	-0.24140	–	–	–	–	19.55	0.19	17.41	0.07	16.45	0.08	1.06	–	y	Eruptive	–
VVVv387	VVV J170300.08-423144.81	17:03:00.08	-42:31:44.81	343.92764	-0.53630	20.31	0.18	19.18	0.10	17.55	0.03	16.39	0.03	15.74	0.04	1.08	–	y	STV	–
VVVv388	VVV J170302.23-422515.48	17:03:02.23	-42:25:15.48	344.01736	-0.47555	–	–	–	–	–	–	–	–	16.10	0.06	1.64	0.84	y	Eruptive	–
VVVv389	VVV J170317.18-422549.88	17:03:17.18	-42:25:49.88	344.03782	-0.51780	–	–	–	–	–	–	16.69	0.04	13.51	0.01	1.56	0.71	y	Eruptive	–
VVVv390	VVV J170203.10-420332.27	17:02:03.10	-42:03:32.27	344.19236	-0.10990	–	–	–	–	19.49	0.19	17.46	0.08	15.82	0.05	1.06	-0.58	y	LPV-YSO	–
VVVv391	VVV J170430.33-422215.38	17:04:30.33	-42:22:15.38	344.22202	-0.66025	–	–	–	–	–	–	–	–	15.88	0.05	1.35	0.39	y	STV	–
VVVv392	VVV J170310.35-415131.99	17:03:10.35	-41:51:31.99	344.47807	-0.15256	–	–	–	–	–	–	16.19	0.04	12.31	0.01	1.38	-0.20	y	LPV-Mira	531
VVVv393	VVV J170436.13-415410.75	17:04:36.13	-41:54:10.75	344.60491	-0.39061	–	–	–	–	18.08	0.07	16.71	0.06	15.74	0.05	1.05	–	n	STV	–
VVVv394	VVV J170507.70-414631.38	17:05:07.70	-41:46:31.38	344.76581	-0.39125	–	–	–	–	–	–	15.65	0.02	13.89	0.01	1.02	–	n	LPV	1500
VVVv395	VVV J170724.60-415541.50	17:07:24.60	-41:55:41.50	344.89996	-0.82239	–	–	–	–	18.92	0.15	17.27	0.11	16.35	0.09	2.68	–	n	Rare	–
VVVv396	VVV J170347.02-412326.48	17:03:47.02	-41:23:26.48	344.91895	0.04206	–	–	–	–	–	–	14.23	0.01	12.23	0.01	1.16	-0.15	y	Eruptive	–
VVVv397	VVV J170501.10-413310.92	17:05:01.10	-41:33:10.92	344.93032	-0.24027	–	–	–	–	–	–	–	–	13.98	0.01	1.17	0.33	y	LPV-Mira	515
VVVv398	VVV J170818.57-414440.23	17:08:18.57	-41:44:40.23	345.14743	-0.84651	–	–	–	–	18.91	0.15	16.52	0.05	15.12	0.03	1.11	-0.11	y	STV	–
VVVv399	VVV J170523.37-411925.23	17:05:23.37	-41:19:25.23	345.15502	-0.15685	–	–	–	–	18.42	0.10	16.98	0.08	15.64	0.05	1.24	0.10	y	STV	–
VVVv400	VVV J170805.25-414002.24	17:08:05.25	-41:40:02.24	345.18452	-0.76711	–	–	–	–	19.27	0.21	17.03	0.08	15.53	0.04	1.02	-0.43	y	STV	16.73
VVVv401	VVV J170528.32-411709.21	17:05:28.32	-41:17:09.21	345.19448	-0.14634	–	–	–	–	–	–	17.39	0.12	12.09	0.01	3.00	0.35	y	LPV-Mira	671
VVVv402	VVV J170533.12-411547.18	17:05:33.12	-41:15:47.18	345.22171	-0.14452	–	–	–	–	–	–	–	–	15.07	0.03	1.19	1.34	y	Eruptive	–
VVVv403	VVV J170645.11-412444.47	17:06:45.11	-41:24:44.47	345.23847	-0.41420	–	–	–	–	18.76	0.13	16.84	0.07	15.39	0.04	1.12	–	n	Rare	–
VVVv404	VVV J170936.20-414740.73	17:09:36.20	-41:47:40.73	345.25111	-1.07003	–	–	–	–	–	–	16.23	0.04	13.00	0.01	1.49	1.15	y	Eruptive	–
VVVv405	VVV J170938.62-413851.81	17:09:38.62	-41:38:51.81	345.37370	-0.98868	–	–	–	–	–	–	17.50	0.13	13.50	0.01	1.99	1.77	y	Dipper	–
VVVv406	VVV J170957.47-413548.87	17:09:57.47	-41:35:48.87	345.44947	-1.00565	–	–	18.89	0.12	17.51	0.04	14.61	0.01	12.57	0.01	2.06	1.10	y	Dipper	–
VVVv407	VVV J171014.46-413159.13	17:10:14.46	-41:31:59.13	345.53228	-1.01036	–	–	–	–	18.73	0.13	17.24	0.11	16.32	0.10	1.07	0.60	y	Eruptive	–
VVVv408	VVV J170719.60-405954.28	17:07:19.60	-40:59:54.28	345.63430	-0.25183	–	–	19.75	0.25	18.82	0.14	16.90	0.08	15.27	0.04	1.40	0.13	y	STV	11.16
VVVv409	VVV J170633.12-405257.01	17:06:33.12	-40:52:57.01	345.63897	-0.06526	19.08	0.07	18.26	0.06	17.05	0.03	15.95	0.03	15.30	0.04	1.41	-1.19	y	STV	9
VVVv410	VVV J170951.32-410424.87	17:09:51.32	-41:04:24.87	345.85893	-0.67912	–	–	–	–	–	–	17.42	0.20	13.37	0.01	1.89	–	n	LPV	699
VVVv411	VVV J170714.78-403616.02	17:07:14.78	-40:36:16.02	345.94021	-0.00312	–	–	–	–	–	–	17.43	0.20	15.95	0.09	1.78	1.27	y	LPV-YSO	307
VVVv412	VVV J170719.21-403041.54	17:07:19.21	-40:30:41.54	346.02292	0.04146	–	–	–	–	–	–	14.86	0.02	12.15	0.01	1.29	0.20	y	Eruptive	–
VVVv413	VVV J171244.60-405917.67	17:12:44.60	-40:59:17.67	346.24984	-1.06791	–	–	–	–	–	–	15.76	0.04	11.66	0.01	1.97	–	n	LPV	672
VVVv414	VVV J170826.92-402011.77	17:08:26.92	-40:20:11.77	346.29166	-0.02571	–	–	–	–	–	–	15.64	0.04	12.14	0.01	1.83	–	n	LPV	670
VVVv415	VVV J170913.65-401051.69	17:09:13.65	-40:10:51.69	346.50518	-0.05205	19.34	0.09	18.22	0.07	16.90	0.04	15.06	0.02	11.55	0.01	1.89	–	n	LPV	583
VVVv416	VVV J170954.59-395612.24	17:09:54.59	-39:56:12.24	346.77920	-0.01154	19.12	0.07	18.20	0.07	17.17	0.06	14.73	0.02	11.69	0.01	1.79	–	n	LPV	646
VVVv417	VVV J171002.75-395634.95	17:10:02.75	-39:56:34.95	346.78961	-0.03624	–	–	–	–	–	–	16.04	0.06	14.38	0.02	1.35	–	n	LPV	750
VVVv418	VVV J170950.73-395404.21	17:09:50.73	-39:54:04.21	346.80045	0.01953	–	–	–	–	–	–	14.71	0.02	11.64	0.01	1.22	–	n	LPV	523
VVVv419	VVV J171322.75-394816.82	17:13:22.75	-39:48:16.82	347.27891	-0.47067	16.34	0.01	15.86	0.01	15.25	0.01	14.68	0.02	14.42	0.03	1.07	–	n	EB	7.2

Continued on next page

Table C1 – *Continued from previous page*

Object ID	VVV Designation	α (J2000)	δ (J2000)	l (degrees)	b (degrees)	Z (mag)	Z_{err} (mag)	Y (mag)	Y_{err} (mag)	J (mag)	J_{err} (mag)	H (mag)	H_{err} (mag)	$K_{\rm s}$ (mag)	$K_{\rm s,err}$ (mag)	$\Delta K_{\rm s}$ (mag)	α_{class}	SFR	Class	Period (days)
VVVv420	VVV J171234.47-393812.04	17:12:34.47	-39:38:12.04	347.32392	-0.24676	–	–	19.20	0.21	17.73	0.12	16.48	0.10	15.65	0.09	1.12	–	n	LPV	–
VVVv421	VVV J171416.64-385217.39	17:14:16.64	-38:52:17.39	348.13698	-0.06482	–	–	17.63	0.05	14.03	0.01	12.47	0.01	11.49	0.01	1.77	–	n	LPV	–
VVVv422	VVV J171910.90-390227.06	17:19:10.90	-39:02:27.06	348.55130	-0.94006	–	–	–	–	–	–	–	–	15.42	0.07	1.85	2.05	y	Eruptive	–
VVVv423	VVV J171803.97-385228.88	17:18:03.97	-38:52:28.88	348.56253	-0.66712	–	–	–	–	–	–	17.23	0.19	15.09	0.05	1.34	-0.79	y	Fader	–
VVVv424	VVV J171929.84-390253.81	17:19:29.84	-39:02:53.81	348.58037	-0.99454	–	–	–	–	17.53	0.11	15.63	0.05	14.66	0.03	1.00	-0.54	y	STV	6.38
VVVv425	VVV J171717.53-382435.22	17:17:17.53	-38:24:35.22	348.85491	-0.27532	–	–	–	–	–	–	14.52	0.01	11.58	0.01	1.79	0.18	y	LPV-Mira	569
VVVv426	VVV J171901.66-381856.10	17:19:01.66	-38:18:56.10	349.12795	-0.49911	–	–	18.90	0.10	16.98	0.04	15.58	0.04	14.68	0.03	1.10	0.28	y	STV	–
VVVv427	VVV J171751.37-375720.53	17:17:51.37	-37:57:20.53	349.28963	-0.10357	–	–	–	–	16.82	0.03	13.67	0.01	12.20	0.01	1.02	-0.50	y	LPV-YSO	176.44
VVVv428	VVV J172200.73-382816.84	17:22:00.73	-38:28:16.84	349.33401	-1.06811	–	–	18.71	0.08	17.30	0.05	15.42	0.03	14.63	0.03	1.16	–	n	Rare	–
VVVv429	VVV J171737.48-375148.58	17:17:37.48	-37:51:48.58	349.33859	-0.01309	–	–	–	–	–	–	14.71	0.02	11.99	0.01	2.05	0.33	y	LPV-Mira	673
VVVv430	VVV J172258.00-381855.60	17:22:58.00	-38:18:55.60	349.56849	-1.13389	–	–	–	–	–	–	15.33	0.03	12.29	0.01	2.11	0.45	y	LPV-YSO	628
VVVv431	VVV J172237.25-380642.48	17:22:37.25	-38:06:42.48	349.69794	-0.96261	19.01	0.05	17.96	0.04	17.59	0.07	15.50	0.03	13.95	0.02	1.44	-1.24	y	LPV-YSO	958
VVVv432	VVV J171827.35-373153.62	17:18:27.35	-37:31:53.62	349.70459	0.04393	–	–	–	–	17.99	0.10	15.12	0.02	11.85	0.01	2.70	0.88	y	LPV-Mira	640
VVVv433	VVV J172230.65-373952.40	17:22:30.65	-37:39:52.40	350.05420	-0.69131	–	–	–	–	–	–	15.49	0.03	12.48	0.01	1.48	0.05	y	LPV-Mira	481
VVVv434	VVV J172412.71-375231.53	17:24:12.71	-37:52:31.53	350.07010	-1.08782	19.70	0.09	18.91	0.10	16.96	0.04	15.64	0.04	14.78	0.03	1.20	–	y	STV	7.89
VVVv435	VVV J114449.44-612030.53	11:44:49.44	-61:20:30.53	295.03186	0.50402	–	–	–	–	19.31	0.23	17.01	0.06	15.27	0.02	1.59	0.13	y	Dipper	–
VVVv436	VVV J114920.18-612533.85	11:49:20.18	-61:25:33.85	295.57625	0.55563	20.07	0.13	18.87	0.08	17.62	0.05	15.29	0.01	13.54	0.01	2.16	0.10	y	LPV-Mira	484
VVVv437	VVV J120800.72-612716.02	12:08:00.72	-61:27:16.02	297.76730	0.98110	18.82	0.06	18.10	0.05	17.07	0.02	16.27	0.02	15.82	0.03	1.10	–	n	STV	–
VVVv438	VVV J121458.74-623509.84	12:14:58.74	-62:35:09.84	298.74931	-0.01075	–	–	–	–	–	–	17.52	0.07	15.26	0.02	1.59	0.16	y	Dipper	–
VVVv439	VVV J121555.97-623408.87	12:15:55.97	-62:34:08.87	298.85571	0.02130	–	–	–	–	–	–	17.74	0.08	15.97	0.03	1.08	0.26	y	STV	5.88
VVVv440	VVV J121710.81-622317.02	12:17:10.81	-62:23:17.02	298.97406	0.22016	18.52	0.04	17.68	0.03	16.76	0.02	16.00	0.02	15.56	0.02	1.14	–	y	STV	–
VVVv441	VVV J122130.75-621939.83	12:21:30.75	-62:19:39.83	299.46516	0.34244	19.72	0.11	17.82	0.04	16.08	0.01	14.63	0.01	13.73	0.01	1.49	–	n	LPV	–
VVVv442	VVV J122346.20-621804.25	12:23:46.20	-62:18:04.25	299.72280	0.39807	20.09	0.15	18.57	0.07	16.88	0.02	15.30	0.01	14.42	0.01	1.91	–	n	LPV	–
VVVv443	VVV J122758.25-624255.21	12:27:58.25	-62:42:55.21	300.24623	0.03400	18.78	0.05	18.01	0.05	17.28	0.03	16.12	0.02	15.33	0.02	1.00	–	n	STV	–
VVVv444	VVV J123511.19-624550.01	12:35:11.19	-62:45:50.01	301.07374	0.04923	19.92	0.14	18.70	0.07	17.32	0.03	15.93	0.02	15.18	0.02	1.26	-0.81	y	Dipper	–
VVVv445	VVV J123605.64-614556.40	12:36:05.64	-61:45:56.40	301.11794	1.05205	–	–	–	–	19.01	0.13	16.42	0.03	14.20	0.01	1.63	-0.24	y	STV	86.26
VVVv446	VVV J123659.77-622732.15	12:36:59.77	-62:27:32.15	301.26334	0.36604	18.77	0.05	18.21	0.05	17.44	0.03	16.45	0.03	16.42	0.05	1.08	–	n	STV	–
VVVv447	VVV J123745.17-622536.29	12:37:45.17	-62:25:36.29	301.34896	0.40295	19.14	0.06	18.24	0.05	17.00	0.02	16.22	0.02	15.75	0.03	1.36	–	n	STV	–
VVVv448	VVV J123746.96-623154.07	12:37:46.96	-62:31:54.07	301.35798	0.29835	18.95	0.06	17.96	0.04	16.98	0.02	16.02	0.02	14.05	0.01	1.68	–	n	LPV	655
VVVv449	VVV J124055.13-615710.28	12:40:55.13	-61:57:10.28	301.69559	0.89366	20.57	0.25	18.94	0.09	17.01	0.02	14.70	0.01	12.84	0.01	2.45	0.03	y	Dipper	–
VVVv450	VVV J124124.20-614717.91	12:41:24.20	-61:47:17.91	301.74609	1.06035	–	–	–	–	18.65	0.09	17.04	0.05	15.77	0.03	1.11	0.24	y	STV	–
VVVv451	VVV J124115.97-623337.44	12:41:15.97	-62:33:37.44	301.76038	0.28823	–	–	–	–	–	–	18.97	0.27	14.89	0.01	1.78	1.26	y	LPV-YSO	675.00
VVVv452	VVV J124158.06-621342.90	12:41:58.06	-62:13:42.90	301.82894	0.62290	–	–	–	–	18.10	0.06	15.68	0.01	13.78	0.01	2.46	0.40	y	Eruptive	–
VVVv453	VVV J124205.43-621621.45	12:42:05.43	-62:16:21.45	301.84484	0.57941	–	–	–	–	18.48	0.08	16.85	0.04	15.81	0.03	1.18	-0.26	y	STV	–
VVVv454	VVV J124228.93-620929.37	12:42:28.93	-62:09:29.37	301.88639	0.69543	–	–	–	–	–	–	17.72	0.08	14.95	0.01	1.15	1.34	y	Dipper	–
VVVv455	VVV J124251.78-621810.74	12:42:51.78	-62:18:10.74	301.93566	0.55220	–	–	–	–	–	–	15.21	0.01	11.92	0.01	1.31	0.22	y	LPV-Mira	550
VVVv456	VVV J124303.86-621246.44	12:43:03.86	-62:12:46.44	301.95610	0.64300	–	–	–	–	18.96	0.12	17.16	0.05	15.77	0.03	1.60	-0.05	y	STV	–
VVVv457	VVV J124316.34-621127.15	12:43:16.34	-62:11:27.15	301.97963	0.66580	–	–	18.19	0.05	14.86	0.01	12.31	0.01	11.26	0.01	2.17	-0.54	y	LPV-Mira	960
VVVv458	VVV J124352.55-615134.62	12:43:52.55	-61:51:34.62	302.04027	0.99906	14.96	0.01	14.27	0.01	13.67	0.01	12.47	0.01	11.80	0.01	1.70	-0.02	y	STV	19.60
VVVv459	VVV J124349.50-625419.27	12:43:49.50	-62:54:19.27	302.06520	-0.04639	20.62	0.21	19.11	0.09	18.21	0.07	17.26	0.06	16.75	0.09	1.22	–	y	LPV-YSO	173.00
VVVv460	VVV J124452.97-623402.84	12:44:52.97	-62:34:02.84	302.17700	0.29470	–	–	19.22	0.10	17.82	0.05	16.30	0.02	15.10	0.02	1.62	–	n	STV	–
VVVv461	VVV J124841.99-623046.38	12:48:41.99	-62:30:46.38	302.61596	0.35721	19.97	0.12	18.81	0.07	17.54	0.04	16.38	0.03	15.79	0.04	1.34	–	n	Rare	–

Continued on next page

Table C1 – *Continued from previous page*

Object ID	VVV Designation	α (J2000)	δ (J2000)	l (degrees)	b (degrees)	Z (mag)	Z_{err} (mag)	Y (mag)	Y_{err} (mag)	J (mag)	J_{err} (mag)	H (mag)	H_{err} (mag)	$K_{\rm s}$ (mag)	$K_{\rm s,err}$ (mag)	$\Delta K_{\rm s}$ (mag)	α_{class}	SFR	Class	Period (days)
VVVv462	VVV J124951.84-620038.13	12:49:51.84	-62:00:38.13	302.74722	0.86061	20.92	0.27	19.78	0.17	18.73	0.11	17.33	0.07	16.75	0.09	3.33	–	n	LPV	–
VVVv463	VVV J125455.60-623638.34	12:54:55.60	-62:36:38.34	303.33315	0.25840	–	–	20.05	0.22	18.14	0.06	16.66	0.03	15.40	0.03	1.78	–	n	LPV	–
VVVv464	VVV J125658.47-622019.66	12:56:58.47	-62:20:19.66	303.57447	0.52607	18.17	0.03	17.22	0.02	16.24	0.01	15.32	0.01	14.79	0.01	1.21	–	n	STV	–
VVVv465	VVV J125710.56-622245.50	12:57:10.56	-62:22:45.50	303.59696	0.48506	18.47	0.03	17.85	0.03	17.05	0.02	16.22	0.02	15.80	0.03	1.04	–	n	STV	–
VVVv466	VVV J125936.70-622418.69	12:59:36.70	-62:24:18.69	303.87834	0.45156	–	–	–	–	–	–	–	–	14.58	0.01	2.41	-0.13	y	Fader	–
VVVv467	VVV J130113.23-622527.93	13:01:13.23	-62:25:27.93	304.06381	0.42584	–	–	–	–	17.05	0.02	14.65	0.01	12.90	0.01	2.26	-0.12	y	Fader	–
VVVv468	VVV J130237.59-623928.81	13:02:37.59	-62:39:28.81	304.21624	0.18586	–	–	–	–	–	–	16.46	0.03	14.29	0.01	1.07	-0.02	y	LPV-YSO	166
VVVv469	VVV J130402.14-621003.89	13:04:02.14	-62:10:03.89	304.40186	0.66806	–	–	18.54	0.07	17.63	0.04	16.31	0.02	13.15	0.01	2.78	–	n	LPV	746
VVVv470	VVV J130653.37-622408.51	13:06:53.37	-62:24:08.51	304.72042	0.41574	13.93	0.01	13.51	0.01	13.08	0.01	12.85	0.01	12.51	0.01	1.01	–	n	LPV	1786
VVVv471	VVV J130819.74-623121.15	13:08:19.74	-62:31:21.15	304.87894	0.28536	–	–	–	–	–	–	17.99	0.11	15.62	0.03	1.30	0.78	y	Dipper	–
VVVv472	VVV J130834.09-621741.78	13:08:34.09	-62:17:41.78	304.92159	0.51064	–	–	–	–	18.47	0.09	16.56	0.04	15.66	0.03	1.04	-0.56	y	STV	11.5
VVVv473	VVV J131057.49-623522.34	13:10:57.49	-62:35:22.34	305.17637	0.19714	–	–	–	–	–	–	–	–	14.53	0.01	1.50	1.82	y	LPV-YSO	275
VVVv474	VVV J131102.14-623513.07	13:11:02.14	-62:35:13.07	305.18548	0.19903	–	–	–	–	–	–	18.11	0.15	16.36	0.06	1.07	–	y	STV	–
VVVv475	VVV J131129.71-623426.91	13:11:29.71	-62:34:26.91	305.23920	0.20774	–	–	–	–	–	–	18.08	0.14	16.18	0.06	1.82	–	y	STV	31
VVVv476	VVV J131204.60-623457.16	13:12:04.60	-62:34:57.16	305.30528	0.19408	–	–	–	–	–	–	–	–	15.57	0.03	1.30	2.10	y	STV	–
VVVv477	VVV J131309.69-624330.96	13:13:09.69	-62:43:30.96	305.41772	0.04161	–	–	–	–	–	–	17.88	0.12	16.52	0.07	1.42	0.79	y	STV	–
VVVv478	VVV J131415.24-622300.25	13:14:15.24	-62:23:00.25	305.57265	0.37133	14.13	0.01	13.80	0.01	12.20	0.01	12.66	0.01	12.05	0.01	1.05	–	n	EB	6.07
VVVv479	VVV J131546.03-624155.02	13:15:46.03	-62:41:55.02	305.71754	0.04149	–	–	19.76	0.20	18.65	0.11	17.41	0.08	16.65	0.08	1.24	–	y	STV	43.25
VVVv480	VVV J131650.32-622341.61	13:16:50.32	-62:23:41.61	305.86975	0.33190	16.94	0.01	16.46	0.01	15.81	0.01	15.08	0.01	14.58	0.01	1.70	-0.28	y	LPV-YSO	159
VVVv481	VVV J131723.85-623904.20	13:17:23.85	-62:39:04.20	305.90837	0.07049	18.85	0.05	18.40	0.06	18.08	0.06	16.93	0.05	16.11	0.05	1.15	0.39	y	STV	–
VVVv482	VVV J131832.04-624000.36	13:18:32.04	-62:40:00.36	306.03658	0.04155	–	–	–	–	19.19	0.18	17.45	0.08	15.95	0.04	1.35	0.68	y	STV	33.92
VVVv483	VVV J131954.87-623001.95	13:19:54.87	-62:30:01.95	306.21246	0.18971	18.42	0.03	17.63	0.03	16.21	0.01	15.06	0.01	14.40	0.01	1.94	-0.39	y	Fader	–
VVVv484	VVV J132049.78-623750.56	13:20:49.78	-62:37:50.56	306.30262	0.04855	15.78	0.01	15.14	0.01	14.37	0.01	13.66	0.01	12.84	0.01	1.42	–	n	Known	–
VVVv485	VVV J132015.07-615257.98	13:20:15.07	-61:52:57.98	306.32004	0.79931	–	–	19.16	0.12	17.33	0.03	15.92	0.02	15.08	0.02	1.00	–	n	STV	–
VVVv486	VVV J132223.72-622522.25	13:22:23.72	-62:25:22.25	306.50625	0.23389	20.13	0.16	18.57	0.07	16.66	0.02	14.44	0.01	12.68	0.01	1.38	0.43	y	Fader	–
VVVv487	VVV J132325.88-622610.52	13:23:25.88	-62:26:10.52	306.62359	0.20597	–	–	–	–	–	–	–	–	17.27	0.15	1.18	–	n	STV	–
VVVv488	VVV J132631.34-621727.54	13:26:31.34	-62:17:27.54	306.99787	0.30349	–	–	–	–	–	–	18.31	0.20	16.07	0.05	1.11	–	n	LPV	1240
VVVv489	VVV J132654.40-620318.49	13:26:54.40	-62:03:18.49	307.07449	0.53101	–	–	–	–	18.50	0.10	15.84	0.02	14.06	0.01	1.29	0.67	y	Eruptive	–
VVVv490	VVV J133104.45-622318.47	13:31:04.45	-62:23:18.47	307.50652	0.13074	16.26	0.01	15.82	0.01	15.65	0.01	14.84	0.01	13.72	0.01	1.24	–	n	Rare	19.75
VVVv491	VVV J133031.03-615116.55	13:30:31.03	-61:51:16.55	307.52336	0.66830	17.70	0.02	17.00	0.02	16.44	0.02	15.76	0.02	15.39	0.03	1.04	–	n	STV	–
VVVv492	VVV J133044.67-614803.84	13:30:44.67	-61:48:03.84	307.55799	0.71714	20.30	0.19	19.21	0.13	17.91	0.06	16.44	0.04	15.61	0.03	1.09	–	n	STV	–
VVVv493	VVV J133425.10-612855.50	13:34:25.10	-61:28:55.50	308.03945	0.96273	19.27	0.06	18.20	0.04	17.10	0.03	16.10	0.02	15.57	0.03	1.10	–	n	EB	4.67
VVVv494	VVV J134038.29-614700.31	13:40:38.29	-61:47:00.31	308.71294	0.53487	–	–	–	–	–	–	19.59	0.58	14.92	0.02	1.35	2.98	y	Eruptive	–
VVVv495	VVV J134030.34-613514.32	13:40:30.34	-61:35:14.32	308.73464	0.73041	–	–	–	–	–	–	18.52	0.21	15.99	0.04	2.43	2.09	y	Eruptive	–
VVVv496	VVV J134148.93-620635.35	13:41:48.93	-62:06:35.35	308.78618	0.18798	–	–	–	–	–	–	17.15	0.06	15.28	0.02	1.55	0.20	y	Eruptive	–
VVVv497	VVV J134202.43-613911.50	13:42:02.43	-61:39:11.50	308.90099	0.63073	19.05	0.05	18.34	0.05	17.63	0.04	16.50	0.03	15.66	0.03	1.25	–	y	STV	–
VVVv498	VVV J134449.97-621446.41	13:44:49.97	-62:14:46.41	309.10389	-0.01601	–	–	–	–	–	–	14.42	0.01	11.30	0.01	1.92	0.61	y	LPV-Mira	464
VVVv499	VVV J134500.58-620616.25	13:45:00.58	-62:06:16.25	309.15326	0.11842	–	–	–	–	–	–	18.45	0.20	16.19	0.05	1.39	0.58	y	LPV-YSO	319
VVVv500	VVV J134346.56-611919.69	13:43:46.56	-61:19:19.69	309.16963	0.91417	–	–	–	–	–	–	17.66	0.10	15.07	0.02	1.10	–	n	STV	–
VVVv501	VVV J134540.86-620350.24	13:45:40.86	-62:03:50.24	309.23854	0.14180	–	–	–	–	–	–	18.05	0.14	16.40	0.06	1.32	-0.15	y	STV	8.35
VVVv502	VVV J134536.57-614435.04	13:45:36.57	-61:44:35.04	309.29723	0.45739	19.24	0.06	18.31	0.05	17.26	0.03	16.44	0.03	16.01	0.04	1.07	–	n	STV	–
VVVv503	VVV J134816.19-615819.55	13:48:16.19	-61:58:19.55	309.55482	0.16669	–	–	–	–	18.97	0.11	17.21	0.05	16.23	0.05	1.40	–	y	STV	–

Continued on next page

Table C1 – *Continued from previous page*

Object ID	VVV Designation	α (J2000)	δ (J2000)	l (degrees)	b (degrees)	Z (mag)	Z_{err} (mag)	Y (mag)	Y_{err} (mag)	J (mag)	J_{err} (mag)	H (mag)	H_{err} (mag)	$K_{\rm s}$ (mag)	$K_{\rm s,err}$ (mag)	$\Delta K_{\rm s}$ (mag)	α_{class}	SFR	Class	Period (days)
VVVv504	VVV J135017.97-614106.77	13:50:17.97	-61:41:06.77	309.85215	0.39315	–	–	–	–	20.07	0.30	16.31	0.02	14.05	0.01	1.14	0.56	y	Dipper	–
VVVv505	VVV J135241.63-613622.63	13:52:41.63	-61:36:22.63	310.14697	0.40440	–	–	20.10	0.20	17.74	0.04	16.32	0.02	15.22	0.02	1.74	-1.34	y	STV	4.46
VVVv506	VVV J135317.06-611021.46	13:53:17.06	-61:10:21.46	310.31808	0.80910	20.08	0.11	18.79	0.06	17.71	0.04	16.28	0.02	15.12	0.02	1.18	–	n	STV	–
VVVv507	VVV J135543.10-615844.13	13:55:43.10	-61:58:44.13	310.40415	-0.04330	20.04	0.10	17.59	0.02	15.39	0.01	13.20	0.01	11.70	0.01	2.08	–	n	LPV	490
VVVv508	VVV J135631.54-613714.61	13:56:31.54	-61:37:14.61	310.58535	0.28008	–	–	–	–	19.53	0.18	17.90	0.10	16.47	0.06	1.89	–	n	LPV	–
VVVv509	VVV J135541.73-605333.65	13:55:41.73	-60:53:33.65	310.66909	1.01015	12.69	0.01	12.60	0.01	13.90	0.01	13.10	0.01	12.91	0.01	1.23	–	n	Known	2.5
VVVv510	VVV J135741.61-611127.48	13:57:41.61	-61:11:27.48	310.82869	0.66087	–	–	19.24	0.09	17.87	0.06	16.39	0.03	15.37	0.03	1.33	-0.82	y	STV	4.08
VVVv511	VVV J135826.40-611522.53	13:58:26.40	-61:15:22.53	310.89890	0.57482	17.48	0.01	17.17	0.02	16.33	0.02	15.86	0.02	15.61	0.03	1.08	–	n	STV	–
VVVv512	VVV J135943.90-614155.63	13:59:43.90	-61:41:55.63	310.93326	0.10746	–	–	–	–	–	–	15.27	0.01	11.79	0.01	1.95	–	n	LPV	646
VVVv513	VVV J135935.48-612208.31	13:59:35.48	-61:22:08.31	311.00322	0.43020	19.07	0.04	18.23	0.04	17.00	0.03	15.84	0.02	15.10	0.02	1.17	-0.85	y	EB	–
VVVv514	VVV J140045.37-613339.95	14:00:45.37	-61:33:39.95	311.08692	0.20826	–	–	–	–	17.40	0.04	14.80	0.01	13.26	0.01	1.73	-1.46	y	Fader	–
VVVv515	VVV J135923.70-605422.36	13:59:23.70	-60:54:22.36	311.10087	0.88316	–	–	–	–	–	–	17.84	0.11	15.74	0.04	1.34	0.86	y	Fader	–
VVVv516	VVV J140017.60-611719.20	14:00:17.60	-61:17:19.20	311.10552	0.48563	–	–	–	–	–	–	14.16	0.01	10.80	0.01	1.95	0.81	y	LPV-Mira	234
VVVv517	VVV J140211.33-610039.77	14:02:11.33	-61:00:39.77	311.40000	0.69215	19.49	0.06	18.71	0.06	17.76	0.05	16.54	0.03	15.48	0.03	1.18	-0.48	y	STV	–
VVVv518	VVV J140513.13-613222.17	14:05:13.13	-61:32:22.17	311.60408	0.08375	–	–	–	–	–	–	17.29	0.06	12.92	0.01	1.63	0.94	y	LPV-YSO	836
VVVv519	VVV J140537.97-610446.32	14:05:37.97	-61:04:46.32	311.78161	0.51097	19.63	0.07	17.31	0.02	15.21	0.01	13.58	0.01	12.63	0.01	1.48	–	n	Rare	–
VVVv520	VVV J140737.39-613408.44	14:07:37.39	-61:34:08.44	311.86998	-0.02642	–	–	–	–	–	–	14.07	0.01	11.15	0.01	1.48	0.16	y	LPV-Mira	532
VVVv521	VVV J140811.24-611646.87	14:08:11.24	-61:16:46.87	312.01884	0.23068	19.63	0.07	18.79	0.06	17.58	0.05	16.48	0.03	16.05	0.05	1.06	–	y	STV	–
VVVv522	VVV J141041.45-611941.89	14:10:41.45	-61:19:41.89	312.29134	0.09498	–	–	–	–	18.59	0.09	16.22	0.03	14.75	0.01	1.08	-0.30	y	Dipper	–
VVVv523	VVV J140956.15-610140.83	14:09:56.15	-61:01:40.83	312.29472	0.40874	–	–	–	–	–	–	17.71	0.10	15.86	0.04	1.40	–	y	STV	67
VVVv524	VVV J141300.81-610550.91	14:13:00.81	-61:05:50.91	312.62817	0.22920	–	–	–	–	18.05	0.06	15.21	0.01	13.22	0.01	1.57	0.27	y	Dipper	–
VVVv525	VVV J141245.69-603242.92	14:12:45.69	-60:32:42.92	312.77000	0.76378	19.22	0.06	18.30	0.04	17.33	0.03	16.28	0.03	15.90	0.04	1.18	–	n	STV	–
VVVv526	VVV J141535.32-605907.91	14:15:35.32	-60:59:07.91	312.95929	0.23732	–	–	–	–	–	–	18.17	0.15	15.79	0.04	1.17	0.73	y	LPV-Mira	1113
VVVv527	VVV J141503.90-604740.38	14:15:03.90	-60:47:40.38	312.95974	0.43864	–	–	–	–	–	–	14.67	0.01	12.12	0.01	1.58	–	n	LPV	426
VVVv528	VVV J141900.72-610554.36	14:19:00.72	-61:05:54.36	313.31429	-0.00438	–	–	–	–	–	–	16.42	0.03	12.22	0.01	2.41	–	n	LPV	694
VVVv529	VVV J142040.61-604133.22	14:20:40.61	-60:41:33.22	313.64094	0.31027	–	–	–	–	–	–	–	–	11.77	0.01	3.04	–	n	LPV	1236.00
VVVv530	VVV J141902.00-600125.01	14:19:02.00	-60:01:25.01	313.67352	1.00864	–	–	–	–	19.10	0.15	14.17	0.01	10.89	0.01	1.72	–	n	LPV	833
VVVv531	VVV J142212.30-604442.26	14:22:12.30	-60:44:42.26	313.79874	0.19726	–	–	19.65	0.16	18.33	0.08	16.25	0.03	14.74	0.01	1.09	-0.35	y	STV	–
VVVv532	VVV J142134.09-603135.20	14:21:34.09	-60:31:35.20	313.80021	0.42940	20.73	0.22	19.60	0.15	18.40	0.08	16.96	0.05	16.52	0.07	1.05	–	y	STV	–
VVVv533	VVV J142226.67-604542.45	14:22:26.67	-60:45:42.45	313.82047	0.17150	–	–	–	–	–	–	–	–	12.96	0.01	1.48	0.06	y	LPV-Mira	419
VVVv534	VVV J142245.57-605018.07	14:22:45.57	-60:50:18.07	313.83014	0.08639	–	–	–	–	–	–	17.70	0.11	14.79	0.02	1.26	1.39	y	Dipper	–
VVVv535	VVV J142440.39-603412.20	14:24:40.39	-60:34:12.20	314.14310	0.25620	–	–	–	–	–	–	17.55	0.09	15.28	0.02	1.08	-0.18	y	LPV-YSO	329
VVVv536	VVV J142524.24-602352.49	14:25:24.24	-60:23:52.49	314.28816	0.38541	–	–	–	–	18.04	0.06	16.28	0.03	15.27	0.02	1.03	0.02	y	Eruptive	–
VVVv537	VVV J142713.67-595918.35	14:27:13.67	-59:59:18.35	314.64640	0.68661	–	–	19.78	0.18	17.87	0.05	16.61	0.04	15.87	0.04	1.08	–	n	EB	2.57
VVVv538	VVV J142815.52-595700.73	14:28:15.52	-59:57:00.73	314.78046	0.67540	19.79	0.10	19.18	0.10	17.30	0.03	16.08	0.02	15.31	0.02	1.02	–	n	EB	2.33
VVVv539	VVV J143013.42-602755.92	14:30:13.42	-60:27:55.92	314.81753	0.10640	–	–	–	–	–	–	–	–	16.20	0.05	1.95	1.29	y	Eruptive	–
VVVv540	VVV J142743.97-593258.83	14:27:43.97	-59:32:58.83	314.86459	1.07255	19.25	0.06	18.92	0.08	18.17	0.07	16.88	0.05	15.88	0.04	1.28	–	y	STV	–
VVVv541	VVV J142831.88-594338.38	14:28:31.88	-59:43:38.38	314.89380	0.87034	19.43	0.07	18.60	0.06	17.06	0.02	15.36	0.01	13.87	0.01	1.74	0.15	y	Fader	–
VVVv542	VVV J143142.37-602810.18	14:31:42.37	-60:28:10.18	314.98545	0.03431	–	–	–	–	19.07	0.15	17.35	0.08	16.18	0.05	1.51	0.12	y	STV	–
VVVv543	VVV J143142.52-602751.76	14:31:42.52	-60:27:51.76	314.98767	0.03893	19.91	0.10	18.75	0.07	17.58	0.04	16.31	0.03	15.66	0.03	1.14	-1.14	y	STV	–
VVVv544	VVV J143506.67-594150.43	14:35:06.67	-59:41:50.43	315.67339	0.58493	–	–	18.92	0.09	17.47	0.03	16.14	0.02	15.44	0.03	1.11	–	n	STV	–
VVVv545	VVV J143742.20-595110.66	14:37:42.20	-59:51:10.66	315.91205	0.31350	–	–	–	–	–	–	15.26	0.01	11.74	0.01	2.43	–	n	LPV	686

Continued on next page

Table C1 – *Continued from previous page*

Object ID	VVV Designation	α (J2000)	δ (J2000)	l (degrees)	b (degrees)	Z (mag)	Z_{err} (mag)	Y (mag)	Y_{err} (mag)	J (mag)	J_{err} (mag)	H (mag)	H_{err} (mag)	$K_{\rm s}$ (mag)	$K_{\rm s,err}$ (mag)	$\Delta K_{\rm s}$ (mag)	α_{class}	SFR	Class	Period (days)
VVVv546	VVV J143752.06-595303.52	14:37:52.06	-59:53:03.52	315.91849	0.27652	19.05	0.08	17.57	0.03	15.93	0.01	14.25	0.01	13.01	0.01	1.53	–	n	LPV	811
VVVv547	VVV J143633.66-590426.59	14:36:33.66	-59:04:26.59	316.08736	1.08617	18.72	0.06	17.78	0.03	16.77	0.02	15.90	0.02	15.47	0.03	1.12	–	n	STV	–
VVVv548	VVV J143915.54-593353.29	14:39:15.54	-59:33:53.29	316.20727	0.49889	–	–	19.08	0.11	17.39	0.03	16.30	0.03	15.64	0.03	1.91	–	n	STV	–
VVVv549	VVV J144040.89-594625.51	14:40:40.89	-59:46:25.51	316.28658	0.23504	–	–	–	–	–	–	–	–	16.22	0.05	3.05	–	n	LPV	1226
VVVv550	VVV J144054.93-593906.08	14:40:54.93	-59:39:06.08	316.36340	0.33438	18.69	0.06	17.39	0.02	16.06	0.01	14.94	0.01	14.32	0.01	1.09	–	n	EB	2.61
VVVv551	VVV J144153.75-595401.48	14:41:53.75	-59:54:01.48	316.37370	0.05693	–	–	–	–	–	–	16.70	0.04	14.34	0.01	1.87	0.67	y	LPV-YSO	289
VVVv552	VVV J144023.74-590454.89	14:40:23.74	-59:04:54.89	316.53560	0.88153	–	–	–	–	–	–	16.54	0.04	12.46	0.01	1.88	–	n	EB	2.67
VVVv553	VVV J144318.26-595246.19	14:43:18.26	-59:52:46.19	316.54309	0.00266	–	–	–	–	–	–	17.65	0.10	15.54	0.03	1.30	0.43	y	Dipper	–
VVVv554	VVV J144315.42-584340.86	14:43:15.42	-58:43:40.86	317.01816	1.05160	–	–	–	–	–	–	–	–	16.80	0.11	1.63	–	y	Eruptive	–
VVVv555	VVV J144553.20-592208.58	14:45:53.20	-59:22:08.58	317.05440	0.32777	18.24	0.03	16.79	0.01	15.52	0.01	14.13	0.01	13.26	0.01	1.45	0.95	y	Dipper	–
VVVv556	VVV J144617.31-592406.72	14:46:17.31	-59:24:06.72	317.08665	0.27626	–	–	–	–	–	–	17.41	0.10	15.84	0.04	1.08	1.36	y	STV	–
VVVv557	VVV J144648.87-592926.55	14:46:48.87	-59:29:26.55	317.10897	0.16735	–	–	–	–	–	–	17.09	0.07	15.25	0.03	1.25	0.49	y	LPV-YSO	–
VVVv558	VVV J144656.53-592936.63	14:46:56.53	-59:29:36.63	317.12240	0.15786	–	–	–	–	–	–	18.70	0.32	16.86	0.11	1.14	0.30	y	Eruptive	–
VVVv559	VVV J144903.47-592411.99	14:49:03.47	-59:24:11.99	317.40378	0.12261	–	–	–	–	–	–	–	–	14.97	0.02	1.73	1.57	y	Dipper	–
VVVv560	VVV J145047.08-592039.71	14:50:47.08	-59:20:39.71	317.62724	0.07882	–	–	–	–	–	–	17.34	0.09	14.95	0.02	1.46	0.45	y	Dipper	–
VVVv561	VVV J145322.68-592024.94	14:53:22.68	-59:20:24.94	317.92475	-0.06533	–	–	–	–	–	–	15.33	0.02	11.73	0.01	1.55	0.56	y	LPV-Mira	537
VVVv562	VVV J145333.59-591021.73	14:53:33.59	-59:10:21.73	318.02120	0.07365	–	–	–	–	16.68	0.02	14.20	0.01	12.46	0.01	2.79	-0.01	y	Fader	–
VVVv563	VVV J145344.28-590933.73	14:53:44.28	-59:09:33.73	318.04759	0.07521	–	–	–	–	–	–	17.51	0.11	15.40	0.03	1.45	-0.04	y	Fader	–
VVVv564	VVV J145047.04-581441.58	14:50:47.04	-58:14:41.58	318.11405	1.06467	17.77	0.02	17.28	0.02	16.49	0.02	15.50	0.02	15.01	0.02	1.20	–	n	STV	–
VVVv565	VVV J145313.19-584603.42	14:53:13.19	-58:46:03.42	318.16502	0.45487	–	–	–	–	18.91	0.14	16.62	0.05	15.34	0.03	2.38	–	n	Rare	–
VVVv566	VVV J145202.35-580908.23	14:52:02.35	-58:09:08.23	318.30337	1.07401	–	–	–	–	–	–	17.82	0.15	14.81	0.02	1.97	1.81	y	STV	–
VVVv567	VVV J145513.69-584957.65	14:55:13.69	-58:49:57.65	318.36715	0.27875	–	–	–	–	–	–	18.76	0.35	15.81	0.05	1.01	–	n	STV	–
VVVv568	VVV J145518.57-582232.03	14:55:18.57	-58:22:32.03	318.58586	0.68029	18.79	0.05	17.77	0.03	16.76	0.02	15.85	0.02	15.28	0.03	1.20	–	y	EB	–
VVVv569	VVV J145617.26-581944.66	14:56:17.26	-58:19:44.66	318.72119	0.66261	–	–	–	–	–	–	15.44	0.02	13.15	0.01	1.21	0.29	y	STV	69.7
VVVv570	VVV J145847.00-575924.03	14:58:47.00	-57:59:24.03	319.17035	0.80954	–	–	–	–	–	–	–	–	16.33	0.07	1.34	1.50	y	STV	73
VVVv571	VVV J145810.12-574249.73	14:58:10.12	-57:42:49.73	319.22752	1.09185	19.17	0.06	18.54	0.06	17.62	0.05	16.47	0.04	15.87	0.05	1.01	–	n	STV	–
VVVv572	VVV J145912.95-575224.81	14:59:12.95	-57:52:24.81	319.27580	0.88531	–	–	–	–	–	–	18.52	0.29	13.74	0.01	1.90	0.98	y	STV	34.37
VVVv573	VVV J150235.15-580550.76	15:02:35.15	-58:05:50.76	319.56183	0.47568	–	–	19.49	0.16	18.08	0.08	16.92	0.06	16.29	0.07	1.04	–	n	STV	–
VVVv574	VVV J150443.18-580654.81	15:04:43.18	-58:06:54.81	319.79961	0.32331	15.81	0.01	15.11	0.01	15.02	0.01	14.24	0.01	13.76	0.01	1.11	–	n	EB	3.98
VVVv575	VVV J150522.47-574002.48	15:05:22.47	-57:40:02.48	320.09491	0.67110	19.40	0.09	18.30	0.05	16.95	0.03	15.54	0.02	14.72	0.02	1.24	-0.44	y	Eruptive	–
VVVv576	VVV J150446.21-573111.93	15:04:46.21	-57:31:11.93	320.09657	0.83924	17.57	0.02	16.65	0.01	15.68	0.01	14.83	0.01	14.37	0.01	1.04	-2.14	y	STV	–
VVVv577	VVV J150523.60-573105.93	15:05:23.60	-57:31:05.93	320.17031	0.79969	–	–	–	–	–	–	17.92	0.16	16.13	0.07	1.96	–	y	STV	10.9
VVVv578	VVV J150813.34-575523.33	15:08:13.34	-57:55:23.33	320.29770	0.26088	–	–	–	–	18.39	0.10	16.76	0.05	15.95	0.05	1.03	–	y	EB	–
VVVv579	VVV J150813.36-573053.59	15:08:13.36	-57:30:53.59	320.50196	0.61437	16.03	0.01	14.44	0.01	12.82	0.01	12.22	0.01	11.60	0.01	1.69	–	n	LPV	410
VVVv580	VVV J150935.66-573522.61	15:09:35.66	-57:35:22.61	320.62350	0.45732	–	–	–	–	18.51	0.11	15.75	0.02	13.70	0.01	3.81	0.75	y	LPV-YSO	930
VVVv581	VVV J151047.12-574616.64	15:10:47.12	-57:46:16.64	320.66875	0.22004	–	–	–	–	17.89	0.07	15.91	0.02	14.43	0.01	1.58	-0.31	y	LPV-YSO	–
VVVv582	VVV J151113.18-574843.98	15:11:13.18	-57:48:43.98	320.69772	0.15535	19.74	0.12	18.45	0.07	17.00	0.03	15.85	0.02	15.24	0.03	1.16	–	y	EB	–
VVVv583	VVV J151051.98-574337.14	15:10:51.98	-57:43:37.14	320.70057	0.25270	–	–	–	–	–	–	16.96	0.06	15.24	0.03	1.21	0.50	y	Eruptive	–
VVVv584	VVV J150936.37-571712.15	15:09:36.37	-57:17:12.15	320.77775	0.71802	–	–	19.42	0.16	16.89	0.03	14.56	0.01	12.79	0.01	2.29	0.61	y	Eruptive	–
VVVv585	VVV J151136.89-565833.71	15:11:36.89	-56:58:33.71	321.17033	0.84723	18.33	0.03	17.52	0.02	16.58	0.02	15.75	0.02	15.26	0.03	1.06	–	n	STV	–
VVVv586	VVV J151319.74-565132.86	15:13:19.74	-56:51:32.86	321.43110	0.82734	–	–	–	–	–	–	18.01	0.17	14.98	0.02	2.52	1.78	y	LPV-YSO	–
VVVv587	VVV J151430.53-564509.59	15:14:30.53	-56:45:09.59	321.62440	0.83466	–	–	–	–	18.72	0.12	16.97	0.06	15.77	0.04	1.56	–	n	STV	–

Continued on next page

Table C1 – *Continued from previous page*

Object ID	VVV Designation	α (J2000)	δ (J2000)	l (degrees)	b (degrees)	Z (mag)	Z_{err} (mag)	Y (mag)	Y_{err} (mag)	J (mag)	J_{err} (mag)	H (mag)	H_{err} (mag)	$K_{\rm s}$ (mag)	$K_{\rm s,err}$ (mag)	$\Delta K_{\rm s}$ (mag)	α_{class}	SFR	Class	Period (days)
VVVv588	VVV J151728.78-572026.38	15:17:28.78	-57:20:26.38	321.65964	0.12213	–	–	–	–	–	–	–	–	14.03	0.01	2.93	1.71	y	LPV-Mira	880
VVVv589	VVV J151802.91-571449.28	15:18:02.91	-57:14:49.28	321.77446	0.16075	20.54	0.25	18.63	0.07	16.84	0.02	15.52	0.02	14.84	0.02	1.01	–	n	EB	2.63
VVVv590	VVV J151817.23-571140.67	15:18:17.23	-57:11:40.67	321.82968	0.18795	18.94	0.06	18.12	0.04	17.31	0.04	16.12	0.03	15.31	0.03	1.11	–	n	STV	–
VVVv591	VVV J152050.24-563327.63	15:20:50.24	-56:33:27.63	322.46519	0.53895	18.69	0.05	18.11	0.04	17.40	0.04	16.71	0.05	16.35	0.07	1.14	–	n	STV	–
VVVv592	VVV J152032.05-562731.91	15:20:32.05	-56:27:31.91	322.48330	0.64470	–	–	–	–	–	–	–	–	16.24	0.07	1.45	1.06	y	STV	–
VVVv593	VVV J152034.71-562800.83	15:20:34.71	-56:28:00.83	322.48413	0.63463	–	–	–	–	17.44	0.04	16.51	0.04	15.69	0.04	1.31	-0.14	y	STV	9.2
VVVv594	VVV J152235.73-565108.49	15:22:35.73	-56:51:08.49	322.50796	0.16049	19.10	0.07	17.23	0.02	15.77	0.01	13.60	0.01	12.14	0.01	1.62	-0.02	y	Fader	–
VVVv595	VVV J152015.17-560443.04	15:20:15.17	-56:04:43.04	322.65521	0.98611	18.79	0.05	17.91	0.03	16.00	0.01	13.20	0.01	11.64	0.01	1.75	–	n	LPV	725
VVVv596	VVV J152203.45-560904.17	15:22:03.45	-56:09:04.17	322.82754	0.78903	–	–	–	–	–	–	17.32	0.08	14.85	0.02	1.40	0.49	y	Eruptive	–
VVVv597	VVV J152535.77-562026.67	15:25:35.77	-56:20:26.67	323.13425	0.36066	–	–	–	–	19.84	0.33	18.03	0.16	17.05	0.14	1.25	–	n	Rare	–
VVVv598	VVV J152332.89-553918.20	15:23:32.89	-55:39:18.20	323.27351	1.09056	–	–	–	–	18.75	0.13	17.02	0.07	16.31	0.07	1.04	–	n	STV	–
VVVv599	VVV J152842.74-563040.60	15:28:42.74	-56:30:40.60	323.39604	-0.02164	19.04	0.06	18.18	0.04	17.10	0.03	16.16	0.03	15.74	0.04	1.03	–	y	STV	–
VVVv600	VVV J152949.95-562243.27	15:29:49.95	-56:22:43.27	323.59868	0.00015	–	–	18.89	0.08	16.92	0.02	14.72	0.01	13.09	0.01	1.00	0.78	y	Dipper	–
VVVv601	VVV J153113.73-560956.68	15:31:13.73	-56:09:56.68	323.87925	0.06486	17.67	0.02	16.49	0.01	15.47	0.01	14.43	0.01	13.94	0.01	1.33	-2.91	y	EB	1.59
VVVv602	VVV J153035.84-555119.45	15:30:35.84	-55:51:19.45	323.98383	0.37009	–	–	–	–	18.86	0.13	16.30	0.04	15.04	0.02	1.14	-0.85	y	EB	5.73
VVVv603	VVV J152919.69-552605.15	15:29:19.69	-55:26:05.15	324.07524	0.81801	–	–	–	–	–	–	13.27	0.01	11.54	0.01	2.08	–	n	LPV	501
VVVv604	VVV J153128.64-554206.72	15:31:28.64	-55:42:06.72	324.17308	0.42551	–	–	–	–	19.83	0.32	17.23	0.09	15.33	0.03	1.61	0.44	y	STV	–
VVVv605	VVV J153126.10-554107.36	15:31:26.10	-55:41:07.36	324.17761	0.44245	–	–	–	–	–	–	16.71	0.05	14.93	0.02	1.09	-0.04	y	STV	18.33
VVVv606	VVV J153331.64-560322.81	15:33:31.64	-56:03:22.81	324.20432	-0.02981	15.66	0.01	14.13	0.01	12.63	0.01	12.22	0.01	11.51	0.01	1.86	–	n	LPV	–
VVVv607	VVV J153300.09-553308.87	15:33:00.09	-55:33:08.87	324.43498	0.42422	–	–	–	–	19.08	0.16	16.94	0.07	15.56	0.04	1.12	–	n	STV	–
VVVv608	VVV J153358.87-553908.22	15:33:58.87	-55:39:08.22	324.49017	0.26278	–	–	–	–	–	–	18.48	0.27	16.57	0.09	1.61	–	n	STV	–
VVVv609	VVV J153341.12-551826.98	15:33:41.12	-55:18:26.98	324.65570	0.56812	17.90	0.02	16.59	0.01	15.28	0.01	14.22	0.01	13.60	0.01	1.49	–	n	EB	2.18
VVVv610	VVV J153445.56-552709.77	15:34:45.56	-55:27:09.77	324.69566	0.36133	–	–	20.20	0.27	17.34	0.03	15.12	0.01	13.56	0.01	1.90	-0.54	y	LPV-Mira	143.67
VVVv611	VVV J153728.01-552400.62	15:37:28.01	-55:24:00.62	325.03772	0.17888	–	–	–	–	20.03	0.39	17.14	0.08	15.10	0.02	1.53	0.45	y	STV	–
VVVv612	VVV J153547.48-550202.45	15:35:47.48	-55:02:02.45	325.05941	0.61557	–	–	–	–	18.16	0.07	16.05	0.03	14.87	0.02	1.12	–	n	EB	3.86
VVVv613	VVV J153517.84-543929.11	15:35:17.84	-54:39:29.11	325.22134	0.96221	19.95	0.14	18.76	0.08	16.90	0.02	14.88	0.01	13.36	0.01	1.99	–	n	STV	–
VVVv614	VVV J153510.45-543257.45	15:35:10.45	-54:32:57.45	325.27035	1.06097	17.57	0.02	17.11	0.02	16.36	0.01	15.56	0.02	15.17	0.03	1.05	–	n	STV	–
VVVv615	VVV J153856.83-550740.23	15:38:56.83	-55:07:40.23	325.36889	0.27354	–	–	–	–	18.87	0.12	16.90	0.05	15.59	0.04	1.15	0.46	y	STV	–
VVVv616	VVV J154024.96-545754.32	15:40:24.96	-54:57:54.32	325.63482	0.27877	–	–	–	–	–	–	16.62	0.04	12.63	0.01	2.38	–	n	LPV	799
VVVv617	VVV J154017.25-544511.18	15:40:17.25	-54:45:11.18	325.74680	0.45971	–	–	20.75	0.33	18.65	0.09	16.51	0.04	15.32	0.03	1.21	–	y	Fader	–
VVVv618	VVV J154254.67-550052.84	15:42:54.67	-55:00:52.84	325.89076	0.02376	20.01	0.10	18.65	0.05	15.74	0.01	13.67	0.01	12.11	0.01	1.14	-0.04	y	LPV-YSO	577
VVVv619	VVV J154228.33-541935.97	15:42:28.33	-54:19:35.97	326.25638	0.61004	–	–	–	–	–	–	13.96	0.01	12.08	0.01	1.08	-0.68	y	LPV-YSO	158
VVVv620	VVV J154157.90-541046.98	15:41:57.90	-54:10:46.98	326.28601	0.77191	–	–	–	–	19.17	0.15	17.36	0.08	15.98	0.05	2.76	–	y	Eruptive	–
VVVv621	VVV J154312.04-542308.80	15:43:12.04	-54:23:08.80	326.30508	0.49874	–	–	–	–	–	–	17.12	0.06	15.49	0.03	1.75	-0.70	y	Eruptive	–
VVVv622	VVV J154110.25-535422.49	15:41:10.25	-53:54:22.49	326.35747	1.06047	–	–	17.94	0.03	15.88	0.01	13.83	0.01	12.46	0.01	1.25	-0.28	y	EB	–
VVVv623	VVV J154225.31-540519.18	15:42:25.31	-54:05:19.18	326.39433	0.80412	19.92	0.09	18.94	0.06	17.47	0.03	16.10	0.02	15.29	0.03	1.04	-1.07	y	STV	–
VVVv624	VVV J154257.11-540416.99	15:42:57.11	-54:04:16.99	326.46668	0.77087	–	–	–	–	19.11	0.15	17.20	0.07	15.77	0.04	1.28	0.32	y	STV	–
VVVv625	VVV J154317.95-540647.29	15:43:17.95	-54:06:47.29	326.48189	0.70679	–	–	–	–	–	–	18.08	0.15	14.49	0.01	1.46	0.33	y	STV	–
VVVv626	VVV J154359.60-541135.69	15:43:59.60	-54:11:35.69	326.51393	0.58141	18.54	0.03	18.03	0.03	17.31	0.03	15.40	0.01	11.90	0.01	1.10	-0.10	y	LPV-YSO	509.43
VVVv627	VVV J154435.13-540903.57	15:44:35.13	-54:09:03.57	326.60840	0.56210	–	–	20.36	0.23	18.07	0.06	16.24	0.03	15.00	0.02	1.33	–	y	STV	13.62
VVVv628	VVV J154449.54-540752.08	15:44:49.54	-54:07:52.08	326.64837	0.55636	–	–	20.46	0.26	17.42	0.03	15.30	0.01	13.76	0.01	1.45	-0.51	y	Dipper	–
VVVv629	VVV J154505.60-540947.91	15:45:05.60	-54:09:47.91	326.65972	0.50694	–	–	20.21	0.21	18.68	0.10	16.48	0.04	15.11	0.02	1.70	-0.25	y	STV	15.13

Continued on next page

Table C1 – *Continued from previous page*

Object ID	VVV Designation	α (J2000)	δ (J2000)	l (degrees)	b (degrees)	Z (mag)	Z_{err} (mag)	Y (mag)	Y_{err} (mag)	J (mag)	J_{err} (mag)	H (mag)	H_{err} (mag)	$K_{\rm s}$ (mag)	$K_{\rm s,err}$ (mag)	$\Delta K_{\rm s}$ (mag)	α_{class}	SFR	Class	Period (days)
VVVv630	VVV J154456.13-540703.18	15:44:56.13	-54:07:03.18	326.66942	0.55727	–	–	–	–	–	–	18.83	0.31	15.76	0.04	1.90	2.70	y	Eruptive	–
VVVv631	VVV J154518.36-541036.87	15:45:18.36	-54:10:36.87	326.67601	0.47714	20.94	0.24	19.53	0.11	17.39	0.03	15.13	0.01	13.41	0.01	2.63	-0.14	y	Eruptive	–
VVVv632	VVV J154409.80-535627.78	15:44:09.80	-53:56:27.78	326.68727	0.76630	16.52	0.01	15.71	0.01	14.35	0.01	12.95	0.01	11.87	0.01	1.51	0.29	y	STV	–
VVVv633	VVV J154503.52-540248.79	15:45:03.52	-54:02:48.79	326.72692	0.60214	–	–	–	–	–	–	18.02	0.15	15.93	0.05	1.53	–	y	Eruptive	–
VVVv634	VVV J154616.79-541206.67	15:46:16.79	-54:12:06.67	326.77318	0.37003	–	–	–	–	–	–	–	–	16.88	0.12	1.54	1.70	y	Eruptive	–
VVVv635	VVV J155022.57-535906.72	15:50:22.57	-53:59:06.72	327.37855	0.16708	–	–	–	–	–	–	16.93	0.05	12.94	0.01	1.31	-0.36	y	LPV-Mira	497
VVVv636	VVV J155146.28-532557.31	15:51:46.28	-53:25:57.31	327.88638	0.46727	–	–	–	–	19.47	0.19	16.15	0.02	13.57	0.01	1.41	0.37	y	LPV-YSO	609
VVVv637	VVV J155206.86-532019.10	15:52:06.86	-53:20:19.10	327.98532	0.50793	–	–	–	–	–	–	17.89	0.12	13.68	0.01	1.98	0.64	y	STV	–
VVVv638	VVV J155319.21-532538.36	15:53:19.21	-53:25:38.36	328.06843	0.32546	–	–	–	–	19.32	0.17	15.33	0.01	12.81	0.01	1.13	0.02	y	Eruptive	–
VVVv639	VVV J155352.73-532223.92	15:53:52.73	-53:22:23.92	328.16705	0.31428	–	–	–	–	–	–	17.03	0.05	11.99	0.01	1.70	0.55	y	LPV-Mira	800
VVVv640	VVV J155303.38-531108.92	15:53:03.38	-53:11:08.92	328.19111	0.53720	–	–	–	–	–	–	17.90	0.12	13.79	0.01	2.08	0.84	y	LPV-Mira	515
VVVv641	VVV J155339.20-530511.82	15:53:39.20	-53:05:11.82	328.32325	0.55705	15.57	0.01	16.00	0.01	16.06	0.01	15.12	0.01	14.85	0.03	1.10	–	y	STV	–
VVVv642	VVV J155510.51-531104.03	15:55:10.51	-53:11:04.03	328.43675	0.33617	–	–	–	–	–	–	12.91	0.01	10.37	0.01	1.59	–	n	LPV	–
VVVv643	VVV J155543.20-531025.97	15:55:43.20	-53:10:25.97	328.50623	0.29203	–	–	–	–	–	–	17.47	0.12	16.22	0.11	1.14	0.64	y	STV	2.84
VVVv644	VVV J155508.35-530130.78	15:55:08.35	-53:01:30.78	328.53443	0.46204	–	–	–	–	–	–	–	–	14.64	0.03	1.36	-0.16	y	LPV-Mira	478
VVVv645	VVV J155555.56-525446.51	15:55:55.56	-52:54:46.51	328.69733	0.47242	–	–	–	–	–	–	–	–	16.96	0.22	1.43	3.85	y	LPV-YSO	154
VVVv646	VVV J155806.68-531630.20	15:58:06.68	-53:16:30.20	328.71482	-0.01592	–	–	–	–	–	–	17.16	0.09	15.47	0.06	1.86	0.26	y	STV	18.16
VVVv647	VVV J155412.81-522943.33	15:54:12.81	-52:29:43.33	328.76478	0.95934	–	–	–	–	–	–	14.62	0.01	12.01	0.01	2.12	–	n	LPV	–
VVVv648	VVV J155542.57-524230.82	15:55:42.57	-52:42:30.82	328.80328	0.65021	–	–	–	–	–	–	–	–	14.76	0.03	1.01	2.97	y	LPV-YSO	478
VVVv649	VVV J155643.04-524815.52	15:56:43.04	-52:48:15.52	328.85865	0.47888	–	–	–	–	–	–	18.31	0.26	14.99	0.04	2.19	0.65	y	Dipper	–
VVVv650	VVV J155734.78-525307.67	15:57:34.78	-52:53:07.67	328.90584	0.33289	–	–	–	–	–	–	–	–	13.50	0.01	1.98	0.79	y	LPV-Mira	578
VVVv651	VVV J155647.56-521908.67	15:56:47.56	-52:19:08.67	329.17983	0.84280	–	–	–	–	17.68	0.05	15.97	0.03	14.76	0.03	1.42	–	n	STV	–
VVVv652	VVV J155929.70-524223.17	15:59:29.70	-52:42:23.17	329.24234	0.28140	–	–	–	–	–	–	17.88	0.17	14.44	0.02	2.84	–	n	LPV	750
VVVv653	VVV J155653.63-521254.18	15:56:53.63	-52:12:54.18	329.25868	0.91241	–	–	–	–	–	–	13.85	0.01	10.77	0.01	1.58	–	n	LPV	729
VVVv654	VVV J155730.34-520227.10	15:57:30.34	-52:02:27.10	329.44281	0.98495	–	–	–	–	–	–	15.26	0.02	11.50	0.01	1.35	–	n	LPV	506
VVVv655	VVV J155842.66-515029.54	15:58:42.66	-51:50:29.54	329.71348	1.01658	–	–	–	–	–	–	16.72	0.06	15.00	0.04	1.35	-1.23	y	STV	–
VVVv656	VVV J160352.97-514258.66	16:03:52.97	-51:42:58.66	330.39955	0.58647	–	–	19.03	0.12	17.46	0.04	16.22	0.03	15.56	0.04	1.04	-1.40	y	EB	22.34
VVVv657	VVV J160501.51-515346.89	16:05:01.51	-51:53:46.89	330.41201	0.33458	–	–	19.28	0.16	17.93	0.06	16.66	0.05	14.72	0.02	1.08	0.60	y	Eruptive	–
VVVv658	VVV J160614.37-515406.13	16:06:14.37	-51:54:06.13	330.54800	0.20564	17.17	0.01	16.18	0.01	14.68	0.01	13.21	0.01	12.37	0.01	1.20	-1.67	y	Eruptive	–
VVVv659	VVV J160436.86-512626.49	16:04:36.86	-51:26:26.49	330.66746	0.71725	–	–	–	–	–	–	14.36	0.01	11.88	0.01	1.85	–	n	LPV	575
VVVv660	VVV J160558.60-513250.32	16:05:58.60	-51:32:50.32	330.75457	0.49647	–	–	–	–	–	–	16.39	0.04	12.62	0.01	1.89	–	n	LPV	649
VVVv661	VVV J160553.34-504722.43	16:05:53.34	-50:47:22.43	331.25047	1.06961	–	–	–	–	17.74	0.05	14.74	0.01	12.40	0.01	1.25	1.25	y	STV	39
VVVv662	VVV J161026.82-512234.13	16:10:26.82	-51:22:34.13	331.38447	0.15390	–	–	–	–	–	–	18.55	0.24	15.30	0.03	1.83	0.81	y	Eruptive	–
VVVv663	VVV J161031.85-510602.50	16:10:31.85	-51:06:02.50	331.58124	0.34711	–	–	–	–	–	–	15.82	0.02	12.26	0.01	1.46	–	n	LPV	885
VVVv664	VVV J160930.62-504822.40	16:09:30.62	-50:48:22.40	331.66287	0.67250	–	–	–	–	–	–	17.12	0.06	14.78	0.02	1.44	-0.11	y	Eruptive	–
VVVv665	VVV J160957.70-504809.42	16:09:57.70	-50:48:09.42	331.71775	0.62685	–	–	–	–	–	–	16.57	0.04	14.09	0.01	1.63	0.95	y	Eruptive	–
VVVv666	VVV J160917.91-503723.65	16:09:17.91	-50:37:23.65	331.76201	0.82992	–	–	–	–	17.91	0.06	16.28	0.03	15.30	0.03	1.17	–	n	EB	7.04
VVVv667	VVV J161200.30-505043.44	16:12:00.30	-50:50:43.44	331.92505	0.37586	–	–	–	–	–	–	17.71	0.11	15.84	0.05	1.24	–	n	LPV	1720
VVVv668	VVV J161146.40-500735.22	16:11:46.40	-50:07:35.22	332.38916	0.92620	18.27	0.03	17.64	0.03	16.52	0.02	15.33	0.01	14.39	0.01	1.17	-1.12	y	Dipper	–
VVVv669	VVV J161155.45-500827.40	16:11:55.45	-50:08:27.40	332.39693	0.89909	18.91	0.06	18.12	0.05	17.55	0.04	16.58	0.04	15.94	0.05	1.06	–	y	STV	–
VVVv670	VVV J161543.48-503433.61	16:15:43.48	-50:34:33.61	332.53779	0.16640	20.08	0.17	–	–	17.70	0.05	15.90	0.02	14.73	0.02	1.42	-0.07	y	STV	4.42
VVVv671	VVV J161238.40-500318.59	16:12:38.40	-50:03:18.59	332.53936	0.88316	–	–	–	–	–	–	17.39	0.08	15.39	0.03	1.67	0.96	y	Eruptive	–

Continued on next page

Table C1 – *Continued from previous page*

Object ID	VVV Designation	α (J2000)	δ (J2000)	l (degrees)	b (degrees)	Z (mag)	Z_{err} (mag)	Y (mag)	Y_{err} (mag)	J (mag)	J_{err} (mag)	H (mag)	H_{err} (mag)	$K_{\rm s}$ (mag)	$K_{\rm s,err}$ (mag)	$\Delta K_{\rm s}$ (mag)	α_{class}	SFR	Class	Period (days)
VVVv672	VVV J161303.16-500721.93	16:13:03.16	-50:07:21.93	332.54124	0.78857	19.52	0.10	18.87	0.10	17.17	0.03	16.12	0.03	15.49	0.04	1.11	-0.95	y	STV	2.3
VVVv673	VVV J161644.12-504321.62	16:16:44.12	-50:43:21.62	332.55147	-0.05037	–	–	–	–	–	–	14.62	0.01	11.37	0.01	1.42	0.12	y	LPV-YSO	576
VVVv674	VVV J161333.07-500522.46	16:13:33.07	-50:05:22.46	332.62215	0.75783	–	–	–	–	–	–	16.30	0.03	15.24	0.03	1.08	–	n	STV	–
VVVv675	VVV J161646.80-503408.73	16:16:46.80	-50:34:08.73	332.66328	0.05515	15.78	0.01	15.08	0.01	14.32	0.01	13.67	0.01	13.46	0.01	1.09	-0.62	y	EB	7.4
VVVv676	VVV J161327.72-494925.09	16:13:27.72	-49:49:25.09	332.79443	0.96095	–	–	–	–	18.80	0.12	16.43	0.04	15.07	0.03	1.48	-0.81	y	STV	6.32
VVVv677	VVV J161708.10-502456.26	16:17:08.10	-50:24:56.26	332.81058	0.12617	–	–	–	–	–	–	16.97	0.07	12.55	0.01	1.20	–	n	LPV	220
VVVv678	VVV J161741.28-502718.42	16:17:41.28	-50:27:18.42	332.84627	0.03651	19.39	0.08	19.00	0.09	18.20	0.07	16.95	0.07	12.61	0.01	1.77	–	n	LPV	610
VVVv679	VVV J161455.50-495908.92	16:14:55.50	-49:59:08.92	332.85355	0.68113	–	–	–	–	–	–	17.44	0.11	13.14	0.01	1.83	–	n	LPV	699
VVVv680	VVV J161830.18-501930.00	16:18:30.18	-50:19:30.00	333.03010	0.03900	–	–	–	–	19.06	0.15	17.12	0.08	15.88	0.06	1.55	-0.78	y	Dipper	–
VVVv681	VVV J161610.85-494746.21	16:16:10.85	-49:47:46.21	333.13083	0.67806	–	–	–	–	–	–	16.97	0.07	14.23	0.01	2.68	0.96	y	Dipper	–
VVVv682	VVV J161854.71-501158.83	16:18:54.71	-50:11:58.83	333.16448	0.08283	19.55	0.10	18.65	0.06	17.49	0.04	16.33	0.04	15.51	0.04	1.56	–	y	EB	3.87
VVVv683	VVV J161533.66-493810.79	16:15:33.66	-49:38:10.79	333.16930	0.86275	–	–	–	–	–	–	16.53	0.05	14.00	0.01	1.31	0.42	y	STV	12.2
VVVv684	VVV J161854.96-500838.21	16:18:54.96	-50:08:38.21	333.20395	0.12217	19.35	0.08	18.82	0.07	18.00	0.06	16.41	0.04	13.17	0.01	1.03	0.90	y	LPV-YSO	675
VVVv685	VVV J161615.48-493458.37	16:16:15.48	-49:34:58.37	333.28778	0.82304	–	–	–	–	–	–	17.16	0.08	15.27	0.03	1.56	-0.37	y	EB	–
VVVv686	VVV J161916.95-500243.18	16:19:16.95	-50:02:43.18	333.31499	0.15137	–	–	–	–	–	–	–	–	16.11	0.07	1.28	1.42	y	Eruptive	–
VVVv687	VVV J161650.93-491901.77	16:16:50.93	-49:19:01.77	333.54143	0.94756	19.24	0.07	18.70	0.07	17.52	0.04	16.77	0.06	15.45	0.04	1.00	–	n	STV	–
VVVv688	VVV J161950.92-493821.50	16:19:50.92	-49:38:21.50	333.66491	0.37663	–	–	–	–	18.92	0.14	–	–	14.57	0.02	1.85	–	n	LPV	782
VVVv689	VVV J162006.05-493656.76	16:20:06.05	-49:36:56.76	333.71051	0.36468	19.64	0.10	18.61	0.06	17.26	0.03	15.70	0.02	14.76	0.02	2.01	-0.39	y	STV	5.08
VVVv690	VVV J161916.31-491409.71	16:19:16.31	-49:14:09.71	333.88107	0.72977	17.18	0.01	16.80	0.01	16.16	0.01	15.39	0.02	15.02	0.03	1.17	–	n	STV	–
VVVv691	VVV J162051.36-492535.05	16:20:51.36	-49:25:35.05	333.93086	0.41295	17.50	0.02	17.08	0.02	16.20	0.01	15.26	0.01	14.55	0.02	1.12	–	n	STV	–
VVVv692	VVV J162059.45-491908.03	16:20:59.45	-49:19:08.03	334.02221	0.47373	18.95	0.06	17.98	0.04	16.66	0.02	15.79	0.02	15.13	0.03	1.00	–	n	STV	–
VVVv693	VVV J162028.12-490800.03	16:20:28.12	-49:08:00.03	334.09242	0.66549	17.35	0.01	16.53	0.01	–	–	14.86	0.01	14.28	0.01	1.01	–	n	STV	–
VVVv694	VVV J162138.12-491021.21	16:21:38.12	-49:10:21.21	334.20001	0.50317	21.04	0.31	19.13	0.11	17.63	0.06	15.70	0.03	14.34	0.02	1.42	0.09	y	Dipper	–
VVVv695	VVV J162337.14-491149.89	16:23:37.14	-49:11:49.89	334.41118	0.25600	17.66	0.02	16.54	0.01	15.48	0.01	14.36	0.01	13.39	0.01	1.66	-0.59	y	Dipper	–
VVVv696	VVV J162050.35-483843.24	16:20:50.35	-48:38:43.24	334.47938	0.96903	18.29	0.03	17.30	0.02	16.10	0.02	15.38	0.02	14.94	0.03	1.08	–	n	EB	2.83
VVVv697	VVV J162327.18-490255.08	16:23:27.18	-49:02:55.08	334.49771	0.37978	–	–	–	–	–	–	14.25	0.01	11.59	0.01	2.44	–	n	LPV	847
VVVv698	VVV J162507.05-491128.22	16:25:07.05	-49:11:28.22	334.58714	0.08569	–	–	–	–	–	–	15.27	0.02	11.85	0.01	1.27	-0.36	y	LPV-Mira	433
VVVv699	VVV J162344.34-485455.29	16:23:44.34	-48:54:55.29	334.62548	0.44010	–	–	–	–	–	–	–	–	16.19	0.09	2.28	2.78	y	Eruptive	–
VVVv700	VVV J162708.19-484400.79	16:27:08.19	-48:44:00.79	335.14625	0.16707	–	–	–	–	–	–	–	–	14.75	0.03	3.66	–	n	LPV	770
VVVv701	VVV J162440.71-475426.69	16:24:40.71	-47:54:26.69	335.45321	1.03612	20.88	0.28	18.99	0.10	17.90	0.08	16.15	0.04	15.41	0.05	1.12	–	n	EB	2.66
VVVv702	VVV J162850.16-481432.68	16:28:50.16	-48:14:32.68	335.69555	0.30415	20.22	0.19	18.96	0.10	17.41	0.05	16.13	0.05	15.31	0.05	1.16	–	y	STV	–
VVVv703	VVV J162726.01-475931.65	16:27:26.01	-47:59:31.65	335.71411	0.64634	–	–	–	–	–	–	15.58	0.03	12.12	0.01	1.87	–	n	LPV	628
VVVv704	VVV J163001.64-481530.95	16:30:01.64	-48:15:30.95	335.82052	0.14929	–	–	–	–	–	–	16.29	0.06	11.86	0.01	1.03	-0.06	y	LPV-Mira	541
VVVv705	VVV J162906.01-480536.96	16:29:06.01	-48:05:36.96	335.83362	0.37501	–	–	–	–	17.84	0.08	15.69	0.03	14.19	0.02	1.21	-0.29	y	STV	–
VVVv706	VVV J163101.05-481842.45	16:31:01.05	-48:18:42.45	335.89495	-0.00698	19.30	0.08	17.03	0.02	14.78	0.01	13.01	0.01	11.90	0.01	1.48	-3.26	y	Fader	–
VVVv707	VVV J162943.72-475759.56	16:29:43.72	-47:57:59.56	335.99810	0.38646	–	–	–	–	–	–	17.97	0.27	13.80	0.01	2.26	–	n	LPV	779
VVVv708	VVV J162939.42-475032.13	16:29:39.42	-47:50:32.13	336.07996	0.48075	–	–	–	–	–	–	17.79	0.22	14.37	0.02	1.95	–	n	LPV	596
VVVv709	VVV J163035.64-474559.55	16:30:35.64	-47:45:59.55	336.24313	0.41855	–	–	–	–	–	–	–	–	16.71	0.17	3.48	3.43	y	LPV-YSO	506
VVVv710	VVV J163225.37-475338.29	16:32:25.37	-47:53:38.29	336.36024	0.10755	–	–	19.56	0.18	17.85	0.08	16.15	0.05	15.37	0.05	1.56	–	y	Eruptive	–
VVVv711	VVV J163438.61-472001.77	16:34:38.61	-47:20:01.77	337.02552	0.21358	20.31	0.20	18.49	0.07	16.72	0.03	14.68	0.01	11.37	0.01	1.28	–	n	LPV	630
VVVv712	VVV J163550.53-472231.49	16:35:50.53	-47:22:31.49	337.13198	0.03578	–	–	–	–	–	–	14.82	0.02	12.56	0.01	2.45	-0.92	y	Fader	–
VVVv713	VVV J163352.79-465218.51	16:33:52.79	-46:52:18.51	337.27716	0.62227	16.91	0.01	16.04	0.01	13.99	0.01	12.61	0.01	11.47	0.01	2.04	-0.08	y	Fader	–

Continued on next page

Table C1 – *Continued from previous page*

Object ID	VVV Designation	α (J2000)	δ (J2000)	l (degrees)	b (degrees)	Z (mag)	Z_{err} (mag)	Y (mag)	Y_{err} (mag)	J (mag)	J_{err} (mag)	H (mag)	H_{err} (mag)	$K_{\rm s}$ (mag)	$K_{\rm s,err}$ (mag)	$\Delta K_{\rm s}$ (mag)	α_{class}	SFR	Class	Period (days)
VVVv714	VVV J163353.64-465134.78	16:33:53.64	-46:51:34.78	337.28772	0.62874	–	–	–	–	–	–	–	–	15.08	0.04	2.18	0.76	y	LPV-YSO	190.42
VVVv715	VVV J163702.59-470039.76	16:37:02.59	-47:00:39.76	337.53883	0.12988	–	–	–	–	–	–	–	–	12.34	0.01	1.46	–	n	LPV	1602.00
VVVv716	VVV J163555.14-464920.63	16:35:55.14	-46:49:20.63	337.54935	0.39883	–	–	–	–	17.14	0.05	15.16	0.02	13.92	0.01	1.02	-1.06	y	LPV-YSO	–
VVVv717	VVV J163605.56-464040.61	16:36:05.56	-46:40:40.61	337.67616	0.47413	–	–	–	–	–	–	–	–	14.37	0.02	2.47	0.80	y	LPV-YSO	844
VVVv718	VVV J163854.24-465446.26	16:38:54.24	-46:54:46.26	337.82422	-0.04043	–	–	–	–	–	–	16.35	0.07	14.73	0.03	1.09	-1.37	y	EB	4.61
VVVv719	VVV J163907.18-464958.72	16:39:07.18	-46:49:58.72	337.90832	-0.01466	–	–	–	–	–	–	14.63	0.01	11.61	0.01	1.65	0.02	y	LPV-Mira	660
VVVv720	VVV J163722.54-461329.11	16:37:22.54	-46:13:29.11	338.16032	0.61494	–	–	–	–	–	–	–	–	14.97	0.04	2.08	1.50	y	Eruptive	–
VVVv721	VVV J163948.77-454847.96	16:39:48.77	-45:48:47.96	338.74912	0.57449	–	–	–	–	18.49	0.16	15.96	0.05	13.98	0.01	1.86	0.87	y	Eruptive	–
VVVv722	VVV J164042.44-453905.82	16:40:42.44	-45:39:05.82	338.97368	0.56500	–	–	–	–	–	–	17.90	0.27	13.53	0.01	1.04	0.06	y	LPV-Mira	123.9
VVVv723	VVV J164231.97-454048.90	16:42:31.97	-45:40:48.90	339.16278	0.30656	–	–	–	–	15.32	0.01	12.99	0.01	11.94	0.01	1.89	-0.21	y	Dipper	–
VVVv724	VVV J164257.47-444743.95	16:42:57.47	-44:47:43.95	339.87852	0.83198	20.17	0.17	18.37	0.06	16.54	0.03	14.92	0.02	14.19	0.02	1.53	–	n	Rare	–
VVVv725	VVV J164624.86-451206.07	16:46:24.86	-45:12:06.07	339.96997	0.10400	18.27	0.03	17.77	0.03	17.13	0.04	16.40	0.05	16.07	0.09	1.16	–	n	STV	–
VVVv726	VVV J164359.99-444504.52	16:43:59.99	-44:45:04.52	340.03324	0.72144	–	–	–	–	–	–	–	–	16.54	0.13	2.07	–	n	LPV	–
VVVv727	VVV J164622.25-445953.10	16:46:22.25	-44:59:53.10	340.11987	0.24200	–	–	–	–	–	–	14.45	0.01	11.91	0.01	1.46	–	n	LPV	549
VVVv728	VVV J164734.30-445638.46	16:47:34.30	-44:56:38.46	340.29861	0.11519	–	–	–	–	–	–	15.35	0.02	11.54	0.01	1.51	0.65	y	LPV-Mira	787
VVVv729	VVV J164803.79-444359.42	16:48:03.79	-44:43:59.42	340.51590	0.18477	–	–	–	–	–	–	16.00	0.04	12.34	0.01	1.50	0.27	y	LPV-Mira	471
VVVv730	VVV J164639.49-443044.62	16:46:39.49	-44:30:44.62	340.52261	0.51824	20.78	0.28	19.00	0.10	17.41	0.05	15.88	0.03	15.03	0.03	1.30	-1.95	y	EB	2.72
VVVv731	VVV J164634.32-442531.34	16:46:34.32	-44:25:31.34	340.57888	0.58638	–	–	–	–	18.30	0.11	15.97	0.04	14.97	0.03	3.70	–	n	Rare	–
VVVv732	VVV J164622.42-441634.06	16:46:22.42	-44:16:34.06	340.66946	0.71018	–	–	–	–	17.77	0.07	15.99	0.04	15.29	0.04	1.31	–	n	STV	–
VVVv733	VVV J164620.85-441447.50	16:46:20.85	-44:14:47.50	340.68894	0.73296	18.92	0.05	17.94	0.04	16.84	0.03	15.81	0.03	15.32	0.04	1.55	–	n	EB	3.53
VVVv734	VVV J164752.96-442816.11	16:47:52.96	-44:28:16.11	340.69533	0.37842	–	–	–	–	–	–	16.78	0.07	15.26	0.04	1.13	–	y	STV	–
VVVv735	VVV J165029.33-441952.02	16:50:29.33	-44:19:52.02	341.10170	0.11162	–	–	–	–	–	–	17.10	0.10	15.35	0.04	1.07	-0.47	y	LPV-YSO	166
VVVv736	VVV J165055.45-440659.40	16:50:55.45	-44:06:59.40	341.31663	0.18874	–	–	–	–	–	–	–	–	15.02	0.03	1.08	1.60	y	Dipper	–
VVVv737	VVV J165131.99-440044.27	16:51:31.99	-44:00:44.27	341.46665	0.17091	–	–	–	–	–	–	15.57	0.02	11.95	0.01	2.07	0.20	y	LPV-Mira	658
VVVv738	VVV J165046.51-435041.49	16:50:46.51	-43:50:41.49	341.50858	0.38280	–	–	–	–	–	–	17.58	0.12	16.30	0.09	1.16	–	y	Eruptive	–
VVVv739	VVV J164822.88-432206.16	16:48:22.88	-43:22:06.16	341.59616	1.02090	18.03	0.02	17.35	0.02	16.60	0.02	15.92	0.03	15.64	0.05	1.02	–	n	STV	–
VVVv740	VVV J165259.55-440203.79	16:52:59.55	-44:02:03.79	341.61623	-0.04574	–	–	–	–	–	–	16.96	0.07	15.44	0.04	1.36	-0.93	y	STV	0.32
VVVv741	VVV J165005.32-432227.21	16:50:05.32	-43:22:27.21	341.79097	0.77929	18.95	0.05	17.98	0.04	17.17	0.03	16.18	0.03	15.84	0.06	1.61	–	n	STV	–
VVVv742	VVV J165053.55-432707.55	16:50:53.55	-43:27:07.55	341.82441	0.61727	19.01	0.05	18.15	0.04	17.20	0.03	16.33	0.04	15.88	0.06	1.06	–	n	STV	–
VVVv743	VVV J165251.56-433950.49	16:52:51.56	-43:39:50.49	341.88755	0.20751	–	–	–	–	19.31	0.21	15.04	0.01	12.42	0.01	1.71	0.93	y	LPV-Mira	649
VVVv744	VVV J165354.84-433809.08	16:53:54.84	-43:38:09.08	342.03005	0.07756	19.36	0.06	18.67	0.06	17.87	0.06	16.56	0.05	13.13	0.01	1.06	-0.05	y	LPV-Mira	527
VVVv745	VVV J165144.08-431111.91	16:51:44.08	-43:11:11.91	342.12662	0.66842	–	–	–	–	18.90	0.15	16.84	0.06	15.51	0.04	1.26	–	n	STV	–
VVVv746	VVV J165344.38-432819.36	16:53:44.38	-43:28:19.36	342.13710	0.20551	–	–	–	–	–	–	18.07	0.19	15.74	0.05	1.27	0.91	y	Eruptive	–
VVVv747	VVV J165205.49-430449.43	16:52:05.49	-43:04:49.43	342.25001	0.68576	–	–	–	–	18.52	0.11	13.76	0.01	11.73	0.01	2.59	–	n	LPV	684
VVVv748	VVV J165331.07-431512.35	16:53:31.07	-43:15:12.35	342.28104	0.37492	–	–	–	–	–	–	17.05	0.08	15.29	0.03	1.15	0.19	y	STV	4.33
VVVv749	VVV J165448.52-432409.89	16:54:48.52	-43:24:09.89	342.31324	0.09858	–	–	–	–	–	–	18.58	0.31	15.33	0.04	1.38	1.69	y	Eruptive	–
VVVv750	VVV J165244.59-430520.02	16:52:44.59	-43:05:20.02	342.31899	0.58841	–	–	–	–	–	–	–	–	16.28	0.08	2.73	2.55	y	STV	75.49
VVVv751	VVV J165249.10-430236.21	16:52:49.10	-43:02:36.21	342.36287	0.60665	18.37	0.03	17.69	0.03	16.19	0.01	14.53	0.01	13.08	0.01	1.22	-0.01	y	Dipper	–
VVVv752	VVV J165507.68-431244.47	16:55:07.68	-43:12:44.47	342.49782	0.17312	–	–	–	–	–	–	17.55	0.12	15.70	0.05	1.03	0.83	y	STV	28.03
VVVv753	VVV J165452.75-430321.11	16:54:52.75	-43:03:21.11	342.59096	0.30682	–	–	–	–	–	–	16.20	0.03	12.68	0.01	1.76	–	n	LPV	504
VVVv754	VVV J165528.31-430602.58	16:55:28.31	-43:06:02.58	342.62406	0.19447	–	–	–	–	–	–	18.57	0.32	12.70	0.01	1.69	–	n	LPV	658
VVVv755	VVV J165504.79-425847.58	16:55:04.79	-42:58:47.58	342.67309	0.32610	–	–	–	–	–	–	17.82	0.16	13.62	0.01	1.86	–	n	LPV	808

Continued on next page

Table C1 – *Continued from previous page*

Object ID	VVV Designation	α (J2000)	δ (J2000)	l (degrees)	b (degrees)	Z (mag)	Z_{err} (mag)	Y (mag)	Y_{err} (mag)	J (mag)	J_{err} (mag)	H (mag)	H_{err} (mag)	$K_{\rm s}$ (mag)	$K_{\rm s,err}$ (mag)	$\Delta K_{\rm s}$ (mag)	α_{class}	SFR	Class	Period (days)
VVVv756	VVV J165225.39-423432.39	16:52:25.39	-42:34:32.39	342.67855	0.95934	21.01	0.29	19.61	0.16	17.16	0.03	15.27	0.02	13.63	0.01	1.94	0.27	y	Fader	–
VVVv757	VVV J165231.55-423049.66	16:52:31.55	-42:30:49.66	342.73837	0.98399	–	–	–	–	18.79	0.14	16.63	0.05	15.61	0.05	1.13	–	n	STV	–
VVVv758	VVV J165625.48-425554.23	16:56:25.48	-42:55:54.23	342.86490	0.16459	19.15	0.15	18.95	0.13	17.80	0.06	14.94	0.01	10.61	0.01	1.34	–	n	LPV	481
VVVv759	VVV J165330.26-422615.00	16:53:30.26	-42:26:15.00	342.91171	0.89267	–	–	–	–	–	–	17.49	0.11	16.30	0.12	2.38	1.75	y	Eruptive	–
VVVv760	VVV J165514.44-424026.62	16:55:14.44	-42:40:26.62	342.92954	0.49531	17.09	0.03	16.54	0.02	16.11	0.01	15.16	0.01	14.79	0.03	1.12	-1.77	y	EB	7
VVVv761	VVV J165639.54-423813.91	16:56:39.54	-42:38:13.91	343.12166	0.31518	–	–	–	–	18.32	0.09	16.46	0.04	15.51	0.06	1.04	–	n	STV	–
VVVv762	VVV J165704.45-423124.12	16:57:04.45	-42:31:24.12	343.25829	0.32656	17.31	0.03	17.13	0.03	16.58	0.02	15.85	0.02	15.28	0.05	1.01	–	n	LPV	513
VVVv763	VVV J165657.89-422955.09	16:56:57.89	-42:29:55.09	343.26505	0.35773	–	–	–	–	18.28	0.09	15.27	0.01	13.63	0.01	3.19	–	n	Rare	–
VVVv764	VVV J165410.03-415356.82	16:54:10.03	-41:53:56.82	343.40683	1.13735	–	–	18.76	0.10	–	–	–	–	11.94	0.01	1.61	0.12	y	LPV-Mira	–
VVVv765	VVV J165452.35-415132.72	16:54:52.35	-41:51:32.72	343.52064	1.06055	–	–	–	–	18.91	0.16	16.97	0.07	14.58	0.03	1.80	-0.52	y	Dipper	–
VVVv766	VVV J165959.76-422759.67	16:59:59.76	-42:27:59.67	343.63706	-0.06055	–	–	–	–	–	–	17.87	0.15	15.78	0.08	1.13	-0.27	y	EB	–
VVVv767	VVV J165646.93-415231.10	16:56:46.93	-41:52:31.10	343.73084	0.77336	14.05	0.01	13.79	0.01	13.46	0.01	–	–	12.25	0.01	1.15	–	n	EB	3.79
VVVv768	VVV J170030.35-421248.67	17:00:30.35	-42:12:48.67	343.89438	0.02131	18.53	0.09	18.04	0.05	18.55	0.11	16.73	0.05	14.95	0.04	1.07	-0.39	y	STV	25.22
VVVv769	VVV J165846.96-414317.51	16:58:46.96	-41:43:17.51	344.08324	0.57717	–	–	–	–	18.30	0.09	14.37	0.01	12.30	0.01	2.06	–	n	LPV	551
VVVv770	VVV J170129.39-413942.90	17:01:29.39	-41:39:42.90	344.44189	0.21617	–	–	–	–	–	–	–	–	15.07	0.03	2.39	0.67	y	Eruptive	–
VVVv771	VVV J165759.50-410834.91	16:57:59.50	-41:08:34.91	344.44477	1.05253	–	–	–	–	16.24	0.01	12.90	0.01	11.63	0.01	1.69	–	n	LPV	227
VVVv772	VVV J165827.14-405409.28	16:58:27.14	-40:54:09.28	344.68722	1.13379	–	–	–	–	17.26	0.03	13.61	0.01	11.74	0.01	2.02	–	n	LPV	585
VVVv773	VVV J170129.82-411022.03	17:01:29.82	-41:10:22.03	344.82892	0.51528	–	–	–	–	–	–	15.49	0.02	12.30	0.01	1.22	–	n	LPV	233
VVVv774	VVV J170028.83-403311.02	17:00:28.83	-40:33:11.02	345.19957	1.04786	18.41	0.03	17.50	0.02	16.48	0.01	15.20	0.01	14.43	0.02	1.17	-0.67	y	STV	–
VVVv775	VVV J170036.85-403207.80	17:00:36.85	-40:32:07.80	345.22906	1.03865	–	–	20.27	0.26	19.17	0.15	17.42	0.09	15.67	0.05	1.45	1.52	y	STV	–
VVVv776	VVV J170041.05-403228.55	17:00:41.05	-40:32:28.55	345.23270	1.02463	–	–	–	–	18.95	0.12	16.23	0.03	14.61	0.02	1.11	-0.09	y	STV	–
VVVv777	VVV J170050.17-403217.91	17:00:50.17	-40:32:17.91	345.25280	1.00368	–	–	–	–	17.52	0.03	15.93	0.02	14.91	0.02	1.38	-0.78	y	STV	11.32
VVVv778	VVV J170038.73-402958.86	17:00:38.73	-40:29:58.86	345.26095	1.05602	–	–	–	–	18.78	0.11	14.92	0.01	12.17	0.01	1.55	1.09	y	STV	–
VVVv779	VVV J170202.20-404118.61	17:02:02.20	-40:41:18.61	345.27405	0.73163	–	–	–	–	–	–	15.53	0.02	12.25	0.01	2.17	0.91	y	LPV-Mira	506
VVVv780	VVV J170104.38-402659.86	17:01:04.38	-40:26:59.86	345.35017	1.02249	19.90	0.11	18.63	0.06	16.85	0.02	15.20	0.01	14.15	0.01	1.07	-0.52	y	STV	9
VVVv781	VVV J170103.96-402640.28	17:01:03.96	-40:26:40.28	345.35366	1.02686	–	–	–	–	18.61	0.09	15.73	0.02	13.90	0.01	1.85	1.51	y	Fader	–
VVVv782	VVV J170558.41-405720.74	17:05:58.41	-40:57:20.74	345.51464	-0.02221	–	–	–	–	–	–	16.64	0.05	14.82	0.02	1.04	-1.07	y	EB	18.17
VVVv783	VVV J170215.24-395854.81	17:02:15.24	-39:58:54.81	345.85827	1.13137	18.74	0.04	18.00	0.04	16.38	0.02	15.12	0.02	14.26	0.02	1.31	-1.01	y	STV	13.08
VVVv784	VVV J170450.47-401830.72	17:04:50.47	-40:18:30.72	345.90020	0.54029	–	–	–	–	–	–	15.58	0.02	13.34	0.01	1.56	0.16	y	STV	–
VVVv785	VVV J170601.51-402746.57	17:06:01.51	-40:27:46.57	345.91354	0.26736	–	–	–	–	–	–	16.55	0.06	12.51	0.01	1.98	0.77	y	LPV-Mira	662
VVVv786	VVV J170448.34-401326.37	17:04:48.34	-40:13:26.37	345.96334	0.59691	–	–	–	–	18.23	0.09	15.30	0.02	13.69	0.01	1.63	0.27	y	Dipper	–
VVVv787	VVV J170648.69-402635.41	17:06:48.69	-40:26:35.41	346.01944	0.15986	–	–	–	–	–	–	–	–	13.75	0.01	1.88	–	n	LPV	638
VVVv788	VVV J170711.21-400902.64	17:07:11.21	-40:09:02.64	346.29617	0.27844	18.59	0.03	17.82	0.03	16.92	0.03	16.04	0.04	15.70	0.06	1.04	–	n	STV	–
VVVv789	VVV J170811.64-392444.91	17:08:11.64	-39:24:44.91	347.00307	0.56616	20.30	0.15	18.79	0.07	17.37	0.04	16.29	0.04	15.52	0.05	1.33	–	n	EB	3.13
VVVv790	VVV J170810.22-391409.92	17:08:10.22	-39:14:09.92	347.14166	0.67538	–	–	–	–	–	–	17.81	0.19	16.60	0.13	1.65	–	n	STV	–
VVVv791	VVV J170806.33-385911.97	17:08:06.33	-38:59:11.97	347.33399	0.83472	–	–	–	–	–	–	–	–	13.13	0.01	2.85	–	n	LPV	699
VVVv792	VVV J170919.43-390259.83	17:09:19.43	-39:02:59.83	347.42453	0.60711	–	–	–	–	–	–	–	–	12.76	0.01	2.01	–	n	LPV	646
VVVv793	VVV J170856.29-385848.19	17:08:56.29	-38:58:48.19	347.43599	0.70892	–	–	–	–	–	–	16.24	0.05	12.72	0.01	2.85	–	n	LPV	653
VVVv794	VVV J171250.14-391027.51	17:12:50.14	-39:10:27.51	347.72752	-0.01558	20.24	0.19	18.85	0.11	17.07	0.04	15.98	0.04	15.40	0.05	1.04	–	y	EB	6.31
VVVv795	VVV J171312.64-385041.41	17:13:12.64	-38:50:41.41	348.03690	0.11908	–	–	–	–	19.32	0.29	17.47	0.16	16.61	0.15	1.53	–	y	Eruptive	–
VVVv796	VVV J171207.43-384126.86	17:12:07.43	-38:41:26.86	348.03683	0.38101	–	–	–	–	–	–	16.87	0.09	12.45	0.01	2.94	1.10	y	LPV-Mira	796
VVVv797	VVV J171219.10-382941.67	17:12:19.10	-38:29:41.67	348.21749	0.46574	–	–	18.89	0.11	17.89	0.08	16.78	0.09	15.90	0.08	1.37	–	y	STV	–

Continued on next page

Table C1 – *Continued from previous page*

Object ID	VVV Designation	α (J2000)	δ (J2000)	l (degrees)	b (degrees)	Z (mag)	Z_{err} (mag)	Y (mag)	Y_{err} (mag)	J (mag)	J_{err} (mag)	H (mag)	H_{err} (mag)	$K_{\rm s}$ (mag)	$K_{\rm s,err}$ (mag)	$\Delta K_{\rm s}$ (mag)	α_{class}	SFR	Class	Period (days)
VVVv798	VVV J171244.16-382639.53	17:12:44.16	-38:26:39.53	348.30653	0.42941	–	–	–	–	–	–	–	–	14.05	0.01	1.03	1.60	y	LPV-Mira	253
VVVv799	VVV J171316.81-383051.00	17:13:16.81	-38:30:51.00	348.31258	0.30220	–	–	–	–	16.25	0.02	13.10	0.01	11.73	0.01	1.38	-1.33	y	Dipper	–
VVVv800	VVV J171246.04-382524.63	17:12:46.04	-38:25:24.63	348.32696	0.43669	–	–	–	–	18.89	0.20	15.80	0.04	12.89	0.01	1.65	1.44	y	Eruptive	–
VVVv801	VVV J171222.63-381837.43	17:12:22.63	-38:18:37.43	348.37339	0.56511	–	–	–	–	–	–	14.13	0.01	11.43	0.01	1.68	0.07	y	LPV-YSO	546
VVVv802	VVV J171410.63-383011.83	17:14:10.63	-38:30:11.83	348.42421	0.16640	19.70	0.12	–	–	18.13	0.10	16.31	0.06	13.30	0.01	1.42	1.38	y	LPV-Mira	1340
VVVv803	VVV J171343.94-381016.01	17:13:43.94	-38:10:16.01	348.64244	0.43158	–	–	–	–	–	–	–	–	13.58	0.01	2.41	–	n	LPV	947
VVVv804	VVV J171504.10-380938.79	17:15:04.10	-38:09:38.79	348.80431	0.22455	–	–	–	–	18.45	0.13	14.38	0.01	11.87	0.01	1.51	0.08	y	LPV-Mira	452
VVVv805	VVV J171524.97-380818.55	17:15:24.97	-38:08:18.55	348.86227	0.18196	–	–	–	–	–	–	16.75	0.10	13.00	0.01	1.22	0.17	y	LPV-Mira	432
VVVv806	VVV J171406.87-374640.84	17:14:06.87	-37:46:40.84	349.00522	0.60069	–	–	–	–	–	–	–	–	14.46	0.02	3.37	–	n	LPV	–
VVVv807	VVV J171643.72-374852.74	17:16:43.72	-37:48:52.74	349.27611	0.15949	–	–	–	–	–	–	–	–	15.52	0.06	2.70	1.29	y	LPV-YSO	546
VVVv808	VVV J171632.78-374609.27	17:16:32.78	-37:46:09.27	349.29224	0.21515	–	–	–	–	–	–	–	–	16.45	0.14	2.26	–	y	Eruptive	–
VVVv809	VVV J171713.14-373941.72	17:17:13.14	-37:39:41.72	349.45704	0.16903	–	–	–	–	–	–	–	–	16.66	0.17	2.01	2.72	y	Eruptive	–
VVVv810	VVV J171707.96-373320.37	17:17:07.96	-37:33:20.37	349.53356	0.24425	–	–	–	–	–	–	–	–	14.70	0.03	2.34	–	n	LPV	811
VVVv811	VVV J171714.07-372347.84	17:17:14.07	-37:23:47.84	349.67499	0.31974	–	–	–	–	–	–	17.32	0.16	12.53	0.01	1.62	–	n	LPV	1472
VVVv812	VVV J171726.31-372352.20	17:17:26.31	-37:23:52.20	349.69743	0.28597	–	–	–	–	–	–	–	–	14.55	0.02	3.47	–	n	LPV	906
VVVv813	VVV J171525.93-364642.02	17:15:25.93	-36:46:42.02	349.97008	0.97119	–	–	–	–	18.06	0.09	14.50	0.01	11.61	0.01	1.42	–	n	LPV	525
VVVv814	VVV J171810.35-370848.64	17:18:10.35	-37:08:48.64	349.98669	0.31152	–	–	–	–	–	–	17.59	0.21	15.82	0.08	1.41	–	n	LPV	–
VVVv815	VVV J142604.95-604116.81	14:26:04.95	-60:41:16.81	314.26286	0.08460	–	–	–	–	19.17	0.16	17.90	0.13	14.94	0.02	1.71	1.58	y	Eruptive	–
VVVv816	VVV J130950.13-624631.76	13:09:50.13	-62:46:31.76	305.03425	0.02114	–	–	–	–	–	–	–	–	15.0	0.03	1.37	2.29	y	LPV-Mira	603